UNIVERSITY OF CALIFORNIA
RIVERSIDE

Regulation of Sporangia Development in *Phytophthora infestans*

A Dissertation submitted in partial satisfaction
of the requirements for the degree of

Doctor of Philosophy

in

Plant Pathology

by

Wiphawee Leesutthiphonchai

June 2020

Dissertation Committee:
Dr. Howard Judelson, Chairperson
Dr. Katherine Borkovich
Dr. Patricia Manosalva

The Dissertation of Wiphawee Leesutthiphonchai is approved:

Committee Chairperson

University of California, Riverside

Acknowledgements

First of all, I would like to thank my PI, Dr. Howard Judelson who always provides great support. I am very grateful for his guidance, encouragement, and being patient with me. Thank you for providing emotional support especially when my experiments failed. His support made me stronger, want to do better, and never give up. Thank you for always being available whenever I needed help. He is my role model for organizing the lab and safety awareness. If one day I have to manage my own lab, I would use what I have learned from this lab.

I would like to thank my dissertation committee, Dr. Katherine Borkovich and Dr. Patricia Manosalva for advice in my research throughout my PhD. I appreciate the guidance from both in my annual review.

I thank you Dr. Audrey Ah-Fong for teaching me *Phytophthora* transformation and helping in lab work. I thank you Amy Boyd who helps me with bioinformatics and encourages me to exercise, and Andrea Vu who shares my lab bench and always helps me to improve my English. I also thank other current and past lab members for providing a good working environment, including Carl Mendoza, Dr. Domingo Martínez-Soto, Nguyen Vo, Tim Harris, Dr. Jolly Shrivastava, Dr. Laetitia Poidevin, Dr. Meenakshi Kagda, Dr. Melania Abrahamian, and Dr. Michael Matson.

My greatest gratitude goes to my parents, my grandmothers and my family who always support me in every way. My special thanks go to Panu who always

shares conversations and gives me the best supports. I thank you Casey, my best yoga and cycling instructor, who always share positive energy. I thank Thanin who always shares conversations at the house. I also thank other Thai friends in Riverside: Jay, Olivia, Nicha, Nuttapon, Ardcha, Watit.

I thank you the Royal Thai Government and Kasetsart University for financial support.

Portions of the Introduction of this dissertation are adapted from an article published in the journal *Phytopathology* [Wiphawee Leesutthiphonchai, Andrea L. Vu, Audrey M. V. Ah-Fong, and Howard S. Judelson 2018]. The co-authors (Andrea L. Vu and Dr. Audrey M. V. Ah-Fong) listed in that publication co-wrote that article.

Chapter I of this dissertation is a reprint of material published in the journal *Molecular Plant-Microbe Interactions* [Wiphawee Leesutthiphonchai and Howard S. Judelson 2019].

Chapter II of this dissertation is a reprint of the material as it appeared in the journal *Molecular Microbiology* [Wiphawee Leesutthiphonchai and Howard S. Judelson 2018].

Portions of chapter III of this dissertation are a reprint of the material as it appeared in *Molecular Plant-Microbe Interactions* [Andrea L. Vu, Wiphawee Leesutthiphonchai, Audrey M. V. Ah-Fong, and Howard S. Judelson 2019]. The co-authors of that publication provided parts of the results.

ABSTRACT OF THE DISSERTATION

Regulation of Sporangia Development in *Phytophthora infestans*

by

Wiphawee Leesutthiphonchai

Doctor of Philosophy, Graduate Program in Plant Pathology
University of California, Riverside, June 2020
Dr. Howard Judelson, Chairperson

Phytophthora infestans causes the late blight disease of potato and tomato. Spores of *Phytophthora* are important for dissemination and causing infection. In this thesis, I studied several aspects of *Phytophthora* spore biology. (1) I performed RNA-seq of sporangia from rye media, potato leaflets, tomato leaflets, and potato tuber slices to investigate whether sporangia from artificial media and from plants are functionally equivalent. I found that sporangia from these different sources had only modest differences in transcriptional profiles, but showed similar infection potential using single-zoospore infection assays. This is an important piece of information indicating that spores from artificial media are good models for the natural situation. (2) I studied a MADS-box transcription factor to understand the regulation of sporangia development in *P. infestans*. MADS was shown to regulate many sporulation-induced genes, to act before previously known regulators, and to be regulated both at the transcriptional and post-translational levels. (3) I checked for potential artifacts associated with the

homology-based gene silencing method that is commonly used to study gene function in *Phytophthora.* Based on studies of two target genes, the *cis*-spread of silencing was frequently observed within 500 nt distance of the target gene; however, this did not occur in all transformants generated by the same silencing vector. This suggests that the expression of neighboring genes should be checked to ensure that phenotypes assigned to genes based on silencing data are reliable.

TABLE OF CONTENTS

LIST OF FIGURES

INTRODUCTION

CHAPTER I

CHAPTER II

CHAPTER III

Introduction

Over a hundred species of *Phytophthora* have been reported (Kroon et al. 2012) including many plant pathogens such as *P. ramorum* causing sudden oak death disease, *P. sojae* causing soybean root rot, and *P. infestans* causing late blight disease of potato and tomato. The disease caused by *P. infestans* was first documented in the United States in 1843 and later became notorious as a cause of the Irish potato famine in 1845 (Judelson 2014). Since then, *P. infestans* still threatens food security and causes an economic loss of around $10 billion annually (Haverkort et al. 2009).

The life and disease cycle of *P. infestans* is illustrated in Figure 1. *P. infestans* can reproduce sexually to yield oospores and asexually to produce sporangia (Judelson and Blanco 2005). The production of asexual sporangia predominates in nature. Asexual sporangia can directly germinate through a germ tube or indirectly, by producing about eight mononucleate zoospores. Zoospores are released within minutes under moist cool conditions. Using their two flagella, zoospores swim toward hosts and readily encyst on a plant surface. The zoospore cyst then extends a germ tube, and often forms an appressorium which penetrates the plant cell wall. This mode of infection is common on foliage, fruits, and stems. Infections also occur on tubers, typically through wounds or natural openings like stomata and lenticels (Judelson 2014). Since *P. infestans* is a hemibiotroph, it colonizes the living host cells and at later stage of infection,

host cells become necrotic. On a leaflet, *P. infestans* initially penetrates host epidermal cells, grows intercellularly and establishes haustoria in host cells, which may be important for nutrition. *P. infestans* then sporulates. Sporulation can occur within 3-4 days after infection under ideal conditions, with more than a thousand new sporangia emerging daily per lesion. Multiple infection cycles can spread disease rapidly through an entire field or a tuber storage facility (Fry et al. 2015).

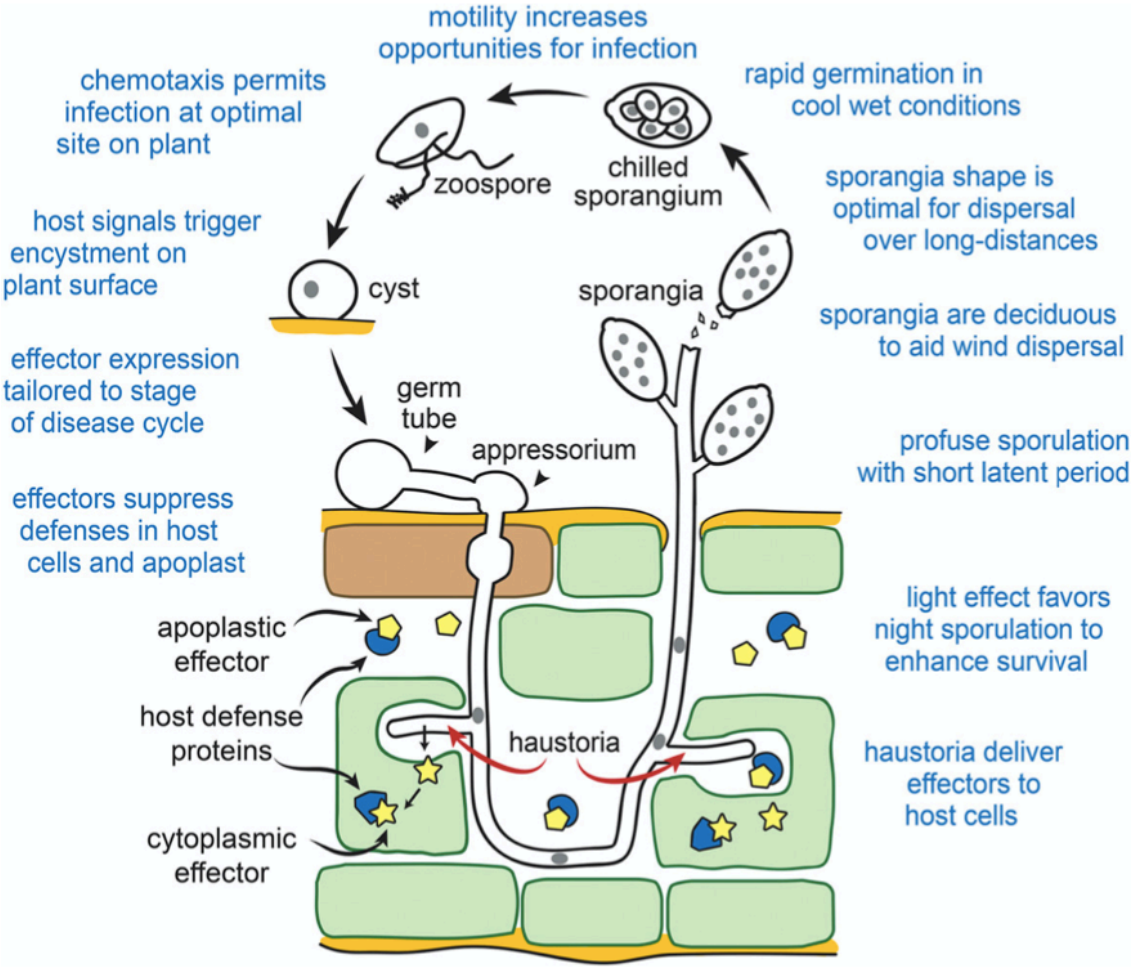

Fig. 1. Disease cycle of *P. infestans* on foliage, with features that contribute to its pathogenic success highlighted. (Leesutthiphonchai et al. 2018)

The first visible sign of sporangia formation are sporangiophores, which develop after a period of vegetative growth. Then, the sporangiophore extends its length while nuclei move along the sporangiophore. The tip of the sporangiophore expands to become a sporangium, followed by the movement of nuclei into sporangium. A septum forms at the base of the sporangium as it matures. The formation of sporangia occurs within 6-7 hours after sporangiophore development initiates (Maltese et al. 1995).

Environmental factors affect sporulation of *P. infestans*. Sporulation requires high humidity and is suppressed by light, and thus occurs at late night (Bashi et al. 1982; Xiang and Judelson 2014). This prevents sporangia from desiccation and UV damage (Mizubuti et al. 2000) since sporangia are hydrated and have no pigments. A fall in humidity, which is typical after sunrise, leads to the hygroscopic twisting of sporangiophores, which releases sporangia to the air (Granke et al. 2009; Hirst 1953). The elongated shape of sporangia aids dispersal, allowing movement up to 10-20 km in less than 3 hours (Aylor 2003; Roper et al. 2008).

Apart from environmental factors, sporulation is controlled by gene expression; however, what regulates sporulation remains to be explored in detail. RNA-seq of *P. infestans* life stages showed that > 4,000 genes were induced in sporangia compared to mycelia (Ah-Fong et al. 2017). More than one-third of these sporangia-induced genes were up-regulated > 100-fold. Over-represented among sporangia-induced genes were those encoding calcium-binding proteins,

signaling proteins, flagellar proteins, and others. The study by Ah-Fong et al also identified many transcription factors induced in sporangia, including a MADS-box transcription factor which is described in Chapter II of this thesis.

Only limited analysis of transcription factors involved in sporulation have been performed. Myb transcription factors are a large group of transcription factors in *P. infestans* and five Myb are induced during sporulation (Xiang and Judelson 2010). The expression of *Myb2R1* and *Myb2R3* mRNA increased 4 to 8 hours before sporulation whereas *Myb2R4* mRNA rose before the other genes, and then was reduced after sporulation started (Xiang and Judelson 2014). The silencing of *Myb2R3* reduced sporangia yield.

Other genes that were shown to be important for sporangia development include the Cdc14 protein phosphatase and G-protein β and γ subunits (Ah-Fong and Judelson 2003; Latijnhouwers and Govers 2003; van den Hoogen et al. 2018). Later in the thesis we describe a role for protein phosphatases in the function of the MADS-box transcription factor.

Overview of this study

In this dissertation, we provide more information about transcriptional regulation during sporangia development, highlight the importance of sporangia handling in laboratory, and demonstrate that homology-based silencing sometimes has off-target effects. This knowledge assists scientists toward

understanding *P. infestans* biology and eventually should help researchers devise new strategies for a disease control.

Chapter I demonstrates that sporangia from media and plants have subtly divergent transcription profiles but equivalent infection potential and aggressiveness. This was a valuable finding since it supports the validity of experiments using lab-raised sporangia. I performed RNA-seq of sporangia from rye media, potato leaflets, tomato leaflets, and potato tuber slices, using sporangia collected on the first and second major days of sporulation. Only modest differences in transcriptional profiles attributable to the sporangia source and the harvest timepoint were observed. Gene ontology (GO term) analysis showed that many of the differentially-expressed genes were related to metabolism. Single-zoospore infection assays showed that spores from artificial media and plant have the same infection potential.

Chapter II shows that a MADS-box transcription factor is an early regulator of *P. infestans* sporulation. It acts before previously published sporulation-associated regulators and controls a majority of sporulation-induced genes. RNA expression suggested that *MADS* mRNA is expressed during sporulation but absent in nonsporulating mycelia. Analysis of RNA-seq and sporangia production data showed *MADS* transcripts accumulate 24 hours before the development of sporangia. MADS protein is expressed during sporulation and remains until germination. MADS protein in zoospores is dephosphorylated, which suggests that MADS may interact with phosphatases such as Cdc14. MADS fused with

fluorescent tag was also shown to localize in nuclei of spores. Silencing experiment confirmed MADS regulates sporulation.

Chapter III emphasized technical aspects to improve silencing vector design and to investigate off-target effects. Using genes encoding an E2F transcription factor and the MADS-box protein as targets, it was found that silencing sometimes spreads to flanking genes. To better understand how often silencing spreads to unintended targets, several transformants of target genes were explored. The frequency of occurrence of the *cis*-spread of silencing diverged between strains, indicating that there is some randomness or transformant-specific variation in how silencing is imposed.

References

Ah-Fong, A.M.V., and Judelson, H.S. 2003. Cell cycle regulator Cdc14 is expressed during sporulation but not hyphal growth in the fungus-like oomycete *Phytophthora infestans*. Molecular Microbiology 50(2):487-494.

Ah-Fong, A. M., Kim, K. S., and Judelson, H. S. 2017. RNA-seq of life stages of the oomycete *Phytophthora infestans* reveals dynamic changes in metabolic, signal transduction, and pathogenesis genes and a major role for calcium signaling in development. BMC Genomics 18:198.

Aylor, D. E. 2003. Spread of plant disease on a continental scale: Role of aerial dispersal of pathogens. Ecology 84:1989-1997.

Bashi, E., Benjoseph, Y., and Rotem, J. 1982. Inoculum potential of *Phytophthora infestans* and the development of potato late blight epidemics. Phytopathology 72:1043-1047.

Blum, M., Waldner, M., and Gisi, U. 2010. A single point mutation in the novel PvCesA3 gene confers resistance to the carboxylic acid amide fungicide mandipropamid in *Plasmopara viticola*. Fungal Genet. Biol. 47:499-510.

Cai, M., Miao, J. Q., Song, X., Lin, D., Bi, Y., Chen, L., Liu, X. L., and Tyler, B. M. 2016. C239s mutation in the beta-tubulin of *Phytophthora sojae* confers resistance to zoxamide. Front. Microbiol. 7:762.

Davidse, L. C., Looijen, D., Turkensteen, L. J., and Vanderwal, D. 1981. Occurrence of metalaxyl-resistant strains of *Phytophthora infestans* in Dutch potato fields. Neth. J. Plant Pathol. 87:65-68.

Fry, W. E., Birch, P. R. J., Judelson, H. S., Grünwald, N. J., Danies, G., Everts, K. L., Gevens, A. J., Gugino, B. K., Johnson, D. A., Johnsone, S. B., McGrath, M. T., Myers, K. L., Ristaino, J. B., Roberts, P. D., Secor, G., and Smart, C. D. 2015. Five reasons to consider *Phytophthora infestans* a reemerging pathogen. Phytopathology 105:966-981.

Granke, L. L., Windstam, S. T., Hoch, H. C., Smart, C. D., and Hausbeck, M. K. 2009. Dispersal and movement mechanisms of *Phytophthora capsici* sporangia. Phytopathology 99:1258-1264.

Haverkort, A. J., Struik, P. C., Visser, R. G. F., and Jacobsen, E. 2009. Applied biotechnology to combat late blight in potato caused by *Phytophthora infestans*. Potato Res. 52:249-264.

Hirst, J. M. 1953. Changes in atmospheric spore content: Diurnal periodicity and the effects of weather. Trans. Br. Mycol. Soc. 36:375-393.

Judelson, H. S. 2014. *Phytophthora infestans*. In: R. Dean, A. Lichens-park and C. Kole (Ed.) Genomics of plant-associated fungi and oomycetes: dicot pathogens. Berlin Heidelberg: Springer, pp.175-208.

Judelson, H. S., and Blanco, F. A. 2005. The spore of *Phytophthora*: weapons of the plant destroyer. Nat. Rev. Microbiol. 3:47-58.

Judelson, H. S., Tyler, B. M., and Michelmore, R. W. 1991. Transformation of the oomycete pathogen, *Phytophthora infestans*. Mol Plan Micro Interac 4:602-607.

Kroon, L. P. N. M., Brouwer, H., de Cock, A. W. A. M., and Govers, F. 2012. The genus *Phytophthora* anno 2012. Phytopathology 102:348-364.

Leesutthiphonchai, W., Vu, A. L., Ah-Fong, A. M. V., and Judelson, H. S. 2018. How Does *Phytophthora infestans* Evade Control Efforts? Modern Insight Into the Late Blight Disease. Phytopathology 108:916-924.

Maltese, C. E., Conigliaro, G., and Shaw, D. S. 1995. The development of sporangia of *Phytophthora infestans*. Mycol. Res. 99:1175-1181.

Miao, J. Q., Cai, M., Dong, X., Liu, L., Lin, D., Zhang, C., Pang, Z. L., and Liu, X. L. 2016. Resistance assessment for oxathiapiprolin in *Phytophthora capsici* and the detection of a point mutation (G769G) in PcOrp1 that confers resistance. Front. Microbiol. 7:615.

Mizubuti, E. S. G., Aylor, D. E., and Fry, W. E. 2000. Survival of *Phytophthora infestans* sporangia exposed to solar radiation. Phytopathology 90:78-84.

Roper, M., Pepper, R. E., Brenner, M. P., and Pringle, A. 2008. Explosively launched spores of ascomycete fungi have drag-minimizing shapes. Proc. Natl. Acad. Sci. U.S.A. 105:20583-20588.

Xiang, Q. J., and Judelson, H. S. 2014. Myb transcription factors and light regulate sporulation in the oomycete *Phytophthora infestans*. PLoS One 9:e92086.

Chapter I

Phytophthora infestans sporangia produced in artificial media and plant lesions have subtly divergent transcription profiles but equivalent infection potential and aggressiveness

Abstract

Sporangia of the potato late blight agent *Phytophthora infestans* are often used in studies of pathogen biology and plant responses to infection. Investigations of spore biology can be challenging in oomycetes because their sporangia are physiologically active and change in response to environmental factors and aging. Whether sporangia from artificial media and plant lesions are functionally equivalent has been a topic of debate. To address these issues, we compared the transcriptomes and infection ability of sporangia from rye-sucrose media, potato and tomato leaflets, and potato tubers. Small differences were observed between the mRNA profiles of sporangia from all sources, including variation in genes encoding metabolic enzymes, cell-wall-degrading enzymes, and ABC transporters. Small differences in sporangia age also resulted in variation in the transcriptome. Taking care to use sporangia of similar maturity, we observed that those sourced from media or plant lesions had similar rates of zoospore release and cyst germination. There were also no differences in infection rates or aggressiveness on leaflets, based on single-spore inoculation assays. Such results are discordant with those of a recent publication in this

journal. Nevertheless, we conclude that sporangia from plant and media cultures are functionally similar and emphasize the importance of using “best practices” in experiments with sporangia to obtain reliable results.

Introduction

Asexual sporangia are made by most oomycete phytopathogens and play central roles in disease. Sporangia travel by wind or water to disseminate the pathogen and initiate infections (Leesutthiphonchai et al. 2018). Unlike conidia of most fungi, which are desiccated, oomycete sporangia are hydrated and physiologically active. This enhances infection potential by enabling sporangia to respond to germination-conducive conditions. For example, exposing sporangia to water triggers zoosporogenesis, in which major cytoplasmic and transcriptomic changes occur within minutes of the stimulus (Tani et al. 2004; Walker and van West 2007). The fact that sporangia are not desiccated makes them prone to damage from laboratory manipulations as well as natural environmental factors such as heat or light (Mizubuti et al. 2000). The ephemeral nature of sporangia and their rapid responses to environmental signals can make the acquisition of highly reproducible experimental results a challenge.

Many laboratories use sporangia produced in artificial media for studying oomycete biology, assessing the effectiveness of plant resistance genes, and characterizing host responses to infection. For example, we and others have employed cultures grown on a rye grain-based medium to study sporulation,

germination, zoospore motility, appressorium formation, and host colonization by wild-type and gene knock-down strains of *Phytophthora infestans*, the potato late blight pathogen (Ah- Fong et al. 2017a; Belhaj et al. 2017; Boevink et al. 2016; Gamboa-Meléndez et al. 2013; Haas et al. 2009; Latijnhouwers et al. 2004; Leesutthiphonchai and Judelson 2018). Sporangia from artificial media are also commonly used in assays of host resistance (Kirk et al. 2005; Naess et al. 2000). However, many researchers prefer to use sporangia produced on host tissue for experiments (Bradshaw et al. 2006; Foolad et al. 2014). Passage through the host may help eliminate deleterious mutations or establish epigenetic states that contribute to fitness. There may also be physiological differences between sporangia from plants and artificial media. Oomycete hyphae lack septa and their cytoplasm flows into sporangial initials during sporulation (Hardham and Hyde 1997). Therefore, proteins and mRNAs made during plant colonization may be deposited in sporangia, where they may later contribute to pathogenesis. Many defense-suppressing effectors and cell-wall-degrading enzymes are expressed by *P. infestans* primarily during plant infection (Ah-Fong et al. 2017b; Haas et al. 2009).

It was suggested recently that differences between *P. infestans* sporangia from artificial media compared with plant lesions may explain why some crop protection strategies that initially looked promising in laboratory assays failed upon further testing (Fry 2016). To explore that concept and test the validity of past research on *P. infestans* spore biology, we compared the transcriptomes

and infection potential of sporangia produced on artificial media, tomato and potato leaflets, and potato tubers. Taking precautions to ensure that the sporangia from each source were of equal age and harvested carefully, we found that the origin of sporangia had only subtle effects on their transcriptomes. We failed to observe differences in the abilities of sporangia generated in artificial media or in planta to cause infection. Our results conflict with those reported in a recent study by another laboratory (Fry et al. 2019).

Results

Strategy for collecting and handling sporangia

We believe that sporangia need to be treated with special care to allow their infection potential, transcriptome content, and other characteristics to be assessed accurately. This applies when comparing sporangia from cultures grown under different conditions or a parental strain with transformants that over-express or are silenced for a gene of interest. Although our detailed protocols for manipulating sporangia are documented in Materials and Methods, an overview is presented in the following paragraphs.

Our preferred method for obtaining sporangia from artificial media is to start by inoculating the entire surface of a rye-sucrose culture plate with sporangia. This leads to uniform hyphal growth, followed by sporulation. Depending on the amount of inoculum and incubation temperature (typically 18ºC), we start to observe a tiny number of new sporangia after approximately 5

days, which is recorded as day 0 in Figure 1A. Sporulation plateaus on day +3, with 70% of sporangia produced on days +1 and +2. The kinetics of sporulation obtained with this protocol match closely that obtained with zoospore-sprayed tomato leaflets, where most sporangia also appear on days +1 and +2 (Fig. 1A). These data were obtained using isolate 1306 but other isolates have yielded similar results.

Based on the literature, most laboratories obtain sporangia from plates inoculated with a plug from a stock culture. Cultures grown in this matter accrue sporangia over at least 6 days (Fig. 1A, dashed line). Many articles describe collecting sporangia after 10 to 14 days; the sporangia would thus range from approximately 1 to 10 days in age.

That age is an important variable is illustrated in Figure 1.1B, which shows the relative fraction of sporangia releasing zoospores (i.e., indirect germination) in isolates 1306 and 88069 after 3 h at 10ºC. Germination was highest in sporangia from cultures 4 to 5 days after inoculation but declined dramatically by day 14. We frequently observe up to 90% germination, which is similar to that reported for *P. infestans* by many other laboratories (Elsner et al. 1970; Latijnhouwers et al. 2004). It should be noted that germination rates in the literature may vary due to many factors, including the incubation conditions and when germination is assessed. Nevertheless, other researchers have also reported that zoospore release decreases in cultures that have aged over a time period similar to that shown in Figure 1.1B (King et al. 1968).

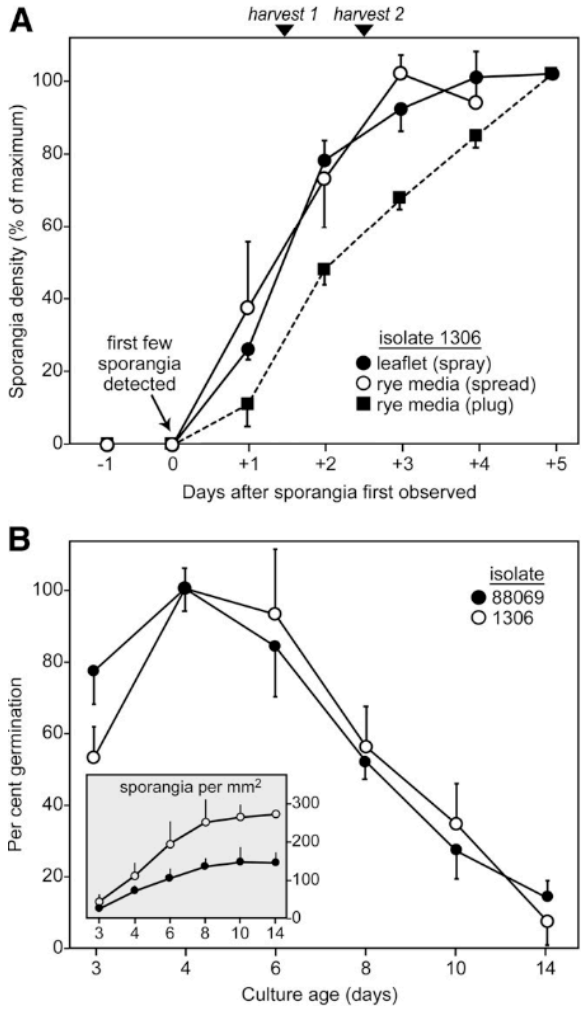

Fig. 1. Influence of age on sporulation and germination in *Phytophthora infestans*. **A**, Time-course of sporulation using isolate 1306. Sporangia were harvested from spray-inoculated tomato leaflets (black circles), rye-sucrose agar inoculated with a lawn of sporangia (open circles), or rye-sucrose agar inoculated with a plug (black squares). Time 0 is when a few sparse sporangia were first observed on leaflets or agar plates. Values are expressed as the percentage of maximum, which equaled 710 ± 69, 247 ± 25, and 331 ± 56 sporangia/mm^2 for the infected leaflet (day +5), spread-inoculated rye media (day +3), and plug-inoculated rye media samples (day +5), respectively. Error bars represent standard deviation of biological replicates. **B**, Effect of culture age on indirect germination. Indicated are the fractions of sporangia that had released zoospores 3 h after being placed in Petri's solution at 10ºC. Values are expressed relative to the maximum for each isolate, which equaled 82 and 71% germination for isolates 88069 and 1306, respectively, on day 4. Direct germination was not observed under the conditions of the experiment. The inset graph shows the density of sporangia at each timepoint in the cultures, which were inoculated with plugs.

We paid close attention to the methods used to harvest sporangia. We typically collect sporangia in a modified version of Petri's solution (0.25 mM $CaCl_2$, 1 mM $MgSO_4$, 1 mM KH_2PO_4, and 0.8 mM KCl; unadjusted pH is 4.9), which was first developed to stimulate sporulation and zoospore release from P. cambivora (Petri 1917). Sporangia are also diluted in this buffer when equalizing their concentrations for germination and infection assays. We have found that the use of the buffer reduces batch-to-batch variation in germination, possibly by equalizing pH or replenishing ions that leach from sporangia during harvesting. Dew on leaf surfaces is typically slightly acidic, and ion levels as well as pH both affect zoospore release (Byrt and Grant 1979; Halsall and Forrester 1977; Sato 1994b; Vanbruggen et al. 1987).

The swift harvesting of sporangia is also important because changes begin when they are placed in water. It may take 60 min for cytoplasmic reorganization to be visually evident but many zoosporogenesis-associated genes are induced within 20 min of exposure to cool water (Tani et al. 2004). Placing sporangia in water at room temperature also causes the abundance of some mRNAs to rise rapidly and others to fall (Tani et al. 2004). Our past attempts to block such changes by harvesting sporangia in high concentrations of actinomycin D (100 µg/ml) had only limited success, possibly because this transcriptional inhibitor slowly crosses the sporangial wall (Judelson and Roberts 2002). Instead, we rushed to harvest each batch of sporangia within 8 to 10 min. For RNA or protein analysis, this means that sporangia are washed from leaf or

culture plate surfaces, filtered to remove contaminating hyphae, concentrated by centrifugation, and flash-frozen within 10 min. Some researchers describe harvesting *P. infestans* sporangia by centrifugation at very high speeds (Fry et al. 2019) but we use the minimum possible (700 × g) because even moderate g-forces trigger rapid changes in most eukaryotic cells (Soto et al. 2007). Transcriptomes are influenced modestly by the source of sporangia.

We employed RNA-seq to compare sporangia from rye media, potato leaflets, tomato leaflets, and potato tuber slices using isolate 1306, with three biological replicates. We were careful to use sporangia of similar age and to harvest the sporangia rapidly. Samples were obtained from time points matching “harvest 1” and “harvest 2” in Figure 1.1A in order to represent sporangia on the first and second major days of sporulation. This corresponded to 4.5 and 5.5 days postinfection on plant tissue, and 6.5 and 7.5 days on rye-sucrose media. The sporangia were passed through a 50-µm mesh filter to eliminate hyphal fragments that may have been dislodged from the cultures. A minimum of 25 million 75-nucleotide (nt) single-end reads were then obtained from each replicate (Supplementary Table S1). Principal component analysis (PCA) identified fairly tight clustering of the replicates, with the least variation seen between those from rye-sucrose media (Fig. 2B).

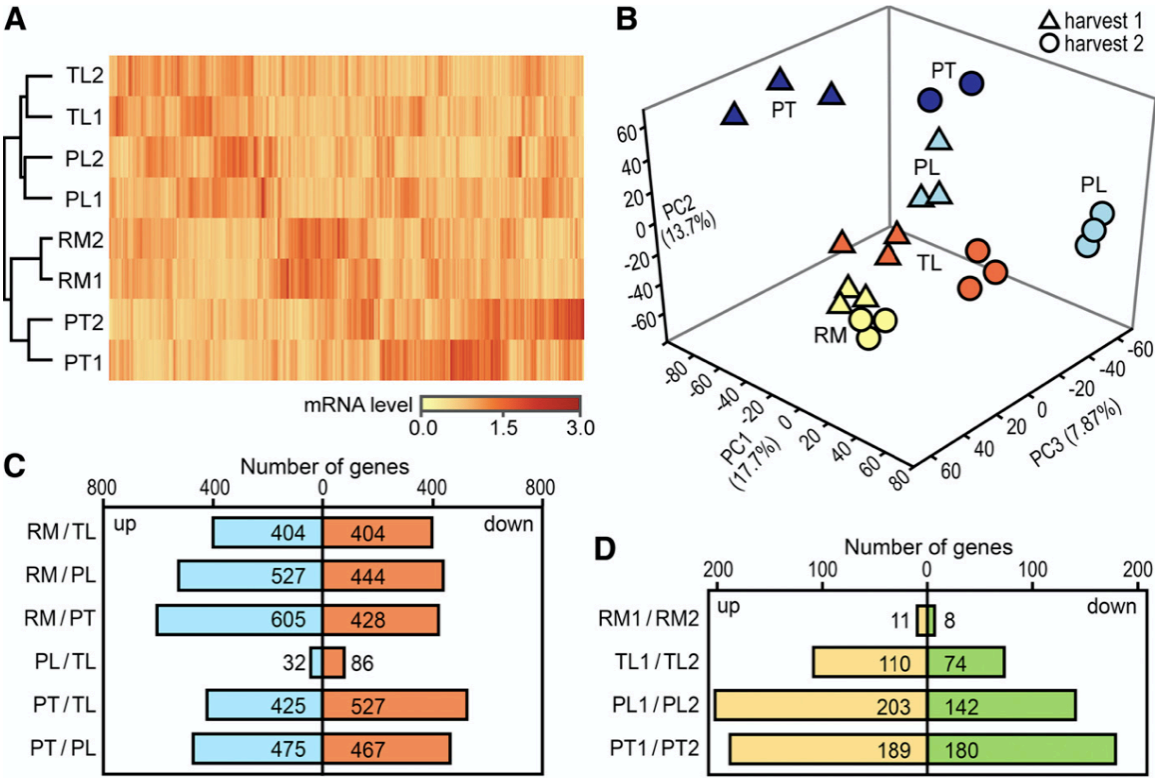

Fig. 2. mRNA levels in sporangia from different culture conditions. **A**, Heatmap representing mRNA from tomato leaflets (TL), potato leaflets (PL), rye-sucrose media (RM), and potato tubers (PT). Samples were taken at the harvest 1 and harvest 2 timepoints, representing sporangia on the first (e.g., TL1) and second (e.g., TL2) major days of sporulation. **B**, Principal component analysis of the RNA samples. Each symbol represents a biological replicate. **C**, Number of genes that were differentially expressed between culture conditions, based on thresholds of >twofold change and false discovery rate < 0.05 at the two timepoints. **D**, Number of genes differentially expressed between sporangia from the harvest 1 and harvest 2 timepoints; these timepoints correspond to 4.5 and 5.5 days postinfection on plant tissue and 6.5 and 7.5 days on rye-sucrose media.

We identified modest differences in mRNA profiles attributable to both the source of sporangia and the harvest date. This and subsequent analyses were limited to the 15,522 genes having counts per million mapped reads (CPM) > 1.0 in at least one condition. When pairwise comparisons were made of sporangia

from rye-sucrose media, potato leaflets, tomato leaflets, or potato tubers, an average of 804 genes or 5.2% of the total exhibited >twofold differences based on a Benjamini-Hochberg false discovery rate (FDR) threshold of 0.05. This variation is evident in the heatmap in Figure 2A and enumerated in Figure 2C. The fewest differences were between sporangia from potato and tomato leaflets. Expression values for the genes and differential expression statistics are shown in Supplementary Tables S2 and S3.

Although growth conditions (e.g., media versus leaflets) contributed most to the differences, age was also a factor. Although little variation was observed between the harvest 1 and harvest 2 sporangia from rye media, an average of 316 genes exhibited >twofold differences between timepoints in one or more of the leaflet and tuber samples (Fig. 2D). That differences would arise between the two timepoints is unsurprising because sporulation in planta occurs during the transition of *P. infestans* from biotrophy to necrotrophy, which would presumably alter the host environment. More age-specific differences were observed in the potato compared with tomato infections, which may reflect the fact that host necrosis with isolate 1306 is typically more extensive in potato than tomato.

The RNA-seq data were also used to scrutinize the quality of the sporangia samples. One check was to ensure that zoosporogenesis-specific genes had not been induced. This might have occurred if our harvesting protocol was slow, resulting in false positives in the differential expression studies. This inspection used several genes, including transporter gene PITG_13579, which is

induced rapidly when sporangia are placed in water (Fig. 3A). The two left-most lanes in Figure 3B show a similar experiment using RNA-seq, where chilling increased the fragments per kilobase of exon per million mapped reads (FPKM) value by at least 100-fold. The other lanes represent the 24 sporangia samples from rye media, potato and tomato leaflets, and potato tubers. None expressed much PITG_13579 mRNA, and similar results were obtained with other zoosporogenesis-induced genes, including PITG_13496, PITG_09169, and PITG_13170. This indicates that the transcriptomes of the 24 sporangia samples are representative of proper ungerminated sporangia, and helps confirm the fidelity of the differential expression data in Figure 2 and our supplementary tables.

A second quality-control check examined genes that are normally expressed at high levels during hyphal growth but are repressed during sporulation. If sporangia were contaminated with hyphal fragments or sporangiophores, then these genes would show a substantial signal in the RNA-seq data. In addition, if some samples had much higher signals than the others, that might mean that we had mistimed the two harvests. One gene used for this analysis was PITG_21410, which encodes elicitin-like protein INF4 (Jiang et al. 2006). The mRNA level of this gene declines in sporulating cultures and is very low in sporangia (Fig. 3C, left side). All 24 rye media, leaflet, and tuber samples exhibited very low levels of expression of this gene (Fig. 3C, right side). Similar results were obtained with other sporulation-repressed genes such as

PITG_09454 and PITG_12556. The finding that the signal was low in all samples supports the fidelity of the comparisons in Figure 2 and our supplementary tables.

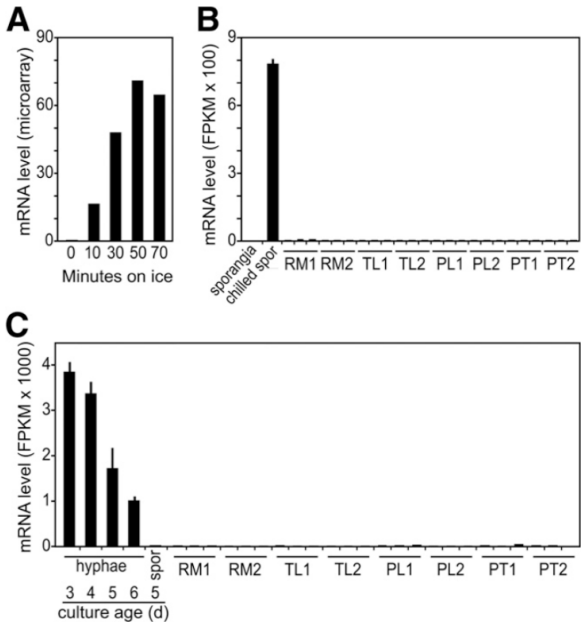

Fig. 3. Quality assessments of the 24 sporangia samples. **A**, Expression of zoosporogenesis-induced gene PITG_13579 in sporangia immediately after harvesting and after 10, 30, 50, and 70 min of chilling in modified Petri's solution. Data are based on microarray analysis. **B**, Abundance of PITG_13579 mRNA based on RNA-seq. The two left samples are freshly harvested sporangia and the same chilled for 0 and 60 min (chilled spor.). Samples labeled RM, TL, PL, and PT are sporangia from rye media, tomato leaflets, potato leaflets, and potato tubers, respectively, from harvest 1 and harvest 2; these timepoints correspond to 4.5 and 5.5 days postinfection on plant tissue and 6.5 and 7.5 days on rye-sucrose media. **C**, Abundance of PITG_21410 mRNA based on RNA-seq. The left side of the panel illustrates expression of the gene in hyphae collected from cultures between 3 and 6 days after inoculation, and sporangia from a 5-day culture. The right side of the panel shows expression in the 24 RM, TL, PL, and PT sporangia samples.

Metabolic functions predominate among differentially expressed genes

Gene ontology (GO term) analyses associated a limited number of functional categories with genes that were differentially expressed between sporangia sourced from media and any of the three types of plant lesions. Many of the differences between the plant and rye-sucrose media samples were related to metabolism. For example, overrepresented GO terms included oxidoreductase activity (GO:0016491, *P adjusted* [*Padj*] = 9e-4), tyrosine catabolism (GO:0006572, *Padj* = 7e-4), and glycosyl hydrolase activity (GO:0016798, *Padj* = 3e-2). A full list is shown in Supplementary Table S4.

Notable differences were seen for genes encoding enzymes that degrade plant cell walls (Fig. 4A). For example, the aggregate level (summed FPKM) of cutinase transcripts was much lower in rye-sucrose media and tubers than the two leaflet samples, which is logical because only the leaflets contain appreciable amounts of cutin. Also logical is our observation that sporangia from rye media contained higher levels of xylosidase mRNA, because rye grain is much richer in xylans than potato or tomato (Blaschek et al. 1981; Jarvis et al. 1981; Knudsen 2014).

A broader analysis of metabolism based on KEGG pathways (Aoki-Kinoshita and Kanehisa 2007) indicated that sporangia from rye-sucrose media clustered separately from the plant samples, with the potato and tomato leaflet samples clustering apart from tubers (Fig. 4B). This pattern had also been observed with total genes (Fig. 2A). Most pathways related to carbohydrate

metabolism such as glycolysis, the TCA cycle, and the pentose phosphate pathway had higher aggregate mRNA levels in sporangia from rye-sucrose media than from leaflets or tubers. This is likely because the concentration of soluble sugars is approximately five times higher in the rye-sucrose media (Judelson et al. 2009). There were also differences in other pathways, including cofactor, fatty acid, and amino acid metabolism. Several transporters were also differentially expressed such as nitrate transporters (PITG_09342 and PITG_25173) which exhibited approximately three times higher transcript levels on leaflets than rye media or tubers. This may be attributable to the fact that our plants were fertilized with nitrate, which is at low levels in tubers and rye-sucrose media (Abrahamian et al. 2016).

An analysis of genes traditionally associated with pathogenesis revealed that ABC transporters tended to have higher mRNA levels in sporangia from leaflets compared with rye-sucrose media. Such proteins are thought to participate in the efflux of toxins, including plant defense molecules (Perlin et al. 2014). The ratio of mRNA abundance in sporangia harvested from tomato leaflets versus rye-sucrose media was skewed toward higher expression in the leaflets (Fig. 4C), with average expression being 23% higher in the leaflets. Based on a *P* value threshold of 0.01, 22 ABC transporter genes had higher transcript levels in sporangia from tomato leaflets compared with artificial media. Similar results were obtained for sporangia from potato leaflets, while mRNA levels of ABC transporters in sporangia from media and potato tubers were

similar. Other genes potentially used to defend against chemical toxicants, such as those encoding catalases and peroxidases, were expressed at similar levels in all samples.

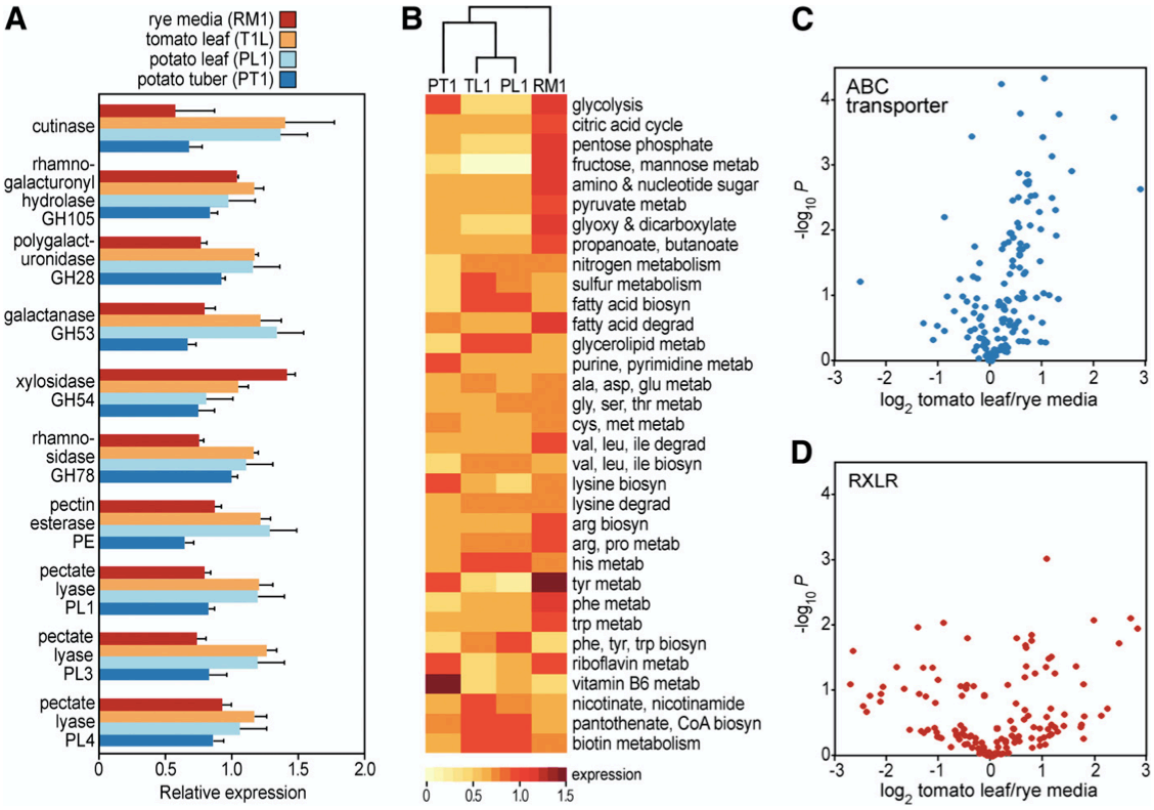

Fig. 4. Effect of sporangia source on mRNA levels of selected functional groups. **A**, Cell-wall-degrading enzymes. Sporangia were from harvest 1 tomato leaflets (TL1), potato leaflets (PL1), rye-sucrose media (RM1), and potato tubers (PT1). Fragments per kilobase of exon per million mapped reads levels of genes in each group were added together and normalized to the average of the group. Results from the harvest 2 sporangia (collected 5.5 days postinfection on plant tissue and 7.5 days postinoculation on rye-sucrose media) were similar. **B**, Metabolic pathways. Samples are the same as those in A, and expression levels were normalized to the average of each functional category. **C**, ABC transporters. Indicated are the ratios of mRNA for each gene in sporangia from tomato leaflets (TL1) versus rye media (RM1). **D**, Same as C but for RXLRs.

Few genes encoding RXLR proteins exhibited significant differential expression between the types of sporangia, based on analysis of the 200 genes that had CPM > 1 in any sample. A volcano plot of their transcript levels in tomato leaflets versus rye-sucrose media showed only three with higher mRNA in the leaflets at a $P < 0.01$ threshold (Fig. 4D). Only two RXLRs that were infection induced, PITG_05846 and PITG_06375, had higher mRNA in each of the three types of plant-derived sporangia compared with rye-sucrose. The horizontal dispersion of RXLR signals in the plot was wider than that of ABC trans- porters because many RXLR genes are up- or downregulated during sporulation, leading to greater statistical noise (Ah-Fong et al. 2017a).

Expressed at CPM > 1 in sporangia were 114 CRN genes. However, none of their mRNA levels were consistently higher in sporangia from a plant source compared with rye-sucrose media, although PITG_19565 was twofold higher in potato leaflets compared with media. Instead, CRN genes were more likely to exhibit higher mRNA levels in sporangia from media.

Transcript levels of genes associated with sporulation varied little between sporangia sourced from plants and media. This conclusion is based on the analysis of genes that encode proteins specific to the flagellar axoneme (Judelson et al. 2012). This is expected because inhibitor studies demonstrated that most zoospore proteins are preformed in sporangia and not translated during germination (Clark et al. 1978). Due to normal mRNA decay in aging sporangia, it was also not surprising that the transcript levels of most flagella-associated

genes were lower in harvest 2 versus the harvest 1 sporangia, because the latter tend to be younger. For example, genes encoding intraflagellar transport, basal body, and mastigoneme proteins exhibited median declines in mRNA of 7, 15, and 29%, respectively, between the timepoints. This decline highlights the importance of using sporangia of similar age in critical experiments. A prior study identified much greater differences in the mRNA levels of flagellar protein genes in sporangia from plants 6 days after infection than from artificial media cultures 12 days after inoculation (Fry et al. 2019). Although that study concluded that this meant that plant-sourced sporangia are more primed for indirect germination, our interpretation of their result is that it provides further proof of the importance of controlling for sporangia age in such experiments.

Sporangia size varies with their origin

The dimensions of *P. infestans* sporangia differed depending on their source. In particular, those generated on rye-sucrose media tended to be larger than those from potato or tomato leaflets, although the length/breadth ratio was not significantly different (Fig. 5). That growth conditions affect sporangial geometry has been reported previously for other members of the genus (Brasier and Griffin 1979). Based on concepts derived from mathematical modeling of fungal growth (Lew 2011), our observations suggest either that extensibility of the sporangial wall is greater on rye media compared with on plants or that cytoplasm flows faster into sporangial initials formed on media.

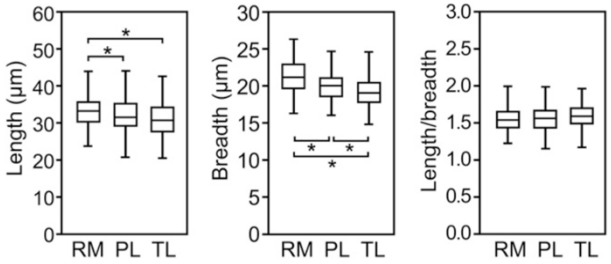

Fig. 5. Sporangia shapes from rye-sucrose media (RM), potato leaflets (PL), and tomato leaflets (TL). Values are based on a minimum of 200 sporangia per sample at the harvest 1 timepoint (4.5 days postinfection on plant tissue and 6.5 days postinoculation on media). Variation was assessed using a paired t test, and pairs differing at $P < 0.01$ are marked by an asterisk.

Spores from all sources have the same infection potential

The dissimilarities in the shapes and transcriptomes of sporangia from media and plant lesions were modest but might signal that propagules from different sources would vary in their infection ability. This was tested by comparing sporangia of isolate 1306 from rye-sucrose media with those from lesions on potato leaflets. To begin, sporangia of the same age were harvested from the two sources in parallel. Indirect germination was then stimulated using cold modified Petri's solution. After 3 h, zoospores were separated from sporangia by filtration through 15-µm mesh and diluted to 100 zoospores/ml, and individual leaflets were inoculated with a single drop bearing 1 zoospore. This was repeated in three separate experiments, using 100 leaflets per treatment per experiment, which after inoculated leaflets were positioned in a plant growth chamber using a randomized complete block design. Materials were rotated daily to ensure that the leaflets were exposed to equivalent light and humidity.

The results from these single-zoospore infection assays indicated that the infection potential of spores from plants and artificial media were equivalent (Fig. 6A and B). There was no significant difference based on one-way analysis of variance and Wilcoxon signed-rank tests. The average infection potential of each zoospore was 32%, which is in the range described for *P. nicotianae* (Kong and Hong 2016). The average infection rate varied in our single-zoospore experiments from 10 to 58%, which we believe is due to differences in the age of the plants. Infection assays performed using five zoospores per inoculum drop also resulted in similar rates of infection by the media and leaflet-sourced spores, although these experiments were less informative because close to 100% of leaflets were often infected.

The source of spores also had no significant effect on the pace of lesion expansion. This conclusion is based on measurements taken between 5 and 8 days postinfection in the three single-zoospore experiments (Fig. 6C). Moreover, the total amount of sporangia produced on the leaflets by day 8 was similar regardless of whether the inoculum was from leaflets or artificial media (Fig. 6D). Therefore, similar aggressiveness was exhibited by sporangia from both sources.

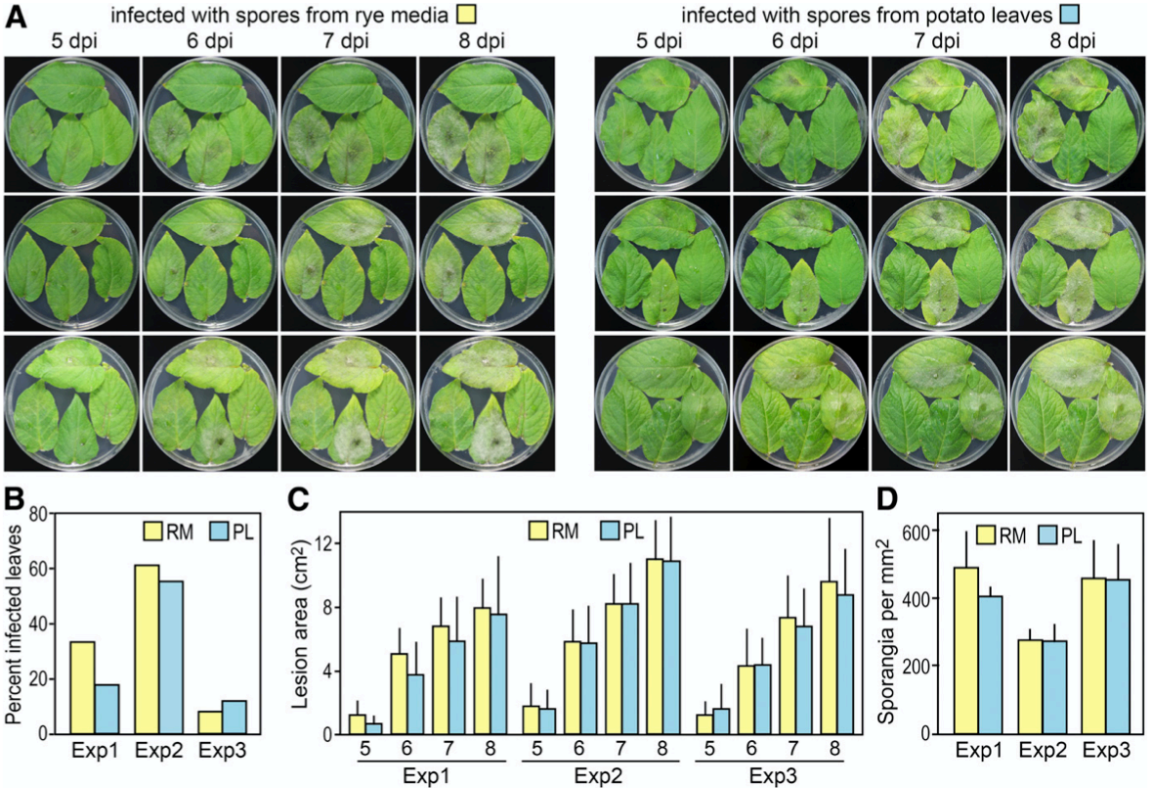

Fig. 6. Infection assays using zoospores from rye-sucrose media (RM) or potato leaflets (PL). **A**, Representative infected leaflets. Each row illustrates the same four leaflets between 5 and 8 days postinfection (dpi). In total, 100 leaflets were used per treatment per experiment. **B**, Percentage of leaflets showing infection in three independent experiments. **C**, Average size of lesions in each experiment. **D**, Sporangial density on infected leaflets.

Because foliage infections are usually initiated by sporangia, we also attempted to assess whether sporangia from plants and rye-sucrose media had similar infection potentials. This involved placing a droplet of water containing a single sporangium on each of multiple leaflets, which were placed at 10ºC for 4 h to trigger zoosporogenesis and then incubated at 18ºC in a plant growth chamber. Excluding cases where the inoculum drop appeared to have run off the leaflet, close to 100% of leaflets became infected. Because the rate of

colonization was so high, we cannot exclude the possibility that miniscule differences may exist in the infection potential of sporangia from plants and media but such small differences may not be biologically relevant.

Sporangia from plants and artificial media germinate at similar rates

Although the rates of zoosporogenesis of the two types of sporangia were not quantified precisely in the plant infection experiments described above, they appeared similar based on microscopic examination. Several additional studies confirmed that zoosporogenesis progresses similarly in plant and media-sourced sporangia.

In the first experiment, we quantified zoospore release from isolates 1306 and 88069. This used sporangia that had been harvested from tomato leaflets and media 6 days after inoculation. With both strains, the source of sporangia had little if any effect on germination based on observations made 2 and 12 h after chilling the spores (Fig. 7A). For example, after 12 h, 76 ± 10 and 69 ± 5% of sporangia from isolate 1306 sourced from tomato leaflets and rye-sucrose media had germinated, respectively. Because zoospores from plant and media were shown above to have similar infection potentials, it follows that the same should hold for sporangia.

A second study also compared the germination of sporangia obtained from tomato leaflets, potato leaflets, and media, this time using only isolate 1306 (Fig. 7B). This experiment also evaluated sporangia harvested 5, 6, and 8 days

after inoculation. Based on observations made 3 and 6 h after chilling, the source of sporangia had little effect on germination. This provides further support to the hypothesis that growing *P. infestans* on a plant does confer upon its sporangia a higher infection potential. It is interesting that the 5- and 8-day sporangia germinated at similar rates in this study, whereas germination was impaired in the older cultures in the Figure 1B experiment. We believe that this is because the cultures in Figure 1B were plug inoculated, whereas those in Figure 7B were initiated by spreading sporangia. Because hyphal growth is dense in plug-inoculated cultures, sporangia germination may be influenced by concentrations of nutrients or waste products in the underlying media. This observation stresses the importance of preparing sporangia under standardized conditions.

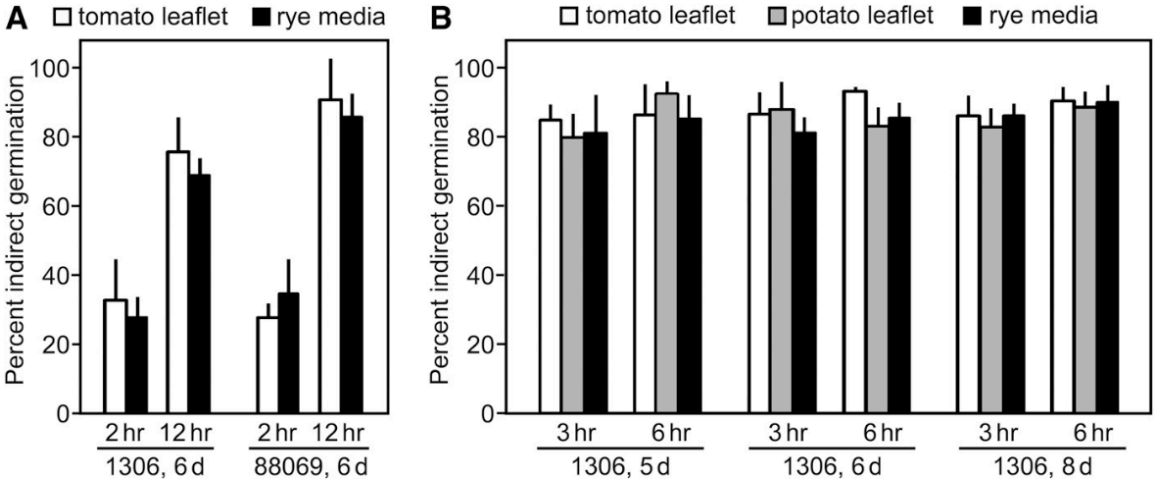

Fig. 7. Germination rates of sporangia. **A**, Indirect germination of isolates 1306 and 88069 measured 2 and 12 h after sporangia were cold treated. Sporangia were harvested from 6-day tomato leaflets or rye-sucrose cultures (inoculated by spreading with sporangia). Concentrations adjusted to 10^4 sporangia/ml prior to the cold treatment. **B**, Indirect germination of sporangia from isolate 1306 grown on tomato leaflets, potato leaflets, and spread-inoculated rye-sucrose media. Measurements were made 3 and 6 h after the cold treatment, using sporangia harvested 5, 6, and 8 days after inoculation.

We also measured the germination of cysts derived from the plant- and media-sourced zoospores used in the infection assays shown in Figure 6. This involved placing aliquots of the zoospores in clarified rye-sucrose broth to trigger encystment and germination. The cyst germination rates in the three experiments in Figure 6 averaged 69 and 78% for sporangia from rye-sucrose media and leaflets, respectively. Although the difference was not significant (P = 0.13), the trend toward higher germination in the plant-sourced material was interesting.

Discussion

This study had two principal goals. One was to test whether sporangia from artificial media and plants were functionally equivalent. We conclude that the source of sporangia has a small effect on their transcriptomes but little or no impact on infection potential, germination, or pathogenic fitness. A second objective was to stress the importance of following “best practices” for handling sporangia. Not all experiments need to follow an exacting protocol but attention should be paid to the age of sporangia and how they treated during harvesting and germination. Marker genes that can indicate the purity, maturity, and germination status of sporangia were also described.

We are not the first to observe the finicky nature of *P. infestans* sporangia. For example, Sato (1994a) found that indirect germination varied depending on how long sporangia were allowed to mature after sporulation. After speculating that germination depended on the source of water in which sporangia were

placed, he showed that pH and small differences in ion concentration influenced germination (Sato 1994b). This helps to explain why we believe that germination occurs more reliably in Petri's solution than water. Many laboratories germinate sporangia in deionized water (Boevink et al. 2016; Foolad et al. 2014; Fry et al. 2019) but this is an unnatural environment because leaf surfaces contain ions exuded from plant cells (Tukey 1970).

The extent of variation in the mRNA content of sporangia from artificial media compared with plant lesions was slight yet interesting, with an average of approximately 800 genes (4.4% of the total) exhibiting >twofold differences. We consider this to be a small number because, by comparison, 40 and 55% of genes were shown to vary by >twofold between mycelia and sporangia and between sporangia and chilled sporangia, respectively (Ah-Fong et al. 2017a). Because hyphae from plant tissues express more pathogenesis-promoting proteins such as RXLRs than do hyphae from artificial media, we had originally hypothesized that such factors would be inherited by plant-sourced sporangia and provide an advantage during early infection. However, this was not supported by our results. Nevertheless, we did see differences related to metabolism and possibly toxin efflux. Some of this could be attributed to the composition of the growth substrate such as the types and concentrations of cell wall glucans and soluble sugars. To understand such differences more fully, it would be necessary to study gene expression in hyphae, which was beyond the scope of this study.

As the writing of our manuscript was being completed, another laboratory reported using RNA-seq to compare *P. infestans* sporangia from plants and media (Fry et al. 2019). Sporangia from plug-inoculated rye-pea agar cultures after 12 days of growth were compared with sporangia from potato leaflets at 6 days postinfection. Approximately one-third of expressed genes (4,791 genes) were described as being >two- fold differentially expressed between plant and media-sourced sporangia, which is 5.9 times more than in our analysis. Sporangia from plants were also reported to germinate >10-fold more than those from media, and to produce larger lesions on leaves. In contrast, our studies identified no differences in these characters. Several factors may explain the discrepancies. For example, the plant and media-sourced sporangia used in their RNA-seq study were very different in age, although we were careful to use sporangia of equal maturity. In addition, their germination assays were performed in water instead of Petri's solution, and different isolates, artificial media, and protocols for collecting sporangia were used. Our plant-sourced sporangia had also passed through plant tissue once, whereas they usually used two rounds of infection.

Although our study failed to repeat the findings of the other study, we do not dispute that passage through a host may be beneficial. Reports that the phenotypes of *Phytophthora* strains can change during culture go back at least 100 years (Rosenbaum 1917). The isolate used for most of our experiments, 1306, is diploid based on genome-wide counts of allele ratios (Matson 2018).

However, many isolates of *P. infestans* exist in apparently unstable polyploid or aneuploid states which, in addition to point mutations, may cause variation in fitness (Li et al. 2017; Matson et al. 2015). Fitness may also change due to mitotic crossing-over, gene conversion, and epigenetic phenomena (Chamnanpunt et al. 2001; Lamour et al. 2012; Shrestha et al. 2016). Isolates may also acquire viruses which could affect phenotype (Cai et al. 2019). Passage through a plant may help eliminate some of these potentially deleterious features.

Despite the reputed variability of *P. infestans*, we do not believe that the species accumulates point mutations at unusually high rates. Based on the analysis of strains that have been serially propagated over five or more years and then subjected to Illumina sequencing, we calculate that approximately 10^{-8} changes occur per nucleotide per nuclear division. This is nearly identical to the mutation rates reported for human germline cells and *Arabidopsis thaliana*, which are approximately 1.4×10^{-8} and 7×10^{-7}, respectively (Acuna-Hidalgo et al. 2016; Watson et al. 2016). We calculate that two nucleotide changes may occur in genes during the growth of *P. infestans* across a 100-mm culture plate.

In summary, we agree with other researchers that changes in fitness (pathogenic or otherwise) can occur during the long-term cultivation of a pathogen. This phenomenon is well described in *P. infestans* (Hodgson and Sharma 1967) and is not unique to oomycetes or phytopathogens (Maury et al. 2017). Nevertheless, because we did not detect evidence of significant short-

term effects resulting from cultivation in rye-sucrose media, studies of sporangia and other preinfection stages from media should yield results that are representative of the natural situation. This assumes that the delicate spore life stages are handled with appropriate care to avoid experimental artifacts. A more important question is whether results from one isolate of *P. infestans* can be extrapolated to others because much intraspecies diversity exists in traits relevant to disease such as host species preference, optimal temperature for spore germination, chemical sensitivity, and sexuality (Danies et al. 2013; Matson et al. 2015; Zhu et al. 2016). Isolate-specific transposons or chromosomal abnormalities may also increase the background mutation rate.

Materials and methods

Strains and culture conditions

P. infestans strain 1306 was isolated from tomato in San Diego County, CA. Subsequent laboratory tests indicated that it is equally pathogenic to potato. The isolate was stored in liquid nitrogen, thawed, and then transferred approximately 10 times before being used for the experiments in this article. Isolate 88069 was isolated from potato in the Netherlands and provided by F. Govers. For routine cultures, plates were inoculated with a plug from an older plate and incubated at 18ºC on rye-sucrose agar (rye A) in the dark (Caten and Jinks 1968). For the RNA-seq and sporulation time-course experiments, the plates were subjected to a cycle of 12 h of light and 12 h of darkness along with

the plant material. For sporulation measurements on plates, the cultures were either plug inoculated or spread with sporangia. The latter involved distributing 10^3 to 10^4 sporangia (in modified Petri's solution) per 100-mm plate with a bent glass rod. Plates were sealed in plastic boxes, which maintained relative humidity above 95% based on digital hygrometers. For some experiments described in the text, plates were viewed with a dissecting microscope to learn when sporangia began.

Sporangia were harvested from culture plates by pouring modified Petri's solution on top of each plate (10 ml for a 100-mm plate), followed by rubbing with a bent glass rod. Hyphal fragments were removed by filtration through 50-µm nylon mesh. Concentrations of sporangia were determined using a hemocytometer. If sporangia needed to be concentrated or pelleted, they were centrifuged at 700 × g in a swinging-bucket rotor for 4 min.

Zoosporogenesis was induced by placing sporangia at 10^4/ml in modified Petri's solution at 10ºC. This involved filling a plastic tub with ice, placing a 6.3 mm thick sheet of acrylic on top of the ice, and then inverting a second tub on top. Temperature throughout the chamber was monitored using thermometers, which indicated that the air above the acrylic sheet became equilibrated to 10ºC. Dishes containing sporangia were then placed on the acrylic sheet. Aliquots were removed at the times noted in Results and viewed under a microscope to assess indirect germination rates, basing measurements on a minimum of 100 sporangia.

Plant colonization

Infections were performed using leaflets of tomato cultivar Pieralbo, leaflets of potato cultivar Russet Burbank, or russet tubers purchased locally. Plant materials were surface sterilized using dilute bleach for 5 min, washed twice in sterile water, blotted dry, and stored for 1 h before use. Leaflets were placed on 0.6% water agar plates in a sealed clear box with moist paper towels. Tuber slices were placed on a metal rack 8 mm above moist paper towels in the same type of box. This maintained the relative humidity between 95 and 98% based on a digital hygrometer. For general infections of leaflets and tubers, each was inoculated on their top surfaces with five drops of 15 µl of sporangia (2.5×10^4 sporangia/ml). Inoculated tubers were incubated in the dark at 18ºC. Leaflets were incubated at 18ºC with a cycle of 12 h of darkness and 12 h of light, using cool-white fluorescent lamps which provided an intensity of 95 µmoles/m^2/s at the leaf surface.

For assessing the infection potential of zoospores from different sources, the adaxial side of each leaflet was inoculated with a single zoospore in 10 µl of modified Petri's solution and incubated in the same way. Zoospores for this application were purified away from sporangia using a 15-µm nylon mesh filter. After inoculation, the infected materials were positioned in the incubator using a randomized complete block design and rotated daily. Starting on day 5, photographs were taken daily and later used to measure lesion sizes using

Adobe Photoshop. At the end of the experiment, sporangia were washed from the leaflets and counted.

RNA analysis

For RNA-seq analysis, sporangia were produced from rye-sucrose agar, infected leaflets, or infected tubers inoculated as described above. The sporangia were then harvested in modified Petri's solution by 30 s of gentle rubbing with a glass rod (agar plates) or vortexing (plant material). The liquid was then passed through a 50-µm nylon mesh, and the sporangia were pelleted at 700 × g for 4 min at room temperature. Care was taken to freeze the sporangia in liquid nitrogen within 10 min of adding Petri's solution. After grinding the tissues under liquid nitrogen, RNA was isolated using the Spectrum Plant Total RNA kit from Sigma.

Indexed libraries for RNA-seq were prepared using the Illumina TruSeq kit and sequenced using an Illumina NextSeq 500, obtaining single-end 75-nt reads. These were filtered and mapped to the *P. infestans* genome using Bowtie 2.2.5 and Tophat 2.0.14, allowing for one mismatch per read (Langmead et al. 2009). Expression and differential expression calls were made with edgeR using TMM normalization, a generalized linear model, and FDR calculations based on the Benjamini- Hochberg method (Robinson et al. 2010). One of the three biological replicates from the harvest 2 tubers was omitted from this analysis because it appeared to be an outlier, apparently due to bacterial growth on the tuber.

Hierarchical clustering, heatmap generation, and PCA were performed using Partek Genomics Suite. GO term enrichment analysis was performed using the GOHyperGAll script (Horan et al. 2008). Analyses of metabolism used functional assignments obtained using a reannotation of the *P. infestans* genome (Kagda 2017), in which enzymes were assigned to pathways based on the KEGG classification scheme (Aoki-Kinoshita and Kanehisa 2007). Expression comparisons entailed adding together the FPKM values of genes with the same function (generally by Enzyme Commission number), and then aggregating the FPKM of all genes encoding all enzymes in each KEGG pathway.

Microarray studies were performed on custom Affymetrix arrays. These were prepared and hybridized with RNA probes, as described (Randall et al. 2005). RNA samples came from sporangia that were harvested from strain 88069 and chilled at 4ºC for the times indicated in Results.

Calculation of mutation rates

After single-nuclear purification through the zoospore stage, independent lineages of isolate 1306 were established and grown for 20 serial transfers on 60-mm cultures of rye-sucrose agar. DNA extracted from the early and terminal stages of each lineage was then used for sequencing, obtaining 50-nt paired-end data to approximately 60-fold coverage using an Illumina HiSeq 2500. The data were then analyzed using the Var-Seq pipeline implemented in systemPipeR (Backman and Girke 2016). In brief, this involved filtering and

alignment to the reference genome using BWA, and the use of GATK (McKenna et al. 2010) to identify sequence polymorphisms. Because *P. infestans* is diploid, only cases where the sequences of the lineages were entirely different or a homozygote changed to a heterozygote (or vice versa) could be scored. We estimate that each lineage had undergone between 162 and 332 nuclear divisions, based on a measurement of the increase in nuclei during growth across a 60-mm culture plate and the doubling time of nuclei determined in a previous study (Ah Fong and Judelson 2003). In comparisons of three lineages, on average, 1,015 single-nucleotide variants were identified per lineage, which corresponds to approximately 10^{-8} changes per nucleotide per nuclear division. This may be an underestimate because some deleterious mutations would be lost during propagation.

Acknowledgements

We thank A. Vu and J. Shrivastava for sharing data. We also would like to thank *Molecular Plant-Microbe Interactions* for letting us use the manuscript as a part of this dissertation. The original article can be found at: https://doi.org/10.1094/MPMI-12-18-0349-TA.

References

Abrahamian, M., Ah-Fong, A. M., Davis, C., Andreeva, K., and Judelson, H. S. 2016. Gene expression and silencing studies in *Phytophthora infestans* reveal infection-specific nutrient transporters and a role for the nitrate reductase pathway in plant pathogenesis. PLoS Pathog. 12: e1006097.

Acuna-Hidalgo, R., Veltman, J. A., and Hoischen, A. 2016. New insights into the generation and role of de novo mutations in health and disease. Genome Biol. 17:241.

Ah Fong, A. M., and Judelson, H. S. 2003. Cell cycle regulator Cdc14 is expressed during sporulation but not hyphal growth in the fungus-like oomycete *Phytophthora infestans*. Mol. Microbiol. 50:487-494.

Ah-Fong, A. M., Kim, K. S., and Judelson, H. S. 2017a. RNA-seq of life stages of the oomycete *Phytophthora infestans* reveals dynamic changes in metabolic, signal transduction, and pathogenesis genes and a major role for calcium signaling in development. BMC Genomics 18:198.

Ah-Fong, A. M. V., Shrivastava, J., and Judelson, H. S. 2017b. Lifestyle, gene gain and loss, and transcriptional remodeling cause divergence in the transcriptomes of *Phytophthora infestans* and *Pythium ultimum* during potato tuber colonization. BMC Genomics 18:764.

Aoki-Kinoshita, K. F., and Kanehisa, M. 2007. Gene annotation and pathway mapping in KEGG. Methods Mol. Biol. 396:71-91.

Backman, T. W. J., and Girke, T. 2016. systemPipeR: NGS workflow and report generation environment. BMC Bioinf. 17:388.

Belhaj, K., Cano, L. M., Prince, D. C., Kemen, A., Yoshida, K., Dagdas, Y. F., Etherington, G. J., Schoonbeek, H. J., van Esse, H. P., Jones, J. D. G., Kamoun, S., and Schornack, S. 2017. Arabidopsis late blight: Infection of a nonhost plant by *Albugo laibachii* enables full colonization by *Phytophthora infestans*. Cell. Microbiol. 19:e12628.

Blaschek, W., Haass, D., Koehler, H., and Franz, G. 1981. Cell-wall regeneration by *Nicotiana tabacum* protoplasts - chemical and biochemical aspects. Plant Sci. Lett. 22:47-57.

Boevink, P. C., Wang, X., McLellan, H., He, Q., Naqvi, S., Armstrong, M. R., Zhang, W., Hein, I., Gilroy, E. M., Tian, Z., and Birch, P. R. J. 2016. A *Phytophthora infestans* RXLR effector targets plant PP1c isoforms that promote late blight disease. Nat. Commun. 7:10311.

Bradshaw, J. E., Bryan, G. J., Lees, A. K., McLean, K., and Solomon- Blackburn, R. M. 2006. Mapping the R10 and R11 genes for resistance to late blight (*Phytophthora infestans*) present in the potato (*Solanum tuberosum*) R-gene differentials of black. Theor. Appl. Genet. 112:744-751.

Brasier, C. M., and Griffin, M. J. 1979. Taxonomy of *Phytophthora palmivora* on cocoa. Trans. Br. Mycol. Soc. 72:111-143.

Byrt, P., and Grant, B. R. 1979. Some conditions governing zoospore production in axenic cultures of *Phytophthora cinnamomi* Rands. Aust. J. Bot. 27:103-115.

Cai, G., Myers, K., Fry, W. E., and Hillman, B. I. 2019. *Phytophthora infestans* RNA virus 2, a novel RNA virus from *Phytophthora infestans*, does not belong to any known virus group. Arch. Virol. 164:567-572.

Caten, C. E., and Jinks, J. L. 1968. Spontaneous variability of single isolates of *Phytophthora infestans*. I. Cultural variation. Can. J. Bot. 46:329-348.

Chamnanpunt, J., Shan, W.-X., and Tyler, B. M. 2001. High frequency mitotic gene conversion in genetic hybrids of the oomycete *Phytophthora sojae*. Proc. Natl. Acad. Sci. U.S.A. 98:14530-14535.

Clark, M. C., Melanson, D. L., and Page, O. T. 1978. Purine metabolism and differential inhibition of spore germination in *Phytophthora infestans*. Can. J. Microbiol. 24:1032-1038.

Danies, G., Small, I. M., Myers, K., Childers, R., and Fry, W. E. 2013. Phenotypic characterization of recent clonal lineages of *Phytophthora infestans* in the united states. Plant Dis. 97:873-881.

Elsner, P., VanderMolen, G., Horton, J. C., and Bowen, C. C. 1970. Fine structure of sporangia of *Phytophthora infestans* during sporangial differentiation and germination. Phytopathology 60:1765-1772.

Foolad, M. R., Sullenberger, M. T., Ohlson, E. W., and Gugino, B. K. 2014. Response of accessions within tomato wild species, *Solanum pimpinellifolium* to late blight. Plant Breed. 133:401-411.

Fry, W. E. 2016. *Phytophthora infestans*: New tools (and old ones) lead to new understanding and precision management. Annu. Rev. Phytopathol. 54:529-547.

Fry, W. E., Patev, S. P., Meyers, K. L., Bao, K., and Fei, Z. 2019. *Phytophthora infestans* sporangia produced in culture and on tomato leaflet lesions

show marked differences in indirect germination rates, aggressiveness, and global transcription profiles. Mol. Plant-Microbe Interact. 32:515-526.

Gamboa-Meléndez, H., Huerta, A. I., and Judelson, H. S. 2013. bZIP transcription factors in the oomycete *Phytophthora infestans* with novel DNA-binding domains are involved in defense against oxidative stress. Eukaryot. Cell 12:1403-1412.

Haas, B. J., Kamoun, S., Zody, M. C., Jiang, R. H., Handsaker, R. E., Cano, L. M., Grabherr, M., Kodira, C. D., Raffaele, S., Torto-Alalibo, T., Bozkurt, T. O., Ah-Fong, A. M., Alvarado, L., Anderson, V. L., Armstrong, M. R., Avrova, A., Baxter, L., Beynon, J., Boevink, P. C., Bollmann, S. R., Bos, J. I., Bulone, V., Cai, G., Cakir, C., Carrington, J. C., Chawner, M., Conti, L., Costanzo, S., Ewan, R., Fahlgren, N., Fischbach, M. A., Fugelstad, J., Gilroy, E. M., Gnerre, S., Green, P. J., Grenville-Briggs, L. J., Griffith, J., Gru¨nwald, N. J., Horn, K., Horner, N. R., Hu, C. H., Huitema, E., Jeong, D. H., Jones, A. M., Jones, J. D., Jones, R. W., Karlsson, E. K., Kunjeti, S. G., Lamour, K., Liu, Z., Ma, L., Maclean, D., Chibucos, M. C., McDonald, H., McWalters, J., Meijer, H. J., Morgan, W., Morris, P. F., Munro, C. A., O'Neill, K., Ospina- Giraldo, M., Pinzo´n, A., Pritchard, L., Ramsahoye, B., Ren, Q., Restrepo, S., Roy, S., Sadanandom, A., Savidor, A., Schornack, S., Schwartz, D. C., Schumann, U. D., Schwessinger, B., Seyer, L., Sharpe, T., Silvar, C., Song, J., Studholme, D. J., Sykes, S., Thines, M., van de Vondervoort, P. J., Phuntumart, V., Wawra, S., Weide, R., Win, J., Young, C., Zhou, S., Fry, W., Meyers, B. C., van West, P., Ristaino, J., Govers, F., Birch, P. R., Whisson, S. C., Judelson, H. S., and Nusbaum, C. 2009. Genome sequence and analysis of the Irish potato famine pathogen *Phytophthora infestans*. Nature 461:393-398.

Halsall, D. M., and Forrester, R. I. 1977. Effects of certain cations on the formation and infectivity of *Phytophthora* zoospores. 1. Effects of calcium, magnesium, potassium, and iron ions. Can. J. Microbiol. 23:994-1001.

Hardham, A. R., and Hyde, G. J. 1997. Asexual sporulation in the oomycetes. Adv. Bot. Res. 24:353-398.

Hodgson, W. A., and Sharma, K. P. 1967. Restoration of virulence of stored cultures of *Phytophthora infestans*. Can. J. Plant Sci. 47:447-449.

Horan, K., Jang, C., Bailey-Serres, J., Mittler, R., Shelton, C., Harper, J. F., Zhu, J. K., Cushman, J. C., Gollery, M., and Girke, T. 2008. Annotating genes of known and unknown function by large-scale coexpression analysis. Plant Physiol. 147:41-57.

Jarvis, M. C., Hall, M. A., Threlfall, D. R., and Friend, J. 1981. The polysaccharide structure of potato cell walls: Chemical fractionation. Planta 152:93-100.

Jiang, R. H., Tyler, B. M., Whisson, S. C., Hardham, A. R., and Govers, F. 2006. Ancient origin of elicitin gene clusters in *Phytophthora* genomes. Mol. Biol. Evol. 23:338-351.

Judelson, H. S., and Roberts, S. 2002. Novel protein kinase induced during sporangial cleavage in the oomycete *Phytophthora infestans*. Eukaryot. Cell 1:687-695.

Judelson, H. S., Shrivastava, J., and Manson, J. 2012. Decay of genes encoding the oomycete flagellar proteome in the downy mildew *Hyaloperonospora arabidopsidis*. PLoS One 7:e47624.

Judelson, H. S., Tani, S., and Narayan, R. D. 2009. Metabolic adaptation of *Phytophthora infestans* during growth on leaves, tubers and artificial media. Mol. Plant Pathol. 10:843-855.

Kagda, M. 2017. Insight into the dynamic metabolism of *Phytophthora infestans*. Ph.D. thesis, University of California, Riverside.

King, J. E., Colhoun, J., and Butler, R. D. 1968. Changes in the ultrastructure of sporangia of *Phytophthora infestans* associated with indirect germination and aging. Trans. Br. Mycol. Soc. 154:1794-1804.

Kirk, W. W., Abu-El Samen, F. M., Muhinyuza, J. B., Hammerschmidt, R., Douches, D. S., Thill, C. A., Groza, H., and Thompson, A. L. 2005. Evaluation of potato late blight management utilizing host plant resistance and reduced rates and frequencies of fungicide applications. Crop Prot. 24:961-970.

Knudsen, K. E. B. 2014. Fiber and nonstarch polysaccharide content and variation in common crops used in broiler diets. Poult. Sci. 93: 2380-2393.

Kong, P., and Hong, C. 2016. Soil bacteria as sources of virulence signal providers promoting plant infection by *Phytophthora* pathogens. Sci. Rep. 6: Article 33239.

Lamour, K. H., Mudge, J., Gobena, D., Hurtado-Gonzales, O. P., Schmutz, J., Kuo, A., Miller, N. A., Rice, B. J., Raffaele, S., Cano, L. M., Bharti, A. K., Donahoo, R. S., Finley, S., Huitema, E., Hulvey, J., Platt, D., Salamov, A., Savidor, A., Sharma, R., Stam, R., Storey, D., Thines, M., Win, J., Haas, B. J., Dinwiddie, D. L., Jenkins, J., Knight, J. R., Affourtit, J. P., Han, C. S.,

Chertkov, O., Lindquist, E. A., Detter, C., Grigoriev, I. V., Kamoun, S., and Kingsmore, S. F. 2012. Genome sequencing and mapping reveal loss of heterozygosity as a mechanism for rapid adaptation in the vegetable pathogen *Phytophthora capsici*. Mol. Plant-Microbe Interact. 25:1350-1360.

Langmead, B., Trapnell, C., Pop, M., and Salzberg, S. L. 2009. Ultrafast and memory-efficient alignment of short DNA sequences to the human genome. Genome Biol. 10:R25.

Latijnhouwers, M., Ligterink, W., Vleeshouwers, V. G. A. A., van West, P., and Govers, F. 2004. A Ga subunit controls zoospore motility and virulence in the potato late blight pathogen *Phytophthora infestans*. Mol. Microbiol. 51:925-936.

Leesutthiphonchai, W., and Judelson, H. S. 2018. A MADS-box transcription factor regulates a central step in sporulation of the oomycete *Phytophthora infestans*. Mol. Microbiol. 110:562-575.

Leesutthiphonchai, W., Vu, A. L., Ah-Fong, A. M. V., and Judelson, H. S. 2018. How does *Phytophthora infestans* evade control efforts? Modern insight into the late blight disease. Phytopathology 108:916-924.

Lew, R. R. 2011. How does a hypha grow? The biophysics of pressurized growth in fungi. Nat. Rev. Microbiol. 9:509-518.

Li, Y., Shen, H., Zhou, Q., Qian, K., van der Lee, T., and Huang, S. 2017. Changing ploidy as a strategy: The Irish potato famine pathogen shifts ploidy in relation to its sexuality. Mol. Plant-Microbe Interact. 30:45-52.

Matson, M. E. H. 2018. A chromosome-scale reference assembly facilitates new insights into fungicide sensitivity and genome plasticity in *Phytophthora infestans*. Ph.D. thesis, University of California, Riverside.

Matson, M. E. H., Small, I. M., Fry, W. E., and Judelson, H. S. 2015. Metalaxyl resistance in *Phytophthora infestans*: Assessing role of Rpa190 gene and diversity within clonal lineages. Phytopathology 105: 1594-1600.

Maury, M. M., Chenal-Francisque, V., Bracq-Dieye, H., Han, L., Leclercq, A., Vales, G., Moura, A., Gouin, E., Scortti, M., Disson, O., Va´zquez-Boland, J. A., and Lecuit, M. 2017. Spontaneous loss of virulence in natural populations of Listeria monocytogenes. Infect. Immun. 85:e00541-e17.

McKenna, A., Hanna, M., Banks, E., Sivachenko, A., Cibulskis, K., Kernytsky, A., Garimella, K., Altshuler, D., Gabriel, S., Daly, M., and DePristo, M. A.

2010. The Genome Analysis Toolkit: A MapReduce framework for analyzing next-generation DNA sequencing data. Genome Res. 20:1297-1303.

Mizubuti, E. S. G., Aylor, D. E., and Fry, W. E. 2000. Survival of *Phytophthora infestans* sporangia exposed to solar radiation. Phytopathology 90:78-84.

Naess, S. K., Bradeen, J. M., Wielgus, S. M., Haberlach, G. T., McGrath, J. M., and Helgeson, J. P. 2000. Resistance to late blight in *Solanum bulbocastanum* is mapped to chromosome 8. Theor. Appl. Genet. 101:697-704.

Perlin, M. H., Andrews, J., and Toh, S. S. 2014. Essential letters in the fungal alphabet: ABC and MFS transporters and their roles in survival and pathogenicity. Adv. Genet. 85:201-253.

Petri, L. 1917. Research on morphology and biology of *Blepharospora cambivora parasitica* from chestnut. Atti R. Accad. Lincei 26:297-299 (in Italian).

Randall, T. A., Dwyer, R. A., Huitema, E., Beyer, K., Cvitanich, C., Kelkar, H., Fong, A. M., Gates, K., Roberts, S., Yatzkan, E., Gaffney, T., Law, M., Testa, A., Torto-Alalibo, T., Zhang, M., Zheng, L., Mueller, E., Windass, J., Binder, A., Birch, P. R. J., Gisi, U., Govers, F., Gow, N. A. R., Mauch, F., van West, P., Waugh, M. E., Yu, J., Boller, T., Kamoun, S., Lam, S. T., and Judelson, H. S. 2005. Large-scale gene discovery in the oomycete *Phytophthora infestans* reveals likely components of phytopathogenicity shared with true fungi. Mol. Plant- Microbe Interact. 18:229-243.

Robinson, M. D., McCarthy, D. J., and Smyth, G. K. 2010. edgeR: A Bioconductor package for differential expression analysis of digital gene expression data. Bioinformatics 26:139-140.

Rosenbaum, J. 1917. Studies of the genus *Phytophthora*. Proc. Natl. Acad. Sci. U.S.A. 3:159-163.

Sato, N. 1994a. Maturation of sporangia of *Phytophthora infestans* affecting the rapidity of indirect germination. Ann. Phytopathol. Soc. Jpn. 60:53-59.

Sato, N. 1994b. Effect of some inorganic salts and hydrogen ion concentration on indirect germination of the sporangia of *Phytophthora infestans*. Ann. Phytopathol. Soc. Jpn. 60:441-447.

Shrestha, S. D., Chapman, P., Zhang, Y., and Gijzen, M. 2016. Strain specific factors control effector gene silencing in *Phytophthora sojae*. PLoS One 11:e0150530.

Soto, T., Núñez, A., Madrid, M., Vicente, J., Gacto, M., and Cansado, J. 2007. Transduction of centrifugation-induced gravity forces through mitogen-activated protein kinase pathways in the fission yeast *Schizosaccharomyces pombe*. Microbiology 153:1519-1529.

Tani, S., Yatzkan, E., and Judelson, H. S. 2004. Multiple pathways regulate the induction of genes during zoosporogenesis in *Phytophthora infestans*. Mol. Plant-Microbe Interact. 17:330-337.

Tukey, H. B. J. 1970. The leaching of substances from plants. Annu. Rev. Plant Physiol. Plant Mol. Biol. 21:305-324.

Vanbruggen, A. H. C., Osmeloski, J. F., and Jacobson, J. S. 1987. Effects of simulated acidic mist on germination of *Alternaria solani* and *Phytophthora infestans* in vitro and their infection efficiency and sporulation on potato. Phytopathology 77:564-570.

Walker, C., and van West, P. 2007. Zoospore development in the oomycetes. Fungal Biol. Rev. 21:10-18.

Watson, J. M., Platzer, A., Kazda, A., Akimcheva, S., Valuchova, S., Nizhynska, V., Nordborg, M., and Riha, K. 2016. Germline replications and somatic mutation accumulation are independent of vegetative life span in *Arabidopsis*. Proc. Natl. Acad. Sci. U.S.A. 113:12226-12231.

Zhu, W., Shen, L. L., Fang, Z. G., Yang, L. N., Zhang, J. F., Sun, D. L., and Zhan, J. 2016. Increased frequency of self-fertile isolates in *Phytophthora infestans* may attribute to their higher fitness relative to the A1 isolates. Sci. Rep. 6: Article 29428.

Chapter II

A MADS-box transcription factor regulates a central step in sporulation of the oomycete *Phytophthora infestans*

Abstract

MADS-box transcription factors play significant roles in eukaryotes, but have not yet been characterized in oomycetes. Here, we describe a MADS-box protein from *Phytophthora infestans*, which causes late blight of potato. *P. infestans* and most other oomycetes express a single MADS-box gene. *PiMADS* is not transcribed during vegetative growth, but is induced early during asexual sporulation. Its mRNA levels oscillate in response to light, which suppresses sporulation. The protein was not detected in nonsporulating mycelia, but was found in sporulating mycelia and spores. Both mRNA and protein levels decline upon spore germination. A similar expression pattern as well as nuclear localization was observed when the protein was expressed with a fluorescent tag from the native promoter. Gene silencing triggered by a construct expressing 478 nt of MADS sequences indicated that *PiMADS* is required for sporulation but not hyphal growth or plant colonization. A comparison of wild type to a silenced strain by RNA-seq indicated that *PiMADS* regulates about 3000 sporulation-associated genes, and acts before other genes previously shown to regulate sporulation. Analysis of the silenced strain also indicated that the native gene was not

transcribed while the transgene was still expressed, which contradicts current models for homology-dependent silencing in oomycetes.

Introduction

Spores are important for the dispersal, infection and survival of many prokaryotic and eukaryotic microbes. A general trend is for asexual sporulation to occur in response to environmental cues, such as nutrition, light, humidity or temperature (Dahlberg and Van Etten 1982; Park and Yu 2012). Such inputs typically set into motion cascades of gene expression that culminate in spore formation. The transcriptional networks that mediate spore formation can be complex. For example, conidiation in *Aspergillus nidulans* is controlled by multiple transcription factors including both activators and repressors (Lee et al. 2016). Even in bacterial systems, spore formation involves the sequential action of multiple regulators (Kovacs 2016).

Research in recent decades has increased our understanding of the molecular events involved in sporulation in the eukaryotic microbes known as oomycetes, especially in the genus *Phytophthora*. For example, transcriptome studies have identified many spore-specific genes (Judelson et al. 2008; Ah-Fong et al. 2017). However, only a few genes that regulate sporulation have been identified. Understanding sporulation is important since oomycetes cause many economically significant dis- eases, in which spores play key roles in dissemination and host infection. The process of sporulation in *Phytophthora*

infestans, the cause of the potato late blight disease, resembles that of many oomycetes. In cultures or plant lesions that reach maturity, sporangiophores emerge from aerial mycelia (Blanco and Judelson 2005). This occurs only under high humidity and is regulated by light (Xiang and Judelson 2014). Nuclei move from mycelia into the sporangiophore, undergo mitosis and transit into terminal swellings destined to become multinucleate sporangia. A basal plug then delimits the sporangium from the sporangiophore. Oomycetes are otherwise aseptate, unlike most fungi where septa divide vegetative cells from cell types that are intermediate to spores. *Phytophthora* sporangia usually germinate by releasing mononucleate zoospores. This involves the cold-triggered cleavage of sporangial cytoplasm into multiple biflagellated zoospores, which swim toward a host, encyst and form germ tubes. At higher temperatures, germ tubes often emerge directly from sporangia.

A few genes that affect sporulation have been identified in *Phytophthora infestans* such as Cdc14 phosphatase (Ah Fong and Judelson 2003; Ah-Fong and Judelson 2011a), G-protein β and γ subunits (Latijnhouwers and Govers 2003; van den Hoogen et al. 2018) and a Myb transcription factor (Xiang and Judelson 2014). The roles in sporulation of Cdc14, G_{β} and G_{γ} were demonstrated through homology-based gene silencing experiments in which sense, antisense or hairpin constructs matching part of the target gene were expressed in transformants. This method was shown to trigger heterochromatinization and the transcriptional quiescence of the native and transgene, and appears to involve a

transient transmissible small RNA signal (Van West et al. 1999; Judelson and Tani 2007; van West et al. 2008).

Prior studies identified several transcription factors that are induced during sporulation in *P. infestans*, including the MADS-box transcription factor *PiMADS* (Ah-Fong et al. 2017). MADS-box proteins occur in nearly all eukaryotes, where they regulate a broad spectrum of cellular processes, such as flower development (Smaczniak et al. 2012), muscle formation (Mughal et al. 2015), and fungal cell wall biosynthesis (Rocha et al. 2016). The MADS-box domain participates in DNA-binding and dimerization, and differences in the C-terminal of region of the domain have been used to classify such proteins as either type I (SRF, human serum response factor) or type II (MEF2, myocyte enhancer factor 2).

To help illuminate the mechanisms that regulate sporulation in *P. infestans*, here we present a detailed analysis of *PiMADS*. The abundance of its mRNA and protein increase during sporulation and decline upon germination, and the protein localizes to nuclei. Silencing experiments indicated that *PiMADS* is essential for sporulation, acts upstream of most sporulation-induced genes but downstream of the light-responsive step, and is not required for growth, spore germination or plant infection. An unexpected finding was that the silencing-inducing transgene was still transcribed in *PiMADS*-silenced strains, which suggests that processes of homology-based silencing may be more diverse than previously thought in oomycetes.

Results and discussion

P. infestans encodes a type II MADS-box protein

A single match to a MADS-box gene was identified in a search of the *P. infestans* genome database (Haas et al. 2009). Gene PITG_07059, referred to hereafter as *PiMADS*, is predicted to encode a protein of 433 amino acids having the domain organization portrayed in Fig. 1A. Eighty-six amino acids at the N-terminus matched the MEF2-like MADS-box domain (Conserved Domain Database accession cd00265, $E = 10^{-36}$), with a weaker hit to the SRF-like domain (cd00266, $E = 10^{-25}$). Phylogenetic analysis was also consistent with *PiMADS* belonging to the MEF2-like lineage (Supporting Information Fig. S1). The C-terminal region of the *P. infestans* protein, which in other taxa serves as the activation domain and contributes to ternary complex formation (Molkentin et al. 1996; Masiero et al. 2002), had a weak match to a microtubule-binding protein domain (pfam10243, $E = 10^{-3}$). This might be a spurious hit since a similar match was observed in some but not all *Phytophthora* orthologs. Consistent with its predicted function as a transcription factor, PiMADS protein was predicted to have an N-terminal nuclear localization signal by SeqNLS (score of 0.904; Lin and Hu 2013) and NucPred (score of 0.87; Brameier et al. 2007), and a C-terminal signal by cNLS Mapper (score of 10.3; Kosugi et al. 2009). These programs identified nuclear localization signals in the same regions of MEF2 proteins from human and *Drosophila melanogaster*.

While *Phytophthora* spp. each encode one MADS-box protein (Supporting Information Fig. S1), larger families have been reported for most other species. Database searches indicate that fungi, animals and plants typically express about two, five and > 100 MADS proteins respectively. Interestingly, while one ortholog was detected in each of all peronosporalean and saprolegnian oomycetes that were examined (*Albugo, Aphanomyces*, *Hyaloperonospora*, *Phytophthora*, *Pythium* and *Saprolegnia*), proteins with MADS-box domains were not detected in other members of the stramenopile group (=heterokonts; Derelle et al. 2016). These included the putative basal member of the group, *Blastocystis hominis*, the pelagophyte *Aureococcus anophagefferens*, the brown alga *Ectocarpus siliculosus*, and the diatoms *Thalassiosira pseudonana* and *Phaeodactylum tricornutum*. The absence of MADS-box proteins from the latter species was reported previously (Thiriet-Rupert et al. 2016). Most alveolates, which bear weak taxonomic affinity with stramenopiles, encode only single or no MADS-box proteins as exemplified by the ciliate *Tetrahymena thermophila* and the apicomplexan *Plasmodium falciparum* respectively.

PiMADS **is induced early during sporulation**

RNA-seq of time courses on rye-sucrose media and tomato leaves indicated that *PiMADS* transcripts begin to accumulate about 24 h prior to the development of sporangia. On rye media in the dark, sporangia began to appear when cultures were 4–4.5 days old, while *PiMADS* mRNA started to rise at about

3–3.5 days (Fig. 1B). A similar trend was seen in rye media cultures exposed to a 12 h light/dark cycle, with *PiMADS* mRNA spiking at the end of each dark cycle (Fig. 1B). This can be explained by the fact that light suppresses sporulation, with more new sporangia made in the dark than the light period (Xiang and Judelson 2014). A similar pattern was seen in infected tomato leaves incubated in a light/ dark cycle, with sporangia and mRNA levels showing more of an increase after the dark incubation period than after the illuminated phase (Fig. 1C).

Transcript levels measured in different life stages in another experiment were also consistent with the involvement of *PiMADS* in spores (Fig. 1D). This compared mRNA levels in purified sporangia, sporangia chilled to initiate the cleavage of their sporangia into zoospores, motile zoospores, encysted zoospores producing germ tubes and nonsporulating and sporulating mycelia; the latter two are analogous to the 2.5 and 6 day timepoints in Fig. 1B. *PiMADS* mRNA was largely absent from non-sporulating mycelia, present at the highest levels in sporangia, and declined in zoospores and germinating cysts.

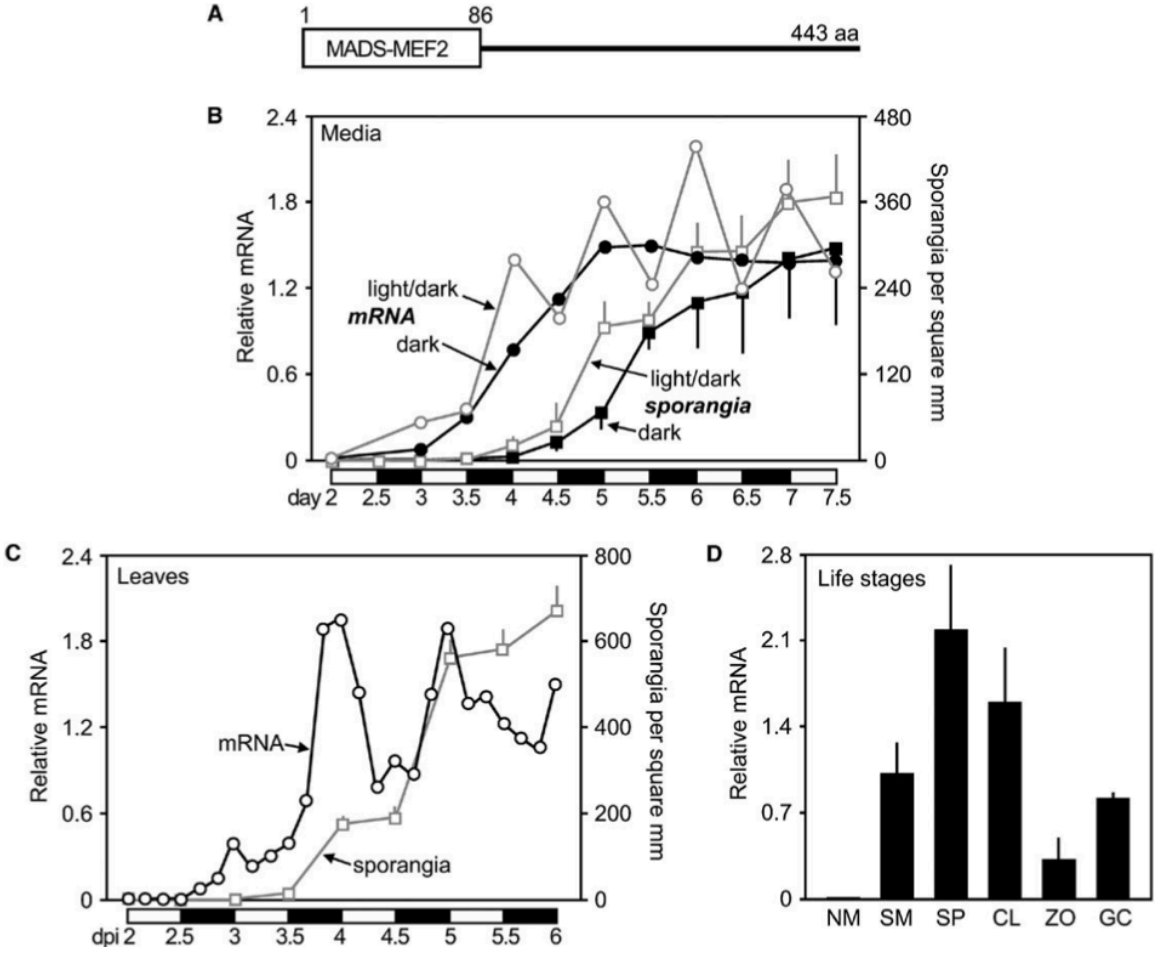

Fig. 1. Structure and expression pattern of *PiMADS*. **A,** Domain organization of PiMADS protein showing N-terminal MADS-box domain. **B,** Timecourse of wild-type *P. infestans* grown on rye-sucrose agar media. Circles indicate per-gene normalized levels of *PiMADS* mRNA determined by RNA-seq in cultures incubated in the dark (filled circles) or a 12 h light/dark cycle (open circles). Squares denote sporangia density in cultures grown in the dark (filled squares) or a light/dark cycle (open squares). The timing of the cycles are indicated below the x-axis. **C,** Levels of *PiMADS* mRNA (open circles) and sporangia (open squares) during tomato leaf infection. **D,** Levels of *PiMADS* mRNA in 3 day cultures (nonsporulating mycelia, NM), 6 day cultures (sporulating mycelia, SM), sporangia (SP), sporangia chilled to initiate cytoplasmic cleavage and zoosporogenesis (CL), zoospores (ZO) and zoospore cysts germinated in water for 6 h (GC).

These results suggest that *PiMADS* is involved in sporulation, or in a later stage such as zoosporogenesis; the latter is possible since studies with actinomycin D and cycloheximide showed that zoospore proteins are preformed in sporangia (Clark et al. 1978; Judelson and Roberts 2002). *PiMADS* mRNA is apparently induced after the light-regulated step of sporulation. A reasonable hypothesis is that a cryptochrome regulates a transcription factor that induces *PiMADS*, since cryptochromes are the only known photoreceptor protein made by *P. infestans* (Xiang and Judelson 2014). Genes acting downstream of *PiMADS* would also be expected to exhibit a light-regulated pattern of expression. This resembles the situation in *Botrytis cinerea*, where a MADS-box transcription factor mediates the transcription of light-responsive genes (Zhang et al. 2016).

PiMADS protein is expressed during sporulation and remains until germination

Antibodies were raised against PiMADS to allow its protein to be quantified during the life cycle. Considering that the transition between sporangia, zoospores, cysts and germinated cysts can take less than 3 h, one cannot assume that RNA and protein levels will always change in concert. To test this, two antibodies (anti-MADS1 and anti-MADS2) were generated using peptides from the C-terminus of the protein.

In western blots, anti-MADS1 detected no band in nonsporulating mycelia, and a 65 kDa band in unchilled sporangia and chilled sporangia (Fig. 2A). In the latter sample, a weak 63 kDa band could also be seen in short exposures of the blot. In zoospores and cysts, only the 63 kDa band was detected, and this mostly disappeared in germinated cysts. When sporangia were placed in broth media to stimulate direct germination, the 65 kDa band was mostly gone by 4 h.

The shift between the 65 and 63 kDa bands was seen in multiple Western blots and does not appear to be a gel artifact. Note that the image in Fig. 2A was cut to remove empty lanes between the chilled sporangia and zoospores. However, the shift was also seen in other blots probed with anti-MADS1 and with anti-MADS2 (Fig. 2B). Other proteins, such as cryptochrome did not show a mobility shift between lanes or heterogeneity within the same lane. The small shift in mobility may be due to a post-translational modification. This would be consistent with a high-throughput study of phosphopeptides in *P. infestans* that identified phosphorylation at amino acids 393 and 395 (Resjo et al. 2014). Other MADS-box proteins are known to undergo modifications that include phosphorylation (Gregoire et al. 2006). To test whether the mobility shift was in fact due to altered phosphorylation, protein from sporangia was treated with lambda phosphatase (Fig. 2D). This reduced the 65 kDa band to 63 kDa, which matched the size of the protein in zoospores.

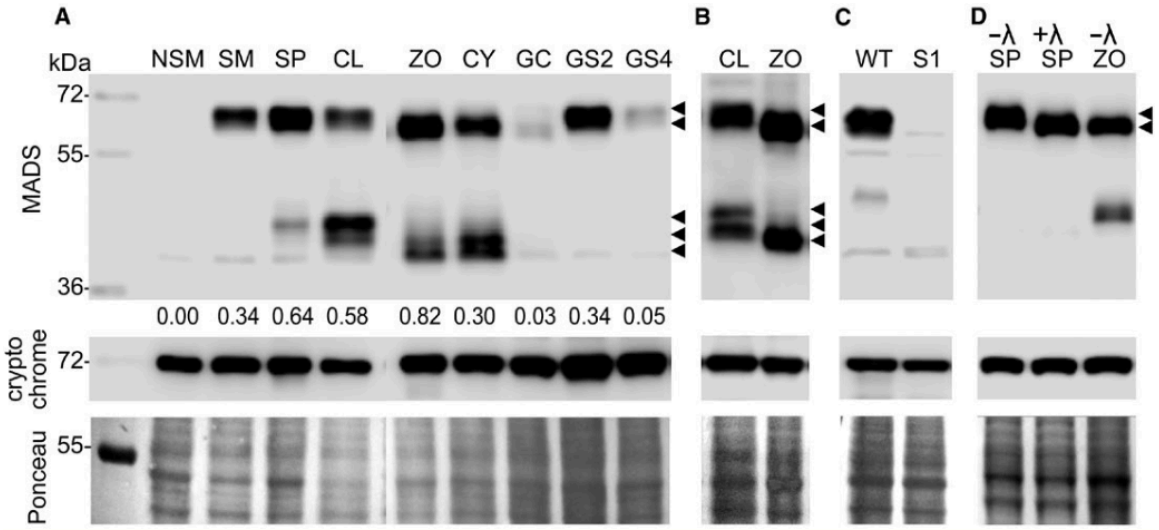

Fig. 2. Levels of PiMADS protein in different life stages of *P. infestans*. **A,** Blot using anti-MADS1 (top panel) and anti-cryptochrome (middle panel, same filter as the top panel). The bottom panel shows Ponceau staining of the membrane after transfer. Life stages are nonsporulating mycelia (NSM), sporulating mycelia (SM), sporangia (SP), chilled sporangia (CL), zoospores (ZO), zoospore cysts (CY), cysts germinated in clarified rye-sucrose broth for 2 h (GC), and sporangia germinated in clarified rye-sucrose broth for 2 and 4 h (GS2, GS4). Numbers below the top panel indicate levels of the MADS protein normalized based on Ponceau staining. **B,** Blot using anti-MADS2 against chilled sporangia (CL) and zoospores (ZO). **C,** Blot using anti-MADS1 against sporulating hyphae from wild type (WT) and the *PiMADS*-silenced strain (S1). **D,** Blot using anti-MADS1 against protein from sporangia (SP) or zoospores (ZO) treated with (+λ) or without (–λ) lambda phosphatase.

Anti-MADS1 and anti-MADS2 also detected several bands between 40 and 45 kDa in sporangia undergoing zoosporogenesis, zoospores and cysts. These bands are proposed to represent in vivo degradation products. They are unlikely to result from alternative splicing since no heterogeneity in transcript structure was evident when RNA-seq reads were mapped against *PiMADS*. They do not appear to be an artifact of cell breakage during centrifugal harvesting of the zoospores, since other proteins, such as cryptochrome only exhibited a

single band and since evidence of generalized protein breakdown was not seen when gels were stained with Coomassie blue. Breakdown of PiMADS protein during germination is probably important for shifting patterns of transcription from genes needed for the formation or germination of sporangia to genes required for hyphal growth. Human MEF2A and MEF2D are also regulated by proteolysis, in which phosphorylation promotes caspase-mediated cleavage within the transactivation domain (Okamoto et al. 2002).

Since there is also a precedent for a MADS-box protein being degraded by the proteasome (MacLean et al. 2014), we tested whether the appearance of the 40–45 kDa bands was inhibited by epoxomicin or MG132. These experiments began by testing whether these proteasome inhibitors impaired the growth of *P. infestans*, since we are unaware of any prior report of their use in an oomycete. Both strongly reduced growth, with epoxomicin being about 10 times more potent than MG132 (Fig. S2A and B). We then poured solutions of the compounds on sporulating mycelia, rubbed off the sporangia, induced zoosporogenesis and harvested zoospores after approximately 150 min. Blot analysis indicated that neither inhibitor reduced the accumulation of the lower bands (Fig. S2C). This suggests that the breakdown of PiMADS occurs through a proteasome-independent pathway.

The predicted size of PiMADS is 48 kDa, not 63–65 kDa as seen in the blots. We believe that the 63–65 kDa species are PiMADS since they were detected by both anti-MADS1 and anti-MADS2, both before and after affinity-

purification of the antiserum using the peptide antigens. In addition, the pattern of expression of the 63–65 kDa bands matches that of *PiMADS* mRNA. Most importantly, the bands were not detected in *P. infestans* transformants in which *PiMADS* was silenced (Fig. 2C); these strains will be discussed in more detail later. The larger-than-expected bands persisted when protein extracts were treated prior to electrophoresis with strong chaotropic agents, such as 8M urea, and both dithiothreitol and β-mercaptoethanol. Therefore, the higher bands are probably not due to dimerization of PiMADS or formation of a ternary complex.

There are many precedents of proteins exhibiting aberrant mobility in electrophoretic separations. For example, 19% of *Saccharomyces cerevisiae* proteins showed a > 20% difference between their predicted and apparent molecular weights in SDS-PAGE (Shirai et al. 2008). Much of this could be attributed to hydrophobicity, with a positive correlation between the degree of hydrophilicity and retarded mobility. PiMADS is very hydrophilic, with a score of –0.968 calculated by GRAVY (Kyte and Doolittle 1982). A large mobility shift can also result from sumoylation, which is known to affect human MADS-box proteins (Shalizi et al. 2006). To investigate whether sumoylation might be responsible for the altered mobility of PiMADS, we first explored the *P. infestans* genome for evidence of a sumoylation pathway. The pathway appears to be present, including genes encoding the small ubiquitin-like modifier (PITG_09611 and PITG_09654) which would be expected to add 11.3 kDa to a protein. We next tested if the PiMADS band was cleaved by SUMO protease Ulp1 from yeast.

This did not alter the 63–65 kDa species, although it is possible that Ulp1 does not recognize the *P. infestans* SUMO sequence.

PiMADS localizes to nuclei of sporulating mycelia and spores

To investigate the subcellular localization of PiMADS, *P. infestans* transformants were generated that express the protein with a C-terminal tdTomato tag, driven by the native promoter. The PiMADS:tdTomato signal was not observed in nonsporulating mycelia, but was detected in nucleus-like structures within sporulating mycelia (Fig. 3A); this pattern of expression is consistent with the RNA-seq and immunoblot results described above. DAPI staining confirmed the nuclear localization of PiMADS (Supporting Information Fig. S3). In later developmental stages, a PiMADS:tdTomato signal was also seen in nuclei of sporangiophores and immature sporangia (Fig. 3B). The latter can be identified as swellings emerging from sporangiophores, which lack the papillae and basal plugs diagnostic of mature sporangia. The strongest signal was observed in nuclei of mature sporangia (Fig. 3C). PiMADS:tdTomato was also detected in the nuclei of sporangia chilled to initiate zoosporogenesis, zoospore nuclei and cyst nuclei (Fig. 3C and D). Once germ tubes emerged from cysts, however, the fluorescent signal became weaker and more cytoplasmic (Fig. 3D). This decline is consistent with the degradation of the protein, as was observed in the immunoblots. Protein degradation may also result in the tdTomato signal to relocalize partially to the cytoplasm.

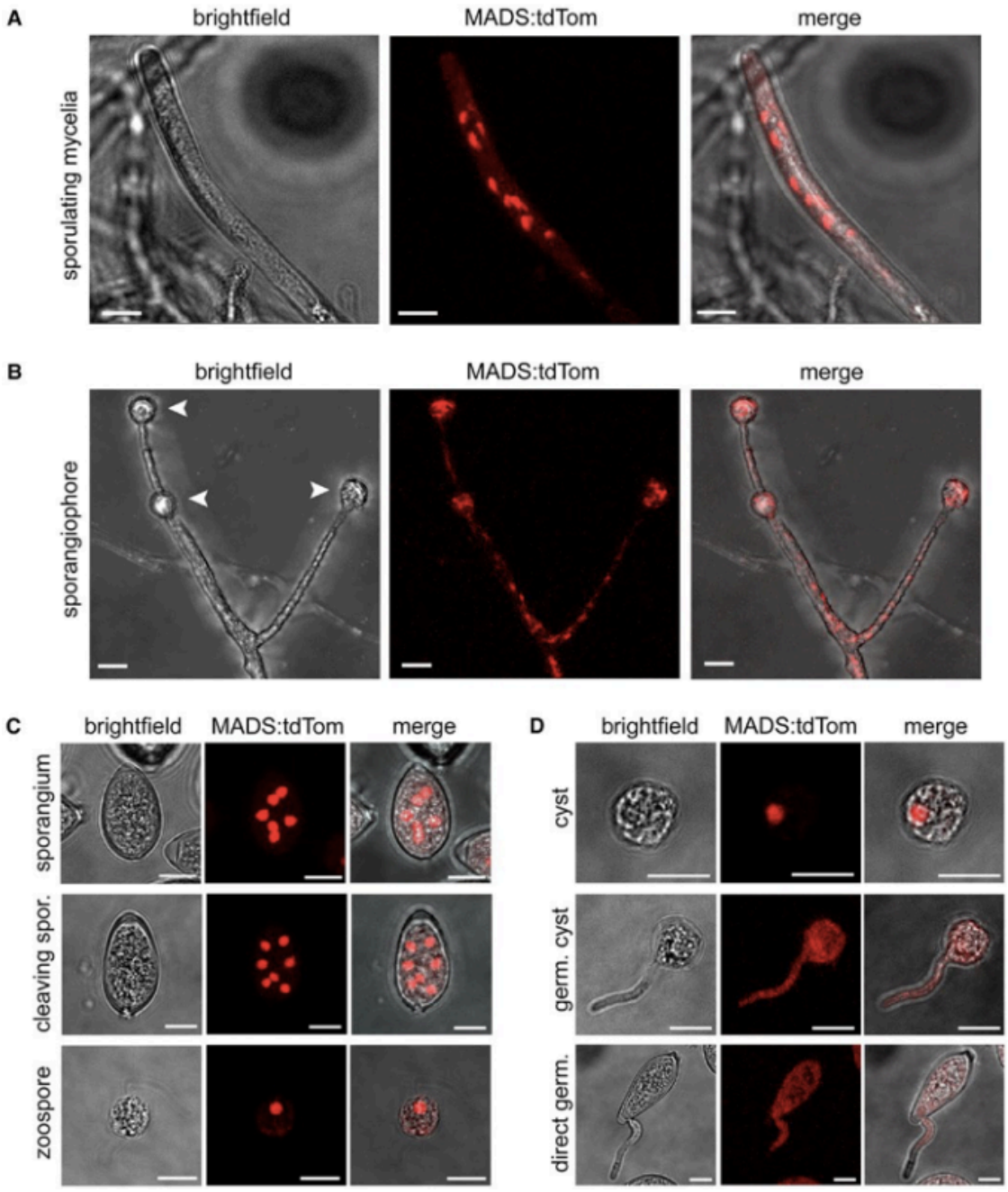

Fig. 3. Transformant expressing PiMADS:tdTomato under the native promoter. Shown are brightfield, red channel (tdTomato), and merged images, with bars representing 10 µm. **A,** mycelium from culture in early stage of sporulation. **B,** sporangiophore from a sporulating culture, with arrows denoting immature sporangia. **C,** shown top to bottom are a mature sporangium, a chilled (cleaving) sporangium, and a zoospore that has exited a sporangium. **D,** shown top to bottom are an encysted zoospore, a cyst after 2 h of germination, and a sporangium germinating directly in media for 4 h.

Silencing *PiMADS* blocks sporulation

The function of *PiMADS* was assessed by homology-directed gene silencing. This involved generating stable transformants that expressed 478 nt from the 3′ exon of the gene, driven by a constitutive promoter in a plasmid backbone that conferred G418-resistance. Strains showing evidence of silencing were identified by reverse transcription-quantitative polymerase chain reaction (RT-qPCR). This is illustrated in Fig. 4A for transformants S1, S2 and S23. Compared to wild type, *PiMADS* mRNA was reduced by 97, 77 and 86% in 8 day cultures of S1, S2 and S23 respectively. Since silencing achieved by this method may potentially spread to adjoining genes, we also tested the two genes flanking *PiMADS*. Those genes, PITG_07058 and PITG_07060, exhibited normal expression in S1, S2 and S23 and this condition persisted over several months of replicated testing.

Western blot analysis of 3 day and 7 day cultures confirmed the silencing of *PiMADS* (Fig. 4B). Compared to wild type, PiMADS protein was not detected in transformant S1 at either timepoint. The protein level in transformant S2 was 16% of wild type, which agreed with the prior RT-qPCR results that indicated that S2 was a partial knock-down. Consistent with the expression data shown earlier, the level of PiMADS protein increased dramatically between days 3 and 7. As mentioned earlier, the results from these blots also help to confirm the specificity of our anti-MADS antibodies.

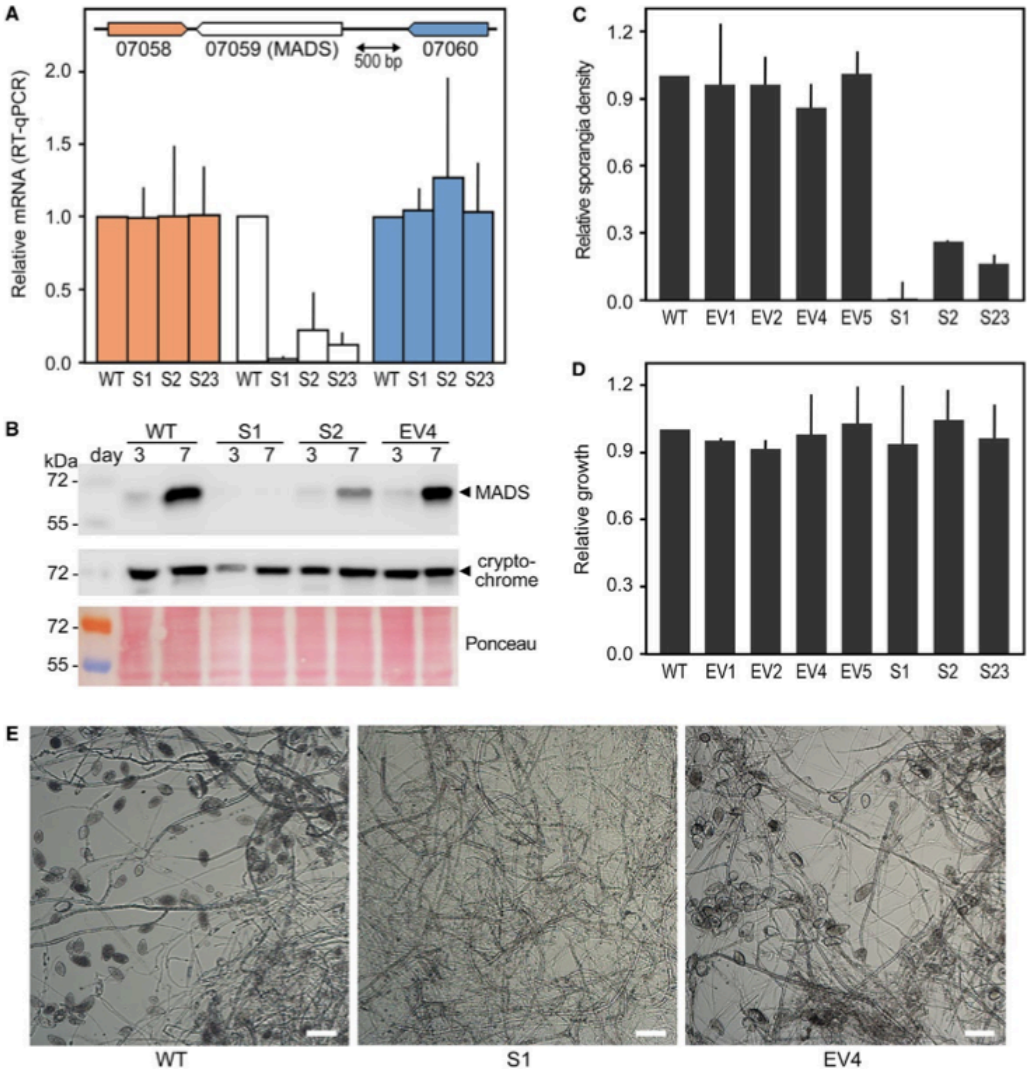

Fig. 4. Effect of silencing of *PiMADS* on growth and sporulation. **A,** RT-qPCR of wild type (WT) and three silenced transformants (S1, S2 and S23). Shown from left to right are gene PITG_07058, which is adjacent to *PiMADS*; PITG_07059, i.e. *PiMADS*; and PITG_07060. The position of the three genes on the chromosome are indicated at the top of the panel. **B,** Levels of PiMADS protein from 3 day and 7 day cultures of wild type, an empty vector transformant (EV4), and *PiMADS*-silenced S1 and S2. The top panels indicate the signal obtained using anti-MADS1. Anti-cryptochrome and Ponceau-stained panels are presented as controls for gel loading. **C,** Relative density of sporangia from 8 day rye-sucrose agar cultures of wild type (WT), empty vector transformants (EV1, EV2, EV4 and EV5), and the three *PiMADS*-silenced strains. Values are normalized relative to wild type. **D,** Relative hyphal growth rates of the strains shown in panel C on rye-sucrose agar. **E,** Culture scrapings from 14 day cultures of wild type, silenced strain S1 and empty vector transformant EV4. The white bar denotes 50 µm.

Phenotypic analysis revealed that silencing was associated with reduced sporulation. Levels of sporulation in 8 day cultures of S1, S2 and S23 were 3, 26 and 16% of wild type respectively (Fig. 4C; Supporting Information Fig. S4). Empty-vector transformants showed normal sporulation. The reduction of sporulation in silenced strain S1 compared to wild-type and empty-vector controls is also illustrated in Fig. 4E, which shows a dearth of sporangia but otherwise normal-looking hyphae in S1.

The few sporangia that were produced by the silenced strains appeared normal with regular dimensions (Supporting Information Fig. S5), released zoospores at normal rates, encysted and produced normal-looking appressoria based on comparisons to wild type and empty-vector transformants. In addition, strains S1, S2 and S23 grew at normal rates on rye media (Fig. 4D), and colonized potato tubers and tomato leaves with equal effectiveness as the non-silenced controls when the same number of sporangia were used as inoculum (Supporting Information Fig. S6). We conclude that *PiMADS* contributes to sporangia production but not growth, germination or plant colonization measured on a per-spore basis.

We next attempted to complement the silenced strains with a recoded form of *PiMADS*. While complementation of silenced genes using RNAi-refractory versions has been reported in other organisms (Binder et al. 2014), this has not been attempted previously in any oomycete. Unfortunately, we did not succeed. Our approach was to employ a synthetic *c-Myc*-tagged gene that

was altered to have ≤8 nt of contiguous sequences matching *PiMADS* while maintaining good codon usage. This was transformed into strain S2 using hygromycin resistance as a second selectable marker. However, immunoblot analysis (using anti-c-Myc) of 20 transformants in which the synthetic gene was driven by the native promoter or the constitutive ham34 promoter failed to identify any expressing the recoded transgene.

We also attempted to test the function of *PiMADS* by overexpression. This involved expressing the open reading frame behind the ham34 promoter with a C-terminal 3 × FLAG epitope tag. No transformants expressing the transgene were detected by immunoblot analysis. The overexpression of *PiMADS* may be lethal, for example, if it diverts cellular activities from vegetative growth toward sporulation or mitotic dormancy.

Current silencing model does not apply to *PiMADS*-silenced strain

In other genes that were silenced in *Phytophthora* using the homology-dependent method that we applied to *PiMADS*, several groups observed that both the transgene and native gene were transcriptionally silenced (van West et al. 1999; Gaulin et al. 2002; Ah Fong and Judelson 2003; Latijnhouwers and Govers 2003; Blanco and Judelson 2005; Judelson and Tani 2007). This was shown to result from heterochromatinization (Ah-Fong et al. 2008; van West et al. 2008). We were therefore surprised to observe that many RNA-seq reads from strain S1 matched the 478-nt region of *PiMADS* that was included in the silencing

vector (Fig. 5A). Reads mapping to other parts of the native gene were reduced by more than 90%. These data indicate that while *PiMADS* was strongly down-regulated, the transgene was not silenced. To confirm this result, we performed RT-qPCR using primer sets specific to the native gene and the transgene (Fig. 5B). This verified that transcripts arising from the transgene, but not the native gene, were abundant in strain S1.

In retrospect, conclusions about the mechanism(s) of homology-dependent silencing in *Phytophthora* may have been premature and based on too few target genes. In plants, fungi and some metazoans, silencing can occur through transcriptional and post-transcriptional processes (Vaucheret et al. 1998; Faugeron 2000; Omotezako et al. 2015). Outcomes can be specific to the plasmid design, target gene and characteristics of the integration event (Lechtenberg et al. 2003). Our results with *PiMADS* resemble a situation observed sometimes in plants, where one transgene has a unidirectional transcriptional silencing effect on another locus that is akin to paramutation (Zheng et al. 2015).

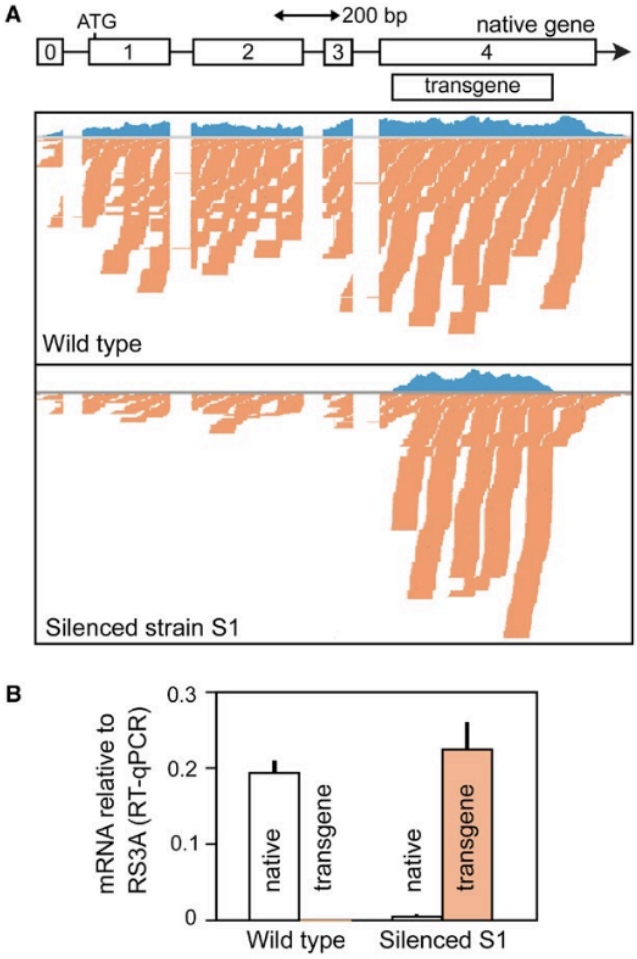

Fig. 5. A, Mapping RNA-seq reads from wild type and silenced strain S1 against the *PiMADS* gene. Images were copied from the Integrated Genomics Viewer. Shown at the top of the figure are the positions of the five exons of the gene (the start codon is in exon 1), and the region expressed in the construct used to silence *PiMADS*. **B,** RT-qPCR analysis using primers specific to the native gene and the transgene.

PiMADS regulates most sporulation-induced genes

To help determine when PiMADS acts in sporulation, RNA-seq was used to compare gene expression in wild type and silenced strain S1 in cultures 2, 4 and 6 days after inoculation. Two biological replicates were obtained for each timepoint for each strain, and each sample was sequenced to a minimum of 28

million 75-nt single-end reads. In wild-type cultures inoculated in parallel, the number of sporangia measured at 2, 4 and 6 days averaged 3, 19 and 183 per mm^2 of culture area (Supporting Information Fig. S4). Defined as 'sporulation-induced' were 3,033 genes that were > 2-fold higher in the 6 day versus 2 day cultures of wild type. Considered to be expressed based on having an average CPM > 1 in at least one timepoint were 15,052 genes. Therefore, 20.1% of genes were sporulation-induced by > 2-fold in wild type. In comparison, only 639 of the 3,033 genes were induced in the silenced strain, although their fold-change was sometimes reduced compared to wild type. Showing > 2-fold differences between the wild type and silenced strains (FDR < 0.05) at any time-point were 5,362 genes, or 35% of the total.

More insight was obtained by *K*-means clustering and GO term analysis (Fig. 6). Cluster 2 includes 2,352 genes that were sporulation-induced in wild type but not in the silenced strain. Over-represented GO terms associated with this cluster were associated with cilia and signaling. Examples of genes in the former category are PITG_01852, PITG_03423 and PITG_12577, each of which encode axonemal dyneins. Included in the signaling category in Cluster 2 were genes encoding regulators that were shown to control sporulation in prior studies, namely transcription factor Myb2R1, protein phosphatase Cdc14, and β and γ G-protein subunits (Latijnhouwers and Govers 2003; Ah-Fong and Judelson 2011a; Xiang and Judelson 2014; van den Hoogen et al. 2018). Thus, PiMADS appears to operate upstream of proteins previously shown to control sporulation.

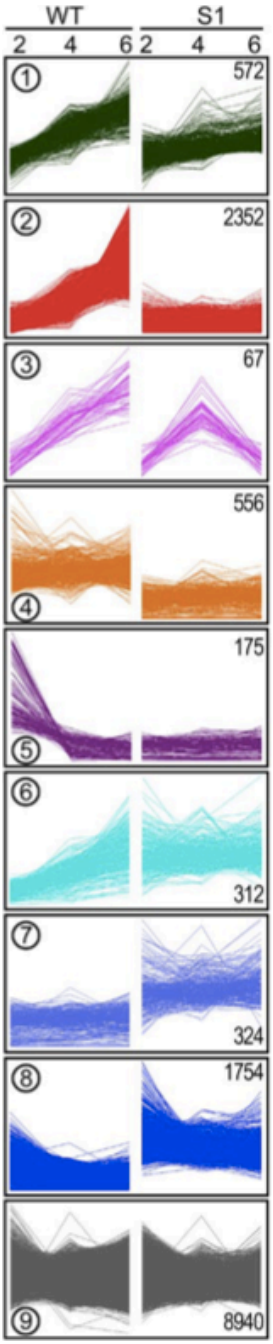

GO ID	Term	Type	FDR
0005929	cilium	CC	6.73E-08
0006928	cell or subcellular component movement	BP	1.90E-07
0007018	microtubule-based movement	BP	4.91E-05
0001578	microtubule bundle formation	BP	2.87E-21
0005216	ion channel activity	MF	6.88E-14
0005929	cilium	CC	1.97E-63
0023052	signaling	BP	6.42E-28
0001510	RNA methylation	BP	9.93E-23
0044249	cellular biosynthetic process	BP	8.89E-05
0031225	anchored component of membrane	CC	1.04E-02
0047066	phospholipid-hydroperoxide glutathione peroxidase	MF	8.69E-04
0005215	transporter activity	MF	5.22E-04
0019321	pentose metabolic process	BP	4.41E-03
0050525	cutinase activity	MF	5.87E-08
0071555	cell wall organization	BP	2.05E-04
0004553	O-glycosyl hydrolase activity	MF	9.90E-03
0005576	extracellular region	CC	1.16E-02
0006732	coenzyme metabolic process	BP	3.63E-08
0016072	rRNA metabolic process	BP	9.36E-27
0019752	carboxylic acid metabolic process	BP	1.69E-27
0072522	purine-containing compound biosyn.	BP	2.22E-10
0016071	mRNA metabolic process	BP	1.10E-21
0019538	protein metabolic process	BP	6.16E-22
0043229	intracellular organelle	CC	5.78E-34
0044265	cellular macromolecule catabolism	BP	3.76E-12

Fig. 6. *K*-means clustering of genes from wild type (WT) and silenced strain S1. Shown in the left column are nine clusters indicating mRNA levels in cultures 2, 4 and 6 days after inoculation. The number of genes in each cluster is indicated in the right side corner of each panel. Shown to the right are over-represented GO terms associated with each cluster with columns indicating the GO term number, description, type (CC, cellular component; BP, biological process; MF, molecular function), and multiple correction-adjusted p-value (FDR).

Cluster 3 was comprised of 67 genes that were induced to similar degrees in the 4 day versus 2 day cultures of both wild type and the silenced strain. This suggests that they are up-regulated initially by a transcription factor other than PiMADS. However, while their mRNAs continued to rise in the 6 day cultures of wild type, they returned to basal levels in the silenced strains. This suggests that Cluster 3 genes are regulated by a positive feedback loop involving PiMADS. RNA methylation was the most over-represented GO term linked to this cluster, reflecting its inclusion of 14 genes encoding RNA methyltransferases. Such modifications determine how much protein is translated from mRNA and influence the function of non-coding RNA (Zhao et al. 2017). In yeast, mRNA methylation is essential for sporulation (Clancy et al. 2002).

Cluster 1 consisted of 572 genes that were sporulation-induced in both the silenced and wild-type strains. The magnitude of their induction was reduced by about one-half in the silenced strain, however. The most over-represented GO term for this cluster was cilium, with examples including PITG_11437, which encodes an axonemal dynein, and PITG_17408, which encodes intraflagellar transport protein 52. Such genes might be induced by transcription factors upstream or independent of the MADS-box protein, but their continued expression appears to be dependent directly or indirectly on PiMADS.

Cluster 8 included 1,754 genes that were expressed at higher levels in the silenced strain than wild type, especially at days 4 and 6. Most GO terms over-represented in this cluster were related to metabolism, which is consistent with

our prior observation that most metabolic mRNAs decline in purified sporangia compared to non- sporulating mycelia (Ah-Fong et al. 2017).

Cluster 9 included 8940 genes, or about 60% of the total. These genes were not sporulation-induced and had similar patterns of expression in wild type and the *PiMADS*-silenced strain. Most were associated with core metabolic and cellular processes.

Transcription of genes in each cluster are undoubtedly governed by multiple proteins. For example, it is unlikely that all 2,352 genes in Cluster 2 are solely or directly regulated by PiMADS. This was explored further using Affymetrix microarray data generated previously for *P. infestans* strains that were silenced for the Cluster 2 gene that encodes Cdc14 phosphatase, *PiCdc14* (Judelson et al. 2009). Those arrays are estimated to detect about half of total *P. infestans* genes (Ah-Fong et al., 2017). Based on that subset, 71% of Cluster 2 genes were not up-regulated in the Cdc14-silenced strains grown under conditions that allow wild type to sporulate. Thus, PiCdc14 represents a regulatory step within Cluster 2. Moreover, nearly all Cluster 3 and Cluster 1 genes were up-regulated in the *PiCdc14*-silenced strains, which is consistent with PiCdc14 acting after PiMADS.

Conclusions

Like many of its non-oomycete orthologs, PiMADS plays an important role in *P. infestans* development. The protein's nuclear localization and influence on

gene expression are consistent with its predicted function as a transcription factor. A model for how sporulation may be regulated is shown in Fig. 7. A yet-unknown signal is proposed to initiate sporulation. This might be a metabolic cue, since nutrient limitation stimulates sporulation in some members of the genus (Ribeiro 1983). The signal is proposed to initiate a gene expression cascade that entails the sequential activation of Cluster 3, Cluster 1, *PiMADS* and Cluster 2 genes. *PiMADS* is proposed to exert two roles. One is to sustain Cluster 3 transcription through a positive feedback loop; this explains why Cluster 3 mRNAs rise but then fall when *PiMADS* was silenced. The lack of this feedback in silenced strains results in transient expression of Cluster 3, and incomplete induction of Cluster 1. The second role of PiMADS protein is to upregulate Cluster 2, which encompasses most sporulation-induced genes, including known sporulation regulators such as Cdc14 and the G-protein subunits. A protein expressed by a Cluster 2 gene is proposed to cause proteolysis of PiMADS upon germination. While this model is speculative, it sets the groundwork for future experimentation.

Our analysis of PiMADS is important since it acts upstream of previously identified regulators. Future studies using methods such as homology-based gene silencing should allow for the development of more detailed and comprehensive model. Our observation that a target gene can sometimes be silenced in *Phytophthora* without concomitantly silencing the transgene will help guide strategies for identifying knock-downs. For example, false negatives may

result unless primers for RT-PCR are specific to the transgene. Regulators of sporulation identified by such techniques may serve as targets for inhibitors that could be used to block the many diseases of plants and animals caused by oomycetes.

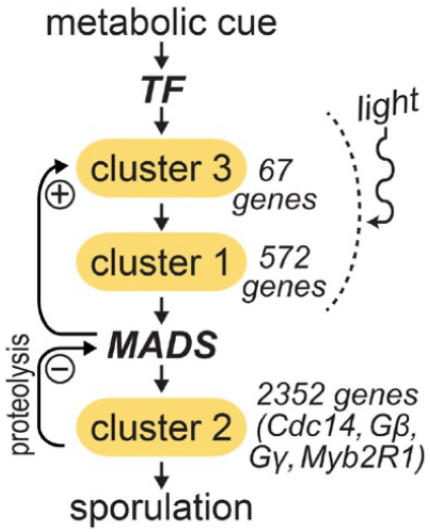

Fig. 7. Model for regulation of sporulation in *P. infestans*. This simplified and parsimonious model invokes PiMADS and an unknown transcription factor (TF) as key regulators of sporulation. An alternative model has Cluster 1 and Cluster 3 genes being activated by independent pathways.

Materials and methods

Sequence analysis

P. infestans genome data were obtained from the FungiDB. org website. MADS-box proteins from other species were collected using BLASTP against FungiDB, GenBank, Ensembl Protists and the Joint Genome Institute of the United States Department of Energy. Protein domains were identified or confirmed using the Conserved Domain Database, Interpro and SMART. For phylogenetic analysis, protein alignments were performed using MUSCLE (Edgar

2004) as implemented in Seaview V4.6.2 (Gouy et al. 2010). Alignments were trimmed using TCS (Chang et al. 2014) prior to the construction of phylogenetic trees. This used PhyML (Guindon et al. 2010), in which branch support was calculated using 1,000 bootstrap replicates, and MrBayes 3.2.6 (Ronquist et al. 2012) using a chain length of 500,000, 4 heated chains, 125,000 burn-in cycles, Poisson model, and gamma rate variation. Clades and tips were colored or collapsed using FigTree V1.4.3 (https://tree.bio.ed.ac.uk/ software/).

Growth and transformation of *P. infestans*

Developmental stages were prepared as described using isolate 1306 (Judelson et al. 2008). In brief, nonsporulating mycelia was collected from 3 day rye-sucrose agar cultures inoculated by spreading with sporangia. Sporulating mycelia and sporangia were obtained from 7 to 9 day cultures. Directly germinated sporangia were generated by placing sporangia in clarified rye broth at 18°C for 4 h. Chilled sporangia and zoospores were prepared by incubating sporangia in 10°C modified Petri's solution (Blanco and Judelson 2005) for 30 and 120 min respectively. Cysts were obtained by vortexing zoospores for 1 min followed by 5 min incubation at room temperature. Germinated cysts were obtained by placing cysts in clarified rye broth at 18°C for 2 h. All life stages except mycelia were pelleted at 1000 × g for 4 min at room temperature while chilled sporangia and zoospores were collected at 4°C, and then frozen in liquid

nitrogen for subsequent analysis. Mycelia were scraped from rye-sucrose agar cultures and frozen in liquid nitrogen.

Transformations were conducted using the protoplast method (Ah-Fong et al. 2008). The silencing construct was generated by inserting nt 718-1196 of *PiMADS* coding sequences in the sense orientation into the *Eco*RI and *Xba*I restriction sites of pTOR, 3′ of the *ham34* promoter. Subcellular localization studies involved cloning the full-length PiMADS open reading frame plus 402 nt of the native promoter into the *Eco*RV and *Nhe*I restriction sites of pTdTomatoN (Abrahamian et al. 2017). Both of these vectors contain the *5′ hsp70:npt:3′ hsp70* selectable marker gene, and transformants were selected on 8–10 µg/ml G418. Primers used in cloning are described in Supporting Information Table S1.

For the silencing rescue construct, a gene fragment that encoded PiMADS but had ≤ 8 nt identity to the native *PiMADS* sequence was synthesized with a C-terminal *c-Myc* tag. This was then inserted into the *Age*I and *Not*I sites of pMCherryH (Ah-Fong and Judelson 2011b). As this backbone contains the *5′ hsp70:hpt:3′ hsp70* marker gene, transformants were selected on 40–50 µg/ml hygromycin.

Confocal microscopy

Life stages prepared as described above were fixed using 4% formaldehyde in 50 mM PIPES pH 6.8 at room tempera- ture for 30 min (Ah-Fong and Judelson 2011a). Fixed tissues were pelleted at 1000 × g for 2 min,

and washed three times with 100 mM PIPES buffer pH 6.8 for 5 min each at room temperature. Microscopy was performed using a Leica SP5 inverted microscope and using settings for TRITC (543 nm excitation and 555–630 nm emission). Images were processed using the Auto Level feature of Adobe Photoshop.

Plant infection

Tubers (cv. Russet Burbank) were surface-sterilized using 10% (v/v) bleach for 15 min and rinsed in distilled water. Slices (4 mm) were obtained using a mandolin, washed in sterile water, blotted dry and incubated for 1 h before infection. Slices were placed on a metal rack above moist paper towels and inoculated by spreading sporangia from 9 day cultures (adjusted to 2.5×10^4 per ml in modified Petri's solution) with a rubber policeman. The slices were then incubated at 18°C in the dark, using a sealed plastic box to maintain high humidity. Tomato leaves (cv. Pieralbo) were surface-sterilized using 10% (v/v) bleach for 5 min, washed in sterile water twice, blotted dry and held for 1 h. The leaves were then placed on 0.6% water agar, inoculated with five 15 µl drops of sporangia prepared as described above, and incubated at 18°C under a 12 h dark/light cycle, using a sealed bag to maintain humidity.

RNA analysis

RNA was isolated using the Spectrum Plant Total RNA kit (Sigma). For RT-qPCR, RNA was treated with the RQ1 DNase (Promega) and cDNA was synthesized using the Maxima First Strand cDNA Synthesis kit (Thermo). Primers for RT-qPCR (Supporting Information Table S1) were tested for efficiency using a dilution series of cDNA template. Amplification was performed using the Dynamo HS SYBR Green qPCR kit (Thermo) and the CFX Connect Real-Time PCR Detection system (BioRad). Controls lacking reverse transcriptase and melt curves were included to help verify the fidelity of the results. Expression levels were calculated using the $\Delta\Delta C_T$ method and normalized to the gene for ribosomal protein S3a. At least three biological replicates were analyzed. For RNA-seq, indexed libraries were prepared and sequenced using an Illumina NextSeq500. Single-end 75-nt reads were aligned and mapped to *P. infestans* gene models using Bowtie2 and Tophat (Langmead et al. 2009). Mapping statistics and library sizes are listed in Supporting Information Table S2. EdgeR was used for differential expression analysis, using TMM-normalized CPM values (Robinson et al. 2010). Visualization of reads mapped to the *P. infestans* genome were performed using the Integrative Genomics Viewer (Robinson et al. 2011). *K*-means clustering was executed using Partek Genomics Suite, and Gene Ontology term enrichment analysis was performed using GOHyperGAll (Horan et al. 2008). Clusters, expression data for genes in each cluster (CPM, fold-change ratios, p-values, and Benjamini-

Hochberg FDR values) and associated GO terms are shown in Supporting Information Table S3. Analyses employed an FDR cut-off of 0.05.

Protein analysis

Protein was extracted by grinding tissue under liquid nitrogen, thawing the tissue in 50 mM Tris pH 7.4, 30 mM NaCl, 1% sodium dodecyl sulfate, 1 mM DTT, 15% glycerol, 1% Sigma protease inhibitor cocktail (catalog number P9599), and clarifying the extract by centrifugation at 18,000 × g for 10 min. For immunoblotting, protein was separated by SDS-10% PAGE, incubated with anti-MADS antibody and then horseradish peroxidase-conjugated goat anti-rabbit IgG (Thermo), and detected using the ECL Prime kit (GE Healthcare) using a C-DiGit Blot Scanner (Li-cor). Quantification of immunoblot and ponceau staining images was performed using C-DiGit Image Studio software. Custom rabbit antibodies against the *P. infestans* MADS- box and cryptochrome proteins were raised and affinity-purified using the peptide RSEVRGSASTSPHKRQRVAV.

To test for protein modifications, 0.2 mg of protein extracts (prepared as described above but with 1% NP-40 in place of the sodium dodecyl sulfate) were incubated with 2,800 units of lambda phosphatase for 30 min at 30°C using the buffer recommended by the manufacturer (New England Biolabs). Treatments of sporangia with epoxomicin and MG132 (Selleck Chemical) were performed at 10 and 100 μM in 0.001% DMSO, respectively. These concentrations totally arrested growth of *P. infestans* and match those used in studies of proteins in

plants (Bos et al. 2010; Gu et al. 2010). Tests of SUMO protease (Ulp1) were performed according to the protocols provided by the manufacturer (Thermo Fisher).

Data availability

All data analyzed during this study are provided in this published article, its additional supporting files, and at the National Center for Biotechnology Information as Bioprojects PRJNA361417 and PRJNA485588.

Acknowledgements

We thank Audrey Ah Fong and Andrea Vu for sharing data, experimental materials, and comments on the manuscript. This work was supported by grants to HSJ from the United States Department of Agriculture National Institute of Food and Agriculture, and a scholarship to WL by the Royal Thai Government. We thank *Molecular Microbiology* for letting us use the manuscript as a part of this dissertation. The original article can be found at: https://onlinelibrary.wiley.com/doi/full/10.1111/mmi.14114.

References

Abrahamian, M., Kagda, M., Ah-Fong, A. M. V., and Judelson, H. S. 2017. Rethinking the evolution of eukaryotic metabolism: novel cellular partitioning of enzymes in stramenopiles links serine biosynthesis to glycolysis in mitochondria. BMC Evol. Biol. 17:241.

Ah Fong, A. M., and Judelson, H. S. 2003. Cell cycle regulator Cdc14 is expressed during sporulation but not hyphal growth in the fungus-like oomycete *Phytophthora infestans*. Mol. Microbiol. 50:487-494.

Ah-Fong, A. M., Bormann-Chung, C. A., and Judelson, H. S. 2008. Optimization of transgene-mediated silencing in *Phytophthora infestans* and its association with small-interfering RNAs. Fungal Genet. Biol. 45:1197-1205.

Ah-Fong, A. M., and Judelson, H. S. 2011a. New role for Cdc14 phosphatase: localization to basal bodies in the oomycete *Phytophthora* and its evolutionary coinheritance with eukaryotic flagella. PLoS One 6:e16725.

Ah-Fong, A. M., and Judelson, H. S. 2011b. Vectors for fluorescent protein tagging in *Phytophthora*: tools for functional genomics and cell biology. Fungal Biol. 115:882-890.

Ah-Fong, A. M. V., Kim, K. S., and Judelson, H. S. 2017. RNA-seq of life stages of the oomycete *Phytophthora infestans* reveals dynamic changes in metabolic, signal transduction, and pathogenesis genes and a major role for calcium signaling in development. BMC Genomics 18:198.

Binder, A., Lambert, J., Morbitzer, R., Popp, C., Ott, T., Lahaye, T., and Parniske, M. 2014. A modular plasmid assembly kit for multigene expression, gene silencing and silencing rescue in plants. PLoS One 9:e88218.

Blanco, F. A., and Judelson, H. S. 2005. A bZIP transcription factor from *Phytophthora* interacts with a protein kinase and is required for zoospore motility and plant infection. Mol. Microbiol. 56:638-648.

Bos, J. I. B., Armstrong, M. R., Gilroy, E. M., Boevink, P. C., Hein, I., Taylor, R. M., Zhendong, T., Engelhardt, S., Vetukuri, R. R., Harrower, B., Dixelius, C., Bryan, G., Sadanandom, A., Whisson, S. C., Kamoun, S., and Birch, P. R. 2010. *Phytophthora infestans* effector avr3a is essential for virulence and manipulates plant immunity by stabilizing host E3 ligase CMPG1. Proc. Natl. Acad. Sci. U.S.A. 107:9909-9914.

Brameier, M., Krings, A., and MacCallum, R. M. 2007. NucPred-predicting nuclear localization of proteins. Bioinformatics 23:1159-1160.

Chang, J. M., Di Tommaso, P., and Notredame, C. 2014. Tcs: a new multiple sequence alignment reliability measure to estimate alignment accuracy and improve phylogenetic tree reconstruction. Mol. Biol. Evol. 31:1625-1637.

Clancy, M. J., Shambaugh, M. E., Timpte, C. S., and Bokar, J. A. 2002. Induction of sporulation in *Saccharomyces cerevisiae* leads to the formation of N-6-methyladenosine in mRNA: a potential mechanism for the activity of the ime4 gene. Nucleic Acids Res. 30:4509-4518.

Clark, M. C., Melanson, D. L., and Page, O. T. 1978. Purine metabolism and differential inhibition of spore germination in *Phytophthora infestans*. Can. J. Microbiol. 24:1032-1038.

Dahlberg, K. R., and Van Etten, J. L. 1982. Physiology and biochemistry of fungal sporulation. In: R.G. Grogan (Ed.) Annual Review of Phytopathology. Palo Alto, CA: Annual Reviews Inc, pp. 281-302.

Derelle, R., Lopez-Garcia, P., Timpano, H., and Moreira, D. 2016. A phylogenomic framework to study the diversity and evolution of stramenopiles (= heterokonts). Mol. Bio. Evol. 33:2890-2898.

Edgar, R. C. 2004. Muscle: multiple sequence alignment with high accuracy and high throughput. Nucleic Acids Res. 32:1792-1797.

Faugeron, G. 2000. Diversity of homology-dependent gene silencing strategies in fungi. Curr. Opin. Microbiol. 3:144-148.

Gaulin, E., Jauneau, A., Villalba, F., Rickauer, M., Esquerre-Tugaye, M. T., and Bottin, A. 2002. The cbel glycoprotein of *Phytophthora parasitica* var. *nicotianae* is involved in cell wall deposition and adhesion to cellulosic substrates. J. Cell Sci. 115:4565-4575.

Gouy, M., Guindon, S., and Gascuel, O. 2010. Seaview version 4: a multiplatform graphical user interface for sequence alignment and phylogenetic tree building. Mol. Biol. Evol. 27:221-224.

Gregoire, S., Tremblay, A. M., Xiao, L., Yang, Q., Ma, K. W., Nie, J., Mao, Z., Wu, Z., Giguère, V., and Yang, X. J. 2006. Control of MEF2 transcriptional activity by coordinated phosphorylation and sumoylation. J. Biol. Chem. 281:8996-8996.

Gu, C., Kolodziejek, I., Misas-Villamil, J., Shindo, T., Colby, T., Verdoes, M., Richau, K. H., Schmidt, J., Overkleeft, H. S., and van der Hoorn, R. A. 2010. Proteasome activity profiling: a simple, robust and versatile method revealing subunit-selective inhibitors and cytoplasmic, defense-induced proteasome activities. Plant J. 62:160-170.

Guindon, S., Dufayard, J. F., Lefort, V., Anisimova, M., Hordijk, W., and Gascuel, O. 2010. New algorithms and methods to estimate maximum-likelihood phylogenies: assessing the performance of PhyML 3.0. Syst. Biol. 59:307-321.

Haas, B. J., Kamoun, S., Zody, M. C., Jiang, R. H., Handsaker, R. E., Cano, L. M., Grabherr, M., Kodira, C. D., Raffaele, S., Torto-Alalibo, T., Bozkurt, T. O., Ah-Fong, A. M., Alvarado, L., Anderson, V. L., Armstrong, M. R., Avrova, A., Baxter, L., Beynon, J., Boevink, P. C., Bollmann, S. R., Bos, J. I., Bulone, V., Cai, G., Cakir, C., Carrington, J. C., Chawner, M., Conti, L., Costanzo, S., Ewan, R., Fahlgren, N., Fischbach, M. A., Fugelstad, J., Gilroy, E. M., Gnerre, S., Green, P. J., Grenville-Briggs, L. J., Griffith, J., Gru¨nwald, N. J., Horn, K., Horner, N. R., Hu, C. H., Huitema, E., Jeong, D. H., Jones, A. M., Jones, J. D., Jones, R. W., Karlsson, E. K., Kunjeti, S. G., Lamour, K., Liu, Z., Ma, L., Maclean, D., Chibucos, M. C., McDonald, H., McWalters, J., Meijer, H. J., Morgan, W., Morris, P. F., Munro, C. A., O'Neill, K., Ospina- Giraldo, M., Pinzo´n, A., Pritchard, L., Ramsahoye, B., Ren, Q., Restrepo, S., Roy, S., Sadanandom, A., Savidor, A., Schornack, S., Schwartz, D. C., Schumann, U. D., Schwessinger, B., Seyer, L., Sharpe, T., Silvar, C., Song, J., Studholme, D. J., Sykes, S., Thines, M., van de Vondervoort, P. J., Phuntumart, V., Wawra, S., Weide, R., Win, J., Young, C., Zhou, S., Fry, W., Meyers, B. C., van West, P., Ristaino, J., Govers, F., Birch, P. R., Whisson, S. C., Judelson, H. S., and Nusbaum, C. 2009. Genome sequence and analysis of the Irish potato famine pathogen *Phytophthora infestans*. Nature 461:393-398.

Horan, K., Jang, C., Bailey-Serres, J., Mittler, R., Shelton, C., Harper, J. F., Zhu J. K., Cushman, J. C., Gollery, M., and Girke, T. 2008. Annotating genes of known and unknown function by large-scale coexpression analysis. Plant Physiol. 147:41-57.

Judelson, H. S., Ah-Fong, A. M., Aux, G., Avrova, A. O., Bruce, C., Cakir, C., da Cunha, L., Grenville-Briggs, L., Latijnhouwers, M., Ligterink, W., Meijer, H. J., Roberts, S., Thurber, C. S., Whisson, S. C., Birch, P. R., Govers, F., Kamoun, S., van West, P., and Windass, J. 2008. Gene expression profiling during asexual development of the late blight pathogen *Phytophthora infestans* reveals a highly dynamic transcriptome. Mol. Plant-Microbe Interact. 21:433-447.

Judelson, H. S., Narayan, R. D., Ah-Fong, A. M., and Kim, K. S. 2009. Gene expression changes during asexual sporulation by the late blight agent *Phytophthora infestans* occur in discrete temporal stages. Mol. Genet. Genomics 281:193-206.

Judelson, H. S., and Roberts, S. 2002. Novel protein kinase induced during sporangial cleavage in the oomycete *Phytophthora infestans*. Eukaryot. Cell 1:687-695.

Judelson, H. S., and Tani, S. 2007. Transgene-induced silencing of the zoosporogenesis-specific NIFC gene cluster of *Phytophthora infestans* involves chromatin alterations. Eukaryot. Cell 6:1200-1209.

Kosugi, S., Hasebe, M., Tomita, M., and Yanagawa, H. 2009. Systematic identification of cell cycle-dependent yeast nucleocytoplasmic shuttling proteins by prediction of composite motifs. Proc. Natl. Acad. Sci. U.S.A. 106:10171-10176.

Kovacs, A.T. 2016. Bacterial differentiation via gradual activation of global regulators. Curr. Genet. 62:125-128.

Kyte, J., and Doolittle, R. F. 1982. A simple method for displaying the hydropathic character of a protein. J. Mol. Biol. 157:105-132.

Langmead, B., Trapnell, C., Pop, M., and Salzberg, S. L. 2009. Ultrafast and memory-efficient alignment of short DNA sequences to the human genome. Genome Biol. 10:R25.

Latijnhouwers, M., and Govers, F. 2003. A *Phytophthora infestans* G-protein subunit is involved in sporangium formation. Eukaryot. Cell 2:971-977.

Lechtenberg, B., Schubert, D., Forsbach, A., Gils, M., and Schmidt, R. 2003. Neither inverted repeat T-DNA configurations nor arrangements of tandemly repeated transgenes are sufficient to trigger transgene silencing. Plant J. 34:507-517.

Lee, M. K., Kwon, N. J., Lee, I. S., Jung, S., Kim, S. C., and Yu, J. H. 2016. Negative regulation and developmental competence in *Aspergillus*. Sci. Rep. 6:28874.

Lin, J. R., and Hu, J. 2013. SeqNLS: nuclear localization signal prediction based on frequent pattern mining and linear motif scoring. PLoS ONE 8:e76864.

MacLean, A. M., Orlovskis, Z., Kowitwanich, K., Zdziarska, A. M., Angenent, G. C., Immink, R. G. H., and Hogenhout, S. A. 2014. Phytoplasma effector

SAP54 hijacks plant reproduction by degrading MADS-box proteins and promotes insect colonization in a RAD23-dependent manner. PLoS Biol. 12:e1001835.

Masiero, S., Imbriano, C., Ravasio, F., Favaro, R., Pelucchi, N., Gorla, M. S., Mantovani, R., Colombo, L., and Kater, M. M. 2002. Ternary complex formation between MADS-box transcription factors and the histone fold protein Nf-Yb. J. Biol. Chem. 277:26429-26435.

Molkentin, J. D., Black, B. L., Martin, J. F., and Olson, E. N. 1996. Mutational analysis of the DNA binding, dimerization, and transcriptional activation domains of MEF2c. Mol. Cell. Biol. 16:2627-2636.

Mughal, W., Nguyen, L., Pustylnik, S., Rosa, S. C. D., Piotrowski, S., Chapman, D., Du, M., Alli, N. S., Grigull, J., Halayko, A. J., Aliani, M., Topham, M. K., Epand, R. M., Hatch, G. M., Pereira, T. J., Kereliuk, S., McDermott, J. C., Rampitsch, C., Dolinsky, V. W., and Gordon, J. W. 2015. A conserved mads-box phosphorylation motif regulates differentiation and mitochondrial function in skeletal, cardiac, and smooth muscle cells. Cell Death Dis. 6:e1944.

Okamoto, S., Li, Z., Ju, C., Scholzke, M. N., Mathews, E., Cui, J. K., Salvesen, G. S., Bossy-Wetzel, E., and Lipton, S. A. 2002. Dominant-interfering forms of MEF2 generated by caspase cleavage contribute to NMDA-induced neuronal apoptosis. Proc. Natl. Acad. Sci. U.S.A. 99:3974-3979.

Omotezako, T., Onuma, T. A., and Nishida, H. 2015. DNA interference: DNA-induced gene silencing in the appendicularian *Oikopleura dioica*. Proc. R. Soc. Lond. B: Biological Sciences 282:20150435.

Park, H. S., and Yu, J. H. 2012. Genetic control of asexual sporulation in filamentous fungi. Curr. Opin. Microbiol. 15:669-677.

Resjo, S., Ali, A., Meijer, H. J. G., Seidl, M. F., Snel, B., Sandin, M., Levander, F., Govers, F., and Andreasson, E. 2014. Quantitative label-free phosphoproteomics of six different life stages of the late blight pathogen *Phytophthora infestans* reveals abundant phosphorylation of members of the CRN effector family. J. Proteome Res. 13:1848-1859.

Ribeiro, O. K. 1983. Physiology of asexual sporulation and spore germination in *Phytophthora*. In: Phytophthora, its biology, taxonomy, ecology, and pathology. St. Paul, MN APS Press, pp. 55-70.

Robinson, J. T., Thorvaldsdottir, H., Winckler, W., Guttman, M., Lander, E. S., Getz, G., and Mesirov J. P. 2011. Integrative genomics viewer. Nat. Biotechnol. 29:24-26.

Robinson, M. D., McCarthy, D. J., and Smyth, G. K. 2010. Edger: a bioconductor package for differential expression analysis of digital gene expression data. Bioinformatics 26:139-140.

Rocha, M. C., Fabri, J. H. T. M., de Godoy, K. F., de Castro, P. A., Hori, J. I., de Cunha, A. F., Arentshorst, M., Ram, A. F. J., van den Hondel, C. A. M. J. J., Goldman, G. H., and Malavazi, I. 2016. *Aspergillus fumigatus* MADS-box transcription factor *rlma* is required for regulation of the cell wall integrity and virulence. G3-Genes Genomes Genetics 6:2983–3002.

Ronquist, F., Teslenko, M., van der Mark, P., Ayres, D. L., Darling, A., Hohna, S., Larget, B., Liu, L., Suchard, M. A., and Huelsenbeck, J. P. 2012. MrBayes 3.2: efficient bayesian phylogenetic inference and model choice across a large model space. Syst. Biol. 61:539-542.

Shalizi, A., Gaudilliere, B., Yuan, Z., Stegmuller, J., Shirogane, T., Ge, Q., Tan, Y., Schulman, B., Harper, J. W., and Bonni, A. 2006. A calcium-regulated MEF2 sumoylation switch controls postsynaptic differentiation. Science 311:1012-1017.

Shirai, A., Matsuyama, A., Yashiroda, Y., Hashimoto, A., Kawamura, Y., Arai, R., Komatsu, Y., Horinouchi, S., and Yoshida, M. 2008. Global analysis of gel mobility of proteins and its use in target identification. J. Biol. Chem. 283:10745-10752.

Smaczniak, C., Immink, R. G. H., Muino, J. M., Blanvillain, R., Busscher, M., Busscher-Lange, J., Dinh, Q. D., Liu, S., Westphal, A. H., Boeren, S., Parcy, F., Xu, L., Carles, C. C., Angenent, G. C., and Kaufmann, K. 2012. Characterization of MADS-domain transcription factor complexes in *Arabidopsis* flower development. Proc. Natl. Acad. Sci. U.S.A. 109:1560-1565.

Thiriet-Rupert, S., Carrier, G., Chenais, B., Trottier, C., Bougaran, G., Cadoret, J. P., Schoefs, B., and Saint-Jean, B. 2016. Transcription factors in microalgae: genome-wide prediction and comparative analysis. BMC Genomics 17:282.

van den Hoogen, J., Verbeek-de Kruif, N., and Govers, F. 2018. The G-protein γ subunit of *Phytophthora infestans* is involved in sporangial development. Fungal Genet. Biol. 116:73-82.

van West, P., Kamoun, S., Van ’t Klooster, J. W., and Govers, F. 1999. Internuclear gene silencing in *Phytophthora infestans*. Mol. Cell 3:339–348.

van West, P., Shepherd, S. J., Walker, C. A., Li, S., Appiah, A. A., Grenville-Briggs, L. J., Govers, F., and Gow N. A. 2008. Internuclear gene silencing in *Phytophthora infestans* is established through chromatin remodelling. Microbiology 154:1482-1490.

Vaucheret, H., Beclin, C., Elmayan, T., Feuerbach, F., Godon, C., Morel, J. B., Mourrain, P., Palauqui, J. C., and Vernhettes, S. 1998. Transgene-induced gene silencing in plants. Plant J. 16:651-659.

Xiang, Q. J., and Judelson, H. S. 2014. Myb transcription factors and light regulate sporulation in the oomycete *Phytophthora infestans*. PLoS One 9:92086.

Zhang, Z. Q., Li, H., Qin, G. Z., He, C., Li, B. Q., and Tian, S. P. 2016. The MADS-box transcription factor BcMads1 is required for growth, sclerotia production and pathogenicity of *Botrytis cinerea*. Sci. Rep. 6:33901.

Zhao, B. X. S., Roundtree, I. A., and He, C. 2017. Post- transcriptional gene regulation by mRNA modifications. Nat. Rev. Mol. Cell Biol. 18:31-42.

Zheng, Z., Yu, H., Miki, D., Jin, D., Zhang, Q., Ren, Z., Gong, Z., Zhang H., and Zhu, J. K. 2015. Involvement of multiple gene-silencing pathways in a paramutation-like phenomenon in *Arabidopsis*. Cell Rep. 11:1160-1167.

Chapter III

Off-target effects of homology-based gene silencing in *Phytophthora infestans*

Abstract

Homology-based gene silencing is extensively used to study gene function in *Phytophthora* but the side-effects of this tool are not well-characterized. In this chapter I investigated the potential existence of off-target effects in knockdown strains to understand the limitation of this tool and to improve the silencing vector design. Transformants from two target genes encoding the MADS protein and an E2F transcription factor were examined the *cis*-spreading events. Cosilencing was frequently observed in adjoining genes within 500 nt distance of the target gene. The cosilencing occurred both in transformants generated using a sense or a hairpin silencing vector. This *cis*-spreading was observed in almost half of *MADS*-silenced strains and all *E2F*-silenced strains. This suggests that the *cis*-spreading is random and the expression of neighboring genes should be checked to ensure the reliable assignment of biological function to genes.

Introduction

Strategies for deciphering the roles of genes in all organisms, including plant pathogens and their hosts, involve tools for functional genomics. These approaches commonly employ gene transfer methods to knock down, knock out,

or overexpress the gene of interest (Jiang et al. 2013). Contributing to the success of these tactics is an understanding of the nature of DNA transformation, including its unplanned consequences. Studies across multiple kingdoms have shown that transformation may cause chromosomal rearrangements, gene-silencing methods (including RNAi) may affect off-targets, gene editing may modify unintended loci, and regenerants may exhibit somaclonal variation (Doench et al. 2016; Firon et al. 2002; Kaelin 2012; Neelakandan and Wang 2012). An awareness of these complications helps direct the judicious use of functional genomics tools.

Methods for DNA transformation have been developed for several members of the genus *Phytophthora*, which includes many important phytopathogens. These eukaryotic microbes belong to the oomycete clade of the stramenopile (heterokont) group. Transformation of oomycetes was first achieved with the potato late blight pathogen *P. infestans* and, later, extended to the soybean pathogen *P. sojae* and others (Judelson et al. 1991, 1993a). The most common strategies for introducing plasmid DNA involve treating protoplasts with polyethylene glycol or electroporating zoospores (Judelson and Ah-Fong 2009). Studies in *P. infestans* have shown that a plasmid usually integrates in tandem arrays at a single locus (Judelson 1993). Microprojectile bombardment and *Agrobacterium*-based methods for transformation have also been described (Cvitanich and Judelson 2003; Wu et al. 2016).

To date, the functions of about 40 *Phytophthora* genes have been tested through overexpression or homology-dependent silencing studies, including genes encoding effectors and diverse cellular proteins (Bos et al. 2010; Hardham and Blackman 2018). The latter method entails knocking down messenger (m)RNA levels of a target gene by expressing sense, antisense, or hairpin sequences from that gene in a stable transformant (Ah-Fong et al. 2008). The expression of hairpin sequences has also been referred to as DNA-directed RNAi by some researchers (Rice et al. 2005). Despite such advances, transformation remains challenging. Many researchers describe difficulty in obtaining sufficient numbers of transformants, transgene expression can be unstable, and the frequency of effective knockdowns can be low. It is, thus, common for studies of gene function to be based on a small number of transformants, sometimes as few as one. This is risky, since phenotypes may be caused by unexpected events. About 20% of *P. infestans* transformants exhibit reduced fitness (Judelson et al. 1993b), which, based on studies of other organisms, might result from mutations caused by plasmid integration (Meng et al. 2007). Oomycetes are normally diploid with complex genomes in which gene-dense clusters are surrounded by repetitive DNA (Haas et al. 2009). For example, the 240-Mb genome of *P. infestans* contains about 18,000 genes and 74% high-copy sequences (Haas et al. 2009). Although the integration of plasmids into oomycete chromosomes is believed to involve nonhomologous recombination, no studies have described where plasmids integrate. It is unknown whether

plasmid DNA inserts preferentially into gene-dense, gene-sparse, intragenic, or intergenic regions.

Although the mechanism of homology-based silencing has been studied in only a few cases, in *P. infestans*, this has been shown to result in small RNA production followed by transcriptional silencing and the formation of repressive chromatin (heterochromatin) at the target site (Ah-Fong et al. 2008; Judelson and Tani 2007; van West et al. 2008). Studies in plants and animals indicate that repressive chromatin can move along a chromosome, although its effect on endogenous genes is limited by barrier insulators or regulated by transcription factors (Elgin and Reuter 2013; Le Thomas et al. 2013). In contrast, transgenes or translocated native genes usually lack such protections and, thus, can become silenced by the cis spreading of heterochromatin (Talbert and Henikoff 2006). It is reasonable to consider that heterochromatin may spread beyond the target of gene silencing in *Phytophthora* spp., causing a phenotype to be ascribed to the incorrect gene. We previously used the spreading phenomenon to our advantage by knocking down a cluster of genes in the same metabolic pathway (Abrahamian et al. 2016). However, no study has examined how often silencing spreads in cis from a target to an unintended gene in any oomycete. Similarly, whether silencing affects off-targets elsewhere in the genome has remained unexplored.

In this chapter, I investigate whether silencing from the target locus spreads to adjoining regions by examining transformants obtained using

constructs targeted against two target genes, *MADS* and *E2F*. My conclusion is that as long as attention is paid to potential off-target effects, homology-based silencing is a useful tool in gene function studies.

Results

The regions of the genes used in silencing vectors of *MADS* (PITG_07059) and *E2F* (PITG_03290) are illustrated in Figure 1. Sense constructs were generated by inserting transgene regions after *Ham34* promoter in pTOR vector (Judelson and Ah-Fong 2009). Hairpin constructs were generated using the sense sequence, the *Ste20* intron (70 nt), and antisense sequence. Protoplast transformation of *P. infestans* was performed to generate stable transformants (Judelson et al. 1991). Strains silenced for the target gene were screened by RT-qPCR. Silencing was defined as the situation when the mRNA level of the target gene was less than 25% of the level in wild type. Six strains silenced for *MADS* (Fig. 2A) were obtained, five from a sense silencing vector (Fig. 2A1 to A5) and one from a hairpin (Fig. 2A6). For *E2F* (Fig. 2B), I acquired one partially knocked down (Fig. 2B5) and three silenced (Fig. 2B1, B2, B4) strains from a sense and two silenced strains from a hairpin (Fig. 2B3, B6). The flanking genes expression of these transformants were then screened by RT-qPCR.

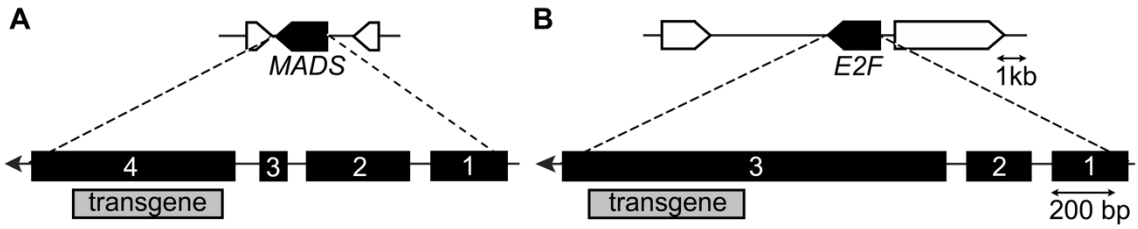

Fig. 1. Genomic region and gene structure of *MADS* and *E2F*. **A**, A schematic representation of *MADS* gene target (black), the neighboring genes (white), and the region used to construct the transgene (gray) in the silencing vector. **B**, Same as A but for the *E2F* gene target.

Using genes encoding the MADS-box protein and an E2F transcription factor as targets, it was found that silencing sometimes spreads to flanking genes. A study of six *MADS*-silenced strains found that silencing spread to flanking untargeted genes about half of the time (Fig. 2A). Both flanking genes, which were 139 and 852 nt away from *MADS* gene, were expressed normally in the first three transformants (Fig. 2A1 to A3). In contrast, both neighboring genes were almost 50% repressed in the transformants shown in Figure 2A4 and A5 even though the same sense silencing vector was used to generate these transformants. One flanking gene of the transformant shown in Figure 2A6 was also suppressed by about 50% using a hairpin silencing construct. The divergent outcomes between strains indicate that there is some randomness or transformant-specific variation in how silencing is imposed.

Another example of silencing spreading to adjacent genes was observed in the case of *E2F* gene target. Analysis of five *E2F*-silenced strains and one partial knockdown (Fig. 2B) found that the flanking gene PITG_03291, which was 544 nt from *E2F* gene, was down-regulated in each strain.

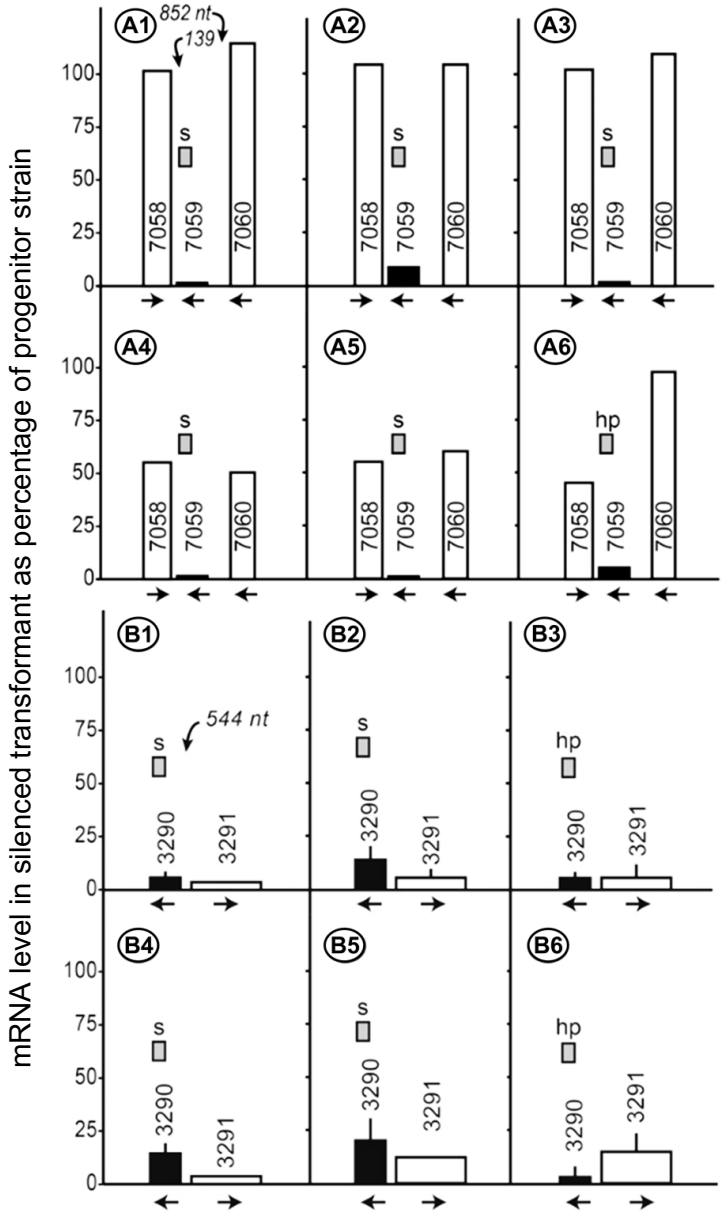

Fig. 2. Expression levels of genes flanking the silenced target. The black bars represent *MADS* gene (PITG_07059) and *E2F* gene (PITG_03290) targeted for silencing and the white bars show the closest genes that flank the target. An arrow under each bar indicates the orientation of transcription. The y axis indicates the mRNA level of each gene relative to wild type. The *x* axis is drawn to scale and portrays the size of each gene and the distance to its neighbors. Distances to flanking genes are denoted in italics. The gray bars indicate the sequences used in the silencing vector as sense (s) or hairpin (hp) constructs. The locations of genes shown were determined using a long read–based assembly of isolate 1306 that allowed contigs used in the Broad Institute's assembly of *P. infestans* T30-4 to be joined and reordered.

Discussion

Data in this chapter is a part of the paper (Vu et al. 2019) in which transformants from ten other targets were also explored. Conclusions from *MADS* and *E2F* are consistent with the analyses of the other genes. Cosilencing commonly occurs within 500 bp from the target. So, assaying flanking gene expression is necessary to ensure that the experimental conclusion regarding to the biological function of a target gene is reliable. Moreover, the results informs how to improve the design of silencing vectors. The sequence homologous to the target gene that is included in the silencing transgene should be designed as far as possible from the nearest gene. In some cases, it may be preferable to use shorter sequences although a previous study showed that a longer hairpin was more effective at triggering silencing (Judelson and Tani 2007). A longer hairpin may be advantageous since it creates a more diverse pool of dsRNAs (Luo et al. 2007).

The *cis*-spread of silencing is random and not correlated to the type of silencing vectors either a sense or a hairpin. So, screening of several transformants increases the chance of identifying a transformant that escaped the cosilencing effect.

In this work we used both a sense and a hairpin, although a hairpin was more effective at triggering silencing in previous studies (Ah-Fong et al. 2008; Wesley et al. 2001). A sense construct is typically an intermediate in the cloning

of a hairpin. Therefore, both constructs were included in many of my gene silencing studies.

Our understanding of the machinery that causes silencing and its *cis*-spread in oomycetes is limited. Homology-based silencing in *P. infestans* has been linked with the transient expression of small RNAs, which arrests transcription based on nuclear run-on assays (Ah-Fong et al. 2008; Judelson and Tani 2007; van West et al. 1999). My study in Chapter II shows the continued expression of transgenes, which could be processed to small RNAs. DNAse protection studies and tests of histone modification inhibitors have suggested that silencing heterochromatinizes the target (Judelson and Tani 2007; van West et al. 2008), although only a few target genes have been studied to date. *P. infestans* encodes the core components for RNA silencing, namely an RNA-dependent RNA polymerase, two Dicers, and five Argonautes (Åsman et al. 2016). Studies in model systems have shown that siRNAs bound to Argonaute guide chromatin-modifying enzymes to complementary loci, leading to transcriptional silencing. Work in fission yeast indicated that siRNA-Argonaute complexes are recruited to their targets through interactions with nascent transcripts (Shimada et al. 2016). The *cis*-spread of silencing may thus occur along mRNA molecules. In plants, the signal involved in post-transcriptional silencing was shown to extend 3'→5' and 5'→3' for up to 300 and 1,000 nt, respectively (Petersen and Albrechtsen 2005; Vaistij et al. 2002). These distances resemble the zone susceptible to the spread of transcriptional silencing

in *P. infestans.* Another mechanism for the *cis*-spread of silencing might involve propagating repressive histone marks. In mammals, histone methyltransferases G9a and GLP forms a complex that binds H3K9me, which allows the enzymes to read their own marks and spread the modification (Shinkai and Tachibana 2011).

Materials and methods

P. infestans transformation

All transformants were obtained using isolate 1306, which is a diploid strain isolated from a tomato field in California. Transformants were maintained on media containing 5 to 10 µg of G418 per milliliter prior to DNA or RNA extraction.

Gene-silencing experiments used sense or hairpin constructs expressed from the *Ham34* promoter. Constructs were generated using pTOR, pSTORA (Judelson and Ah-Fong 2009) or a version modified to include additional cloning sites (pSTORAV). Strains were defined as silenced if the mRNA level of the target gene in RT-qPCR was <25% that of wild type, based on three biological replicates of wild type and the putative silenced strain.

Transformants were obtained using a modification of our original protoplast method (Judelson et al. 1991). Seed cultures for protoplasting were initiated by spreading about 10^4 sporangia per 150-mm plate of rye-sucrose media containing 1.5% agar, typically using 15 plates per experiment. After about 10 days at 18°C in the dark, 15 ml of room-temperature water were spread on

each plate, and sporangia were rubbed from the plate using a flamed bent glass rod. The liquid from the plates was decanted into a 1-liter flask, and hyphal fragments were removed by filtering through 50-µm nylon mesh. An equal amount of clarified amended lima bean media (Bruck et al. 1980) was then added, and additional media (and an equal volume of water) were added to set the sporangia concentration to 4×10^5 per milliliter. The media was then distributed to 1-liter flasks, with 150 ml per flask. After 24 to 36 h of stationary growth at 18°C, the germinated sporangia had formed a thin mat on the bottom of each flask. These were detached from the glass by gentle swirling and were harvested by pouring the culture through 50-µm mesh and rinsing with protoplasting buffer (PB) (0.4 M mannitol, 20 mM KCl, 20 mM MES, pH 5.7, 10 mM $CaCl_2$). This wash was performed by picking up the hyphae from the mesh with bent forceps, placing the hyphae in a 50-ml tube containing PB, and collecting the hyphae again on the nylon mesh. For every milliliter of packed germlings, 3 ml of PB was added, containing 5 mg of filter-sterilized cellulase per milliliter (Sigma) (from *Trichoderma reesi*) and 10 mg of β-glucanase per milliliter; the latter was either Vinoflow NCE (Novozyme) or Extralyse (Laffort). The tube was then shaken gently (40 rpm) on an orbital shaker. During this incubation, 30 µg of DNA (in 40 µl, volume adjusted, as needed, with water) was mixed in a polystyrene tube with 60 µl of Lipofectin (Thermo). When cell-wall digestion was about 90% complete, based on microscopic examination, typically about 20 to 25 min, the protoplast mixture was passed through Miracloth or 50-µm mesh and

was pelleted in a swinging bucket centrifuge at 700 × g at room temperature. The pellet was resuspended gently in 30 ml of PB and respun. The pellet was then resus- pended in 15 ml of PB, and 15 ml of MT (1 M mannitol, 10 mM Tris, pH 7.5) was added. After another round of centrifugation, the pellet was resuspended in 30 ml of MT plus 10 mM $CaCl_2$, was respun, and was resuspended at about 2.5 × 107 protoplasts per milliliter, based on a concentration determined before the final spin. The DNA was then added to 0.7 ml of the protoplast mixture in a 16-ml polystyrene tube, with gentle mixing by inversion or gentle pipetting up and down. After 4 min, 0.7 ml of 50% polyethylene glycol MW 3350 containing 25 mM $CaCl_2$ and 10 mM Tris, pH 7.5, was added slowly by pipetting the fluid down the side of the tube while rotating the tube. After 4 min, 2 ml of clarified rye-sucrose broth containing 1 M mannitol (rye-mannitol) at room temperature was added, the tube was inverted, and, after 1 min, an additional 4 ml of rye-mannitol was added. After 1 min, the contents of the tube were poured into 25 ml of additional rye-mannitol (in a plastic petri plate or a 50-ml tube) and the material was incubated for 20 to 36 h at 18°C. The regenerated tissue was then spun at 1,000 × g for 5 min. The pellet was then resuspended in about 1.5 ml of media containing mannitol with the aid of agitation, using a 1-ml pipette, and was spread on rye-sucrose agar plates containing 7 µg of G418 per milliliter. These plates typically were amended with 40 units of nystatin and 25 µg of penicillin G (or other antibacterial) per milliliter. Colonies typically appeared after 7 days at 18°C.

RT-qPCR

RT-qPCR used primers designed to amplify fragments of 100 to 150 nt from the 3′ ends of the target genes. RNA for RT-qPCR was isolated, using the Sigma kit for plant RNA, was DNase-treated, and cDNA was synthesized using the Maxima (Thermo) first-strand RT-PCR kit. Primers were tested using a dilution series of template and were accepted if efficiencies were above 94%. Amplifications were performed using a Bio-Rad iCycler CFX Connect system using the Dynamo SYBR green qPCR kit (Thermo) with the following program: 95°C for 15 min, followed by 40 cycles of 94°C for 30 s, 52 to 58°C for 30 s, depending on the primer, and 72°C for 30 s. Controls without reverse transcription and melt curves were included to help verify the reliability of the amplification. Expression levels were calculated using the ΔΔcycle threshold method, using constitutive genes (PITG_09862 and PITG_11766) (Niu et al. 2018) as a control, with at least two biological replicates with three technical replicates each.

Acknowledgements

We thank *Molecular Plant-Microbe Interactions* for letting us use a part of the manuscript in this dissertation. The original article can be found at: https://doi.org/10.1094/MPMI-09-18-0265-TA.

References

Abrahamian, M., Ah-Fong, A. M., Davis, C., Andreeva, K., and Judelson, H. S. 2016. Gene expression and silencing studies in *Phytophthora infestans* reveal infection-specific nutrient transporters and a role for the nitrate reductase pathway in plant pathogenesis. PLoS Pathog. 12:e1006097.

Ah-Fong, A. M., Bormann-Chung, C. A., and Judelson, H. S. 2008. Optimization of transgene-mediated silencing in *Phytophthora infestans* and its association with small-interfering RNAs. Fungal Genet. Biol. 45:1197-1205.

Åsman, A. K., Fogelqvist, J., Vetukuri, R. R., and Dixelius, C. 2016. *Phytophthora infestans* Argonaute 1 binds microRNA and small RNAs from effector genes and transposable elements. New Phytol. 211:993-1007.

Bos, J. I. B., Armstrong, M. R., Gilroy, E. M., Boevink, P. C., Hein, I., Taylor, R. M., Zhendong, T., Engelhardt, S., Vetukuri, R. R., Harrower, B., Dixelius, C., Bryan, G., Sadanandom, A., Whisson, S. C., Kamoun, S., and Birch, P. R. J. 2010. *Phytophthora infestans* effector AVR3a is essential for virulence and manipulates plant immunity by stabilizing host E3 ligase CMPG1. Proc. Natl. Acad. Sci. U.S.A. 107:9909-9914.

Bruck, R. I., Fry, W. E., and Apple, A. E. 1980. Effect of metalaxyl an acyl alanine fungicide on developmental stages of *Phytophthora infestans*. Phytopathology 70:597-601.

Cvitanich, C., and Judelson, H. S. 2003. Stable transformation of the oomycete, *Phytophthora infestans*, using microprojectile bombardment. Curr. Genet. 42:228-235.

Doench, J. G., Fusi, N., Sullender, M., Hegde, M., Vaimberg, E. W., Donovan, K. F., Smith, I., Tothova, Z., Wilen, C., Orchard, R., Virgin, H. W., Listgarten, J., and Root, D. E. 2016. Optimized sgRNA design to maximize activity and minimize off-target effects of CRISPR-Cas9. Nat. Biotechnol. 34:184-191.

Elgin, S. C. R., and Reuter, G. 2013. Position-effect variegation, heterochromatin formation, and gene silencing in *Drosophila*. Cold Spring Harb. Perspect. Biol. 5:a017780.

Firon, A., Beauvais, A., Latgé, J. P., Couvé, E., Grosjean-Cournoyer, M. C., and D'Enfert, C. 2002. Characterization of essential genes by parasexual genetics in the human fungal pathogen *Aspergillus fumigatus*: Impact of

genomic rearrangements associated with electroporation of DNA. Genetics 161:1077-1087.

Haas, B. J., Kamoun, S., Zody, M. C., Jiang, R. H., Handsaker, R. E., Cano, L. M., Grabherr, M., Kodira, C. D., Raffaele, S., Torto-Alalibo, T., Bozkurt, T. O., Ah-Fong, A. M., Alvarado, L., Anderson, V. L., Armstrong, M. R., Avrova, A., Baxter, L., Beynon, J., Boevink, P. C., Bollmann, S. R., Bos, J. I., Bulone, V., Cai, G., Cakir, C., Carrington, J. C., Chawner, M., Conti, L., Costanzo, S., Ewan, R., Fahlgren, N., Fischbach, M. A., Fugelstad, J., Gilroy, E. M., Gnerre, S., Green, P. J., Grenville-Briggs, L. J., Griffith, J., Grünwald, N. J., Horn, K., Horner, N. R., Hu, C. H., Huitema, E., Jeong, D. H., Jones, A. M., Jones, J. D., Jones, R. W., Karlsson, E. K., Kunjeti, S. G., Lamour, K., Liu, Z., Ma, L., Maclean, D., Chibucos, M. C., McDonald, H., McWalters, J., Meijer, H. J., Morgan, W., Morris, P. F., Munro, C. A., O'Neill, K., Ospina- Giraldo, M., Pinzo´n, A., Pritchard, L., Ramsahoye, B., Ren, Q., Restrepo, S., Roy, S., Sadanandom, A., Savidor, A., Schornack, S., Schwartz, D. C., Schumann, U. D., Schwessinger, B., Seyer, L., Sharpe, T., Silvar, C., Song, J., Studholme, D. J., Sykes, S., Thines, M., van de Vondervoort, P. J., Phuntumart, V., Wawra, S., Weide, R., Win, J., Young, C., Zhou, S., Fry, W., Meyers, B. C., van West, P., Ristaino, J., Govers, F., Birch, P. R., Whisson, S. C., Judelson, H. S., and Nusbaum, C. 2009. Genome sequence and analysis of the Irish potato famine pathogen *Phytophthora infestans*. Nature 461:393-398.

Hardham, A. R., and Blackman, L. M. 2018. *Phytophthora cinnamomi*. Mol. Plant Pathol. 19:260-285.

Jiang, D., Zhu, W., Wang, Y., Sun, C., Zhang, K. Q., and Yang, J. 2013. Molecular tools for functional genomics in filamentous fungi: Recent advances and new strategies. Biotechnol. Adv. 31:1562-1574.

Judelson, H. S. 1993. Intermolecular ligation mediates efficient cotransformation in *Phytophthora infestans*. Mol. Gen. Genet. 239:241-250.

Judelson, H. S., and Ah-Fong, A. M. V. 2009. Progress and challenges in oomycete transformation. Pages 435-454. in: Oomycete Genetics and Genomics. K. Lamour and S. Kamoun, eds. John Wiley & Sons, Inc., Hoboken, NJ, U.S.A.

Judelson, H. S., Coffey, M. D., Arredondo, F. R., and Tyler, B. M. 1993a. Transformation of the oomycete pathogen *Phytophthora megasperma* f. sp. *glycinea* occurs by DNA integration into single or multiple chromosomes. Curr. Genet. 23:211-218.

Judelson, H. S., Dudler, R., Pieterse, C. M. J., Unkles, S. E., and Michelmore, R. W. 1993b. Expression and antisense inhibition of transgenes in *Phytophthora infestans* is modulated by choice of promoter and position effects. Gene 133:63-69.

Judelson, H. S., and Tani, S. 2007. Transgene-induced silencing of the zoosporogenesis-specific *NIFC* gene cluster of *Phytophthora infestans* involves chromatin alterations. Eukaryot. Cell 6:1200-1209.

Judelson, H. S., Tyler, B. M., and Michelmore, R. W. 1991. Transformation of the oomycete pathogen, *Phytophthora infestans*. Mol. Plant-Microbe Interact. 4:602-607.

Kaelin, W. G., Jr. 2012. Molecular biology. Use and abuse of RNAi to study mammalian gene function. Science 337:421-422.

Le Thomas, A., Rogers, A. K., Webster, A., Marinov, G. K., Liao, S. E., Perkins, E. M., Hur, J. K., Aravin, A. A., and To´th, K. F. 2013. Piwi induces piRNA-guided transcriptional silencing and establishment of a repressive chromatin state. Genes Dev. 27:390-399.

Luo, Q., Kang, Q., Song, W. X., Luu, H. H., Luo, X., An, N., Luo, J., Deng, Z. L., Jiang, W., Yin, H., Chen, J., Sharff, K. A., Tang, N., Bennett, E., Haydon, R. C., and He, T. C. 2007. Selection and validation of optimal siRNA target sites for RNAi-mediated gene silencing. Gene 395:160-169.

Meng, Y., Patel, G., Heist, M., Betts, M. F., Tucker, S. L., Galadima, N., Donofrio, N. M., Brown, D., Mitchell, T. K., Li, L., Xu, J. R., Orbach, M., Thon, M., Dean, R. A., and Farman, M. L. 2007. A systematic analysis of T-DNA insertion events in *Magnaporthe oryzae*. Fungal Genet. Biol. 44:1050-1064.

Neelakandan, A. K., and Wang, K. 2012. Recent progress in the understanding of tissue culture-induced genome level changes in plants and potential applications. Plant Cell Rep. 31:597-620.

Niu, X., Ah-Fong, A. M. V., Lopez, L. A., and Judelson, H. S. 2018. Transcriptomic and proteomic analysis reveals wall-associated and glucan-degrading proteins with potential roles in *Phytophthora infestans* sexual spore development. PLoS One 13:e0198186.

Petersen, B. O., and Albrechtsen, M. 2005. Evidence implying only unprimed RdRP activity during transitive gene silencing in plants. Plant Mol. Biol. 58:575-583.

Rice, R. R., Muirhead, A. N., Harrison, B. T., Kassianos, A. J., Sedlak, P. L., Maugeri, N. J., Goss, P. J., Davey, J. R., James, D. E., and Graham, M. W. 2005. Simple, robust strategies for generating DNA-directed RNA interference constructs. Methods Enzymol. 392:405-419.

Shimada, Y., Mohn, F., and Bühler, M. 2016. The RNA-induced transcriptional silencing complex targets chromatin exclusively via interacting with nascent transcripts. Genes Dev. 30:2571-2580.

Shinkai, Y., and Tachibana, M. 2011. H3K9 methyltransferase G9a and the related molecule GLP. Genes Dev. 25:781-788.

Talbert, P. B., and Henikoff, S. 2006. Spreading of silent chromatin: Inaction at a distance. Nat. Rev. Genet. 7:793-803.

Vaistij, F. E., Jones, L., and Baulcombe, D. C. 2002. Spreading of RNA targeting and DNA methylation in RNA silencing requires transcription of the target gene and a putative RNA-dependent RNA polymerase. Plant Cell 14:857-867.

van West, P., Kamoun, S., van't Klooster, J. W., and Govers, F. 1999. Internuclear gene silencing in *Phytophthora infestans*. Mol. Cell 3:339-348.

van West, P., Shepherd, S. J., Walker, C. A., Li, S., Appiah, A. A., Grenville-Briggs, L. J., Govers, F., and Gow, N. A. 2008. Internuclear gene silencing in *Phytophthora infestans* is established through chromatin remodelling. Microbiology 154:1482-1490.

Vu, A. L., Leesutthiphonchai, W., Ah-Fong, A. M. V., and Judelson, H. S. 2019. Defining transgene insertion sites and off-target effects of homology-based gene silencing informs the application of functional genomics tools in *Phytophthora infestans*. MPMI 32:915–927.

Wesley, S. V., Helliwell, C. A., Smith, N. A., Wang, M. B., Rouse, D. T., Liu, Q., Gooding, P. S., Singh, S. P., Abbott, D., Stoutjesdijk, P. A., Robinson, S. P., Gleave, A. P., Green, A. G., and Waterhouse, P. M. 2001. Construct design for efficient, effective and high-throughput gene silencing in plants. Plant J. 27:581-590.

Wu, D., Navet, N., Liu, Y., Uchida, J., and Tian, M. 2016. Establishment of a simple and efficient Agrobacterium-mediated transformation system for *Phytophthora palmivora*. BMC Microbiol. 16:204.

Conclusions

In this thesis, I addressed several unknown aspects of sporangia in *Phytophthora*. Since spores are important for dissemination and infection, understanding how *Phytophthora* produces spores could lead to new or effective ways for disease management, for example by finding chemicals or peptides that target regulators to disrupt spore production, and thus block the spread of disease.

In Chapter I, my characterization of sporangia from artificial media and those produced *in planta* confirmed that sporangia in laboratory are largely functionally similar to those produced in nature. Therefore, most results from laboratory experiments using sporangia from artificial media should apply to the situation in the field. I also presented guidelines for the handling of sporangia, which is crucial since sporangia are metabolically active and delicate. Checking marker genes of sporangia and other life stages to ensure that collected sporangia have been collected under uniform conditions will help to avoid artifacts in experiments.

I compared the transcriptional profiles of sporangia from media and plants and identified a small number of differentially expressed genes. The majority of those were metabolic genes. Despite having modest differences in the RNA-seq results, sporangia from media and plants were similar in infection potential and germination rate.

Another aspect of *Phytophthora* biology that I have tried to understand is the regulatory network of sporulation. In Chapter II, a study of a MADS-box transcription factor revealed its essential function in sporulation of *P. infestans*. I showed that *MADS* mRNA and protein rose during sporulation and declined when spores germinate. *MADS* mRNA oscillated in response to light, which indicated that at least some factors that activate MADS transcription likely occur downstream of the light regulation step. Cryptochromes were identified as a photoreceptor of *P. infestans* (Xiang and Judelson 2014). It would be interesting to study if these proteins link light to the MADS pathway.

Conserved domain analysis of MADS showed the MEF2-like MADS-box domain at N-terminus. The domain contains the DNA binding site and a dimerization motif. The latter is relevant since MADS-box transcription factors in other organisms were shown to form both homo- and heterodimers (Molkentin et al. 1996; Riechmann et al. 1996; Zhao et al. 1999). Over a hundred *MADS* genes are found in angiosperms while between one and five *MADS* genes are in animals and fungi (De Bodt et al. 2003; Parenicová et al. 2003; Shore and Sharrocks 1995). Oomycetes have one *MADS* gene, which is simpler than the *MADS* gene families of plants or animals. During evolution, gene duplication events enlarged the *MADS* gene family in non-oomycetes (Alvarez-Buylla et al. 2000; De Bodt et al. 2005; Zahn et al. 2005), with homodimerization shifting to obligate heterodimerization (Winter et al. 2002). Since *Phytophthora* have one

MADS gene, I hypothesize that MADS forms a homodimer. This could be tested by yeast two-hybrid or coimmunoprecipitation.

I showed that MADS protein was phosphorylated in sporangia and dephosphorylated in zoospores. The protein's degradation was also observed during zoosporogenesis. This suggests that MADS interacts with other proteins like kinases and phosphatases. A sporulation-induced phosphatase like Cdc14 is a candidate for an interactor with MADS. I hypothesize that the interaction would occur in nuclei since the study from Ah-Fong and Judelson (2011) showed the nuclear localization of Cdc14 in spores. It would be interesting to test this using coimmunoprecipitation or yeast two-hybrid experiments.

MADS appeared larger than its predicted size. I hypothesize that sumoylation would alter the mobility of MADS. Although SUMO protease Ulp1 from yeast does not cleave MADS, it is possible that Ulp1 does not recognize the *P. infestans* SUMO sequence. If an antibody that is specific to the *P. infestans* SUMO sequence could be found, researchers could test my hypothesis concerning the sumoylation of MADS.

I described the localization of the MADS protein expressed with a fluorescent tag driven by the native promoter in sporulating mycelia and spores. In the experiment, the native promoter used included 402 nt of DNA upstream of the transcription start site; however, transcription factor binding sites and response elements within this *MADS* promoter have not been studied. It would be interesting to identify the functional domains of this promoter. Very little about

oomycete promoters is known (Ah-Fong et al. 2007; Roy et al. 2013), hence a study of the *MADS* promoter would provide more information of *Phytophthora* transcriptional mechanisms. Moreover, a promoter study would reveal whether MADS is autoregulated as previously reported in other organisms (Cripps et al. 2004; Ramachandran et al. 2008). It would be interesting to identify the promoter elements that are required for autoactivation and when it occurs.

I showed that MADS localized in nuclei of spores. The nuclear localization signals of oomycetes are not well-defined (Fang et al. 2017). The predicted nuclear localization signals of MADS are at both its N- and C-termini, similar to the predictions of human and *Drosophila* MEF2. The C-terminal NLS of MEF2 is experimentally confirmed (Yu 1996; Borghi et al. 2001) and the predicted region is similar to the region in *P. infestans* MADS. Moreover, the NLS sequence of MEF2 and *P. infestans* MADS are conventional as a class 2 NLS (Kosugi et al. 2009). It would be useful to study the nuclear localization signal of MADS by deletion fragments fused with fluorescent tag.

Using homology-based gene silencing, I demonstrated that MADS was important for sporulation. RNA-seq of wild type and a silenced strain showed that MADS regulates more than 2000 sporulation-associated genes. In theory, the genes targeted directly by MADS could be identified if the DNA-binding specificity of MADS was known. Moreover, a study of the MADS binding site in *P. infestans* would confirm whether it is similar to the motif reported in other organisms (Pollock and Treisman 1991; Thai et al. 1998). In the future, chromatin

immunoprecipitation can be used to identify the binding sites and the target genes of MADS.

In Chapter III, the off-target effects of homology-based gene silencing in knockdown strains were studied to understand the limitation of this tool and to improve silencing vector design. The *cis*-spread of silencing to adjoining genes was frequently observed; however, an absence of this *cis*-spread was observed in many individual transformants. Overall, this suggests that suitably extensive screening of transformants (including neighbor gene analysis) should enable the reliable use of the silencing method. Moreover, in the gene silencing of *MADS*, I found that *MADS* transgenes were not always silenced with the native gene. This contradicted current silencing models in oomycetes which, based on previous studies, indicate that both the transgene and native gene are transcriptionally silenced (van West et al. 1999; Gaulin et al. 2002; Ah Fong and Judelson 2003; Latijnhouwers and Govers 2003; Blanco and Judelson 2005; Judelson and Tani 2007). By exploring more transformants, I observed that continued expression of transgene was occasional (Vu et al. 2019). This suggests that primers used for screening for silencing should be designed outside of the transgene region.

My thesis has helped to expand our knowledge about *Phytophthora* sporangia; however, many more questions related to sporulation remain to be answered. For example, what is required for a culture to reach competence to sporulate? When does *Phytophthora* achieve this competence? What metabolic

and environmental cues trigger the onset of sporulation? What regulators and signaling pathways trigger sporulation?

The regulation of *Phytophthora* sporulation is poorly understood while the regulatory networks of asexual sporulation in many fungi are very well-described (Park and Yu 2016). In fungi, many central regulators of asexual spore development have been identified including BrlA, AbaA, WetA, StuA, and MedA (Adam et al. 1988; Boylan et al. 1987; Sewall et al. 1990; Miller et al. 1992; Busby et al. 1996). Signaling pathways that respond to environmental cues and trigger sporulation have also been studied. These include FluG-mediated signaling pathways, heterotrimeric G proteins, and light signaling pathways (Wieser et al. 1994; Yu 2006; Bayram et al. 2010). Sporulation networks are complex and it will take some time to achieve a similar level of knowledge in *Phytophthora*. Nevertheless, this is a worthy goal since understanding the mechanisms of *Phytophthora* sporulation will lead to more effective strategies for disease control.

References

Adams, T. H., Boylan, M. T., and Timberlake, W. E. 1988. *brlA* is necessary and sufficient to direct conidiophore development in *Aspergillus nidulans*. Cell 54:353-362.

Ah Fong, A. M., and Judelson, H. S. 2003. Cell cycle regulator Cdc14 is expressed during sporulation but not hyphal growth in the fungus-like oomycete *Phytophthora infestans*. Mol. Microbiol. 50:487-494.

Ah-Fong, A. M., and Judelson, H. S. 2011. New role for Cdc14 phosphatase: localization to basal bodies in the oomycete *Phytophthora* and its evolutionary coinheritance with eukaryotic flagella. PLoS One 6:e16725.

Ah-Fong, A. M., Bormann-Chung, C. A., and Judelson, H. S. 2008. Optimization of transgene-mediated silencing in *Phytophthora infestans* and its association with small-interfering RNAs. Fungal Genet. Biol. 45:1197-1205.

Ah-Fong, A. M., Xiang, Q., and Judelson, H. S. 2007. Architecture of the sporulation-specific Cdc14 promoter from the oomycete *Phytophthora infestans* and its association with small-interfering RNAs. Fungal Genet. Biol. 45:1197-1205.

Alvarez-Buylla, E. R., Pelaz, S., Liljegren, S. J., Gold, S. E., Burgeff, C., Ditta, G. S., Ribas de Pouplana, L., Martínez-Castilla, L., and Yanofsky, M. F. 2000. An ancestral MADS-box gene duplication occurred before the divergence of plants and animals. Proc Natl Acad Sci U S A. 97:5328-5333.

Bayram, O., Braus, G. H.., Fischer, R., and Rodriguez-Romero, J. 2010. Spotlight on *Aspergillus nidulans* photosensory systems. Fungal. Genet. Biol. 47:900-908.

Blanco, F. A., and Judelson, H. S. 2005. A bZIP transcription factor from *Phytophthora* interacts with a protein kinase and is required for zoospore motility and plant infection. Mol. Microbiol. 56:638-648.

Borghi, S., Molinari, S., Razzini, G., Parise, F., Battini, R., and Ferrari, S. 2001. The nuclear localization domain of the MEF2 family of transcription factors shows member-specific features and mediates the nuclear import of histone deacetylase 4. J. Cell Sci. 114:4477-4483.

Boylan, M. T., Mirabito, P. M., Willett, C. E., Zimmerman, C. R., and Timberlake, W. E. 1987. Isolation and physical characterization of three essential conidiation genes from *Aspergillus nidulans*. Mol. Cell. Biol. 7:3113-3118.

Busby, T. M., Miller, K. Y., and Miller, B. L. 1996. Suppression and enhancement of the *Aspergillus nidulans medusa* mutation by altered dosage of the bristle and stunted genes. Genetics 143:155-163.

Cripps, R. M., Lovato, T. L., and Olson, E. N. 2004. Positive autoregulation of the myocyte enhancer factor-2 myogenic control gene during somatic muscle development in *Drosophila*. Dev. Biol. 267:536-547.

De Bodt, S., Maere, S., and Van de Peer, Y. 2005. Genome duplication and the origin of angiosperms. Trends Ecol. Evol. 20:591–597.

De Bodt, S., Raes, J., Florquin, K., Rombauts, S., Rouzé, P., Theißen, G., Van de Peer, Y. 2003. Genome-wide structural annotation and evolutionary analysis of the type I MADS-box genes in plants. J. Mol. Evol. 56:573-586.

Fang, Y., Jang, H. S., Watson, G. W., Wellappili, D. P., Tyler, B. M. 2017. Distinctive nuclear localization signals in the oomycete *Phytophthora sojae*. Front. Microbiol. 8:10.

Judelson, H. S., and Tani, S. 2007. Transgene-induced silencing of the zoosporogenesis-specific NIFC gene cluster of *Phytophthora infestans* involves chromatin alterations. Eukaryot. Cell 6:1200-1209.

Gaulin, E., Jauneau, A., Villalba, F., Rickauer, M., Esquerre-Tugaye, M. T., and Bottin, A. 2002. The cbel glycoprotein of *Phytophthora parasitica* var. *nicotianae* is involved in cell wall deposition and adhesion to cellulosic substrates. J. Cell Sci. 115:4565-4575.

Kosugi, S., Hasebe, M., Matsumura, N., Takashima, H., Miyamoto-Sato, E., Tomita, M., and Yanagawa, H. 2009. Six classes of nuclear localization signals specific to different binding grooves of importin α. J. Biol. Chem. 284:478-485.

Latijnhouwers, M., and Govers, F. 2003. A *Phytophthora infestans* G-protein subunit is involved in sporangium formation. Eukaryot. Cell 2:971-977.

Matson, M. E. H. 2018. A chromosome-scale reference assembly facilitates new insights into fungicide sensitivity and genome plasticity in *Phytophthora infestans*. Ph.D. thesis, University of California, Riverside.

Miller, K. Y., Wu, J., and Miller, B. L. 1992. StuA is required for cell pattern formation in *Aspergillus*. Genes Dev. 6: 1770-1782.

Molkentin, J. D., Black, B. L., Martin, J. F., and Olson, E. N. 1996. Mutational analysis of the DNA binding, dimerization, and transcriptional activation domains of MEF2C. Mol. Cell. Biol. 16:2627-2636.

Parenicová, L., de Folter, S., Kieffer, M., Horner, D. S., Favalli, C., Busscher, J., Cook, H. E., Ingram, R. M., Kater, M. M., Davies, B., Angenent, G. C., and Colombo, L. 2003. Molecular and phylogenetic analyses of the complete MADS-box transcription factor family in *Arabidopsis*: new openings to the MADS world. Plant Cell 15:1538-1551.

Park, H. S., and Yu, J. H. 2016. Molecular Biology of Asexual Sporulation in Filamentous Fungi. In: D. Hoffmeister (Ed.) Biochemistry and Molecular Biology. The Mycota (A Comprehensive Treatise on Fungi as Experimental Systems for Basic and Applied Research), vol III. Cham Switzerland: Springer, pp.3-20.

Pollock, R., and Treisman, R. 1991. Human SRF-related proteins: DNA binding properties and potential regulatory targets. Genes Dev. 5: 2327-2341.

Ramachandran, B., Yu, G., Li, S., Zhu, B., and Gulick, T. 2008. Myocyte enhancer factor 2A is transcriptionally autoregulated. J. Biol. Chem. 283:10318-10329.

Riechmann, J. L., Krizek, B. A., and Meyerowitz, E. M. 1996. Dimerization specificity of *Arabidopsis* MADS domain homeotic proteins APETALA1, APETALA3, PISTILLATA, and AGAMOUS. Proc. Nat. Acad. Sci. U.S.A. 93:4793-4798.

Roy, S., Poidevin, L., Jiang, T., and Judelson, H. S. 2013. Novel core promoter elements in the oomycete pathogen *Phytophthora infestans* and their influence on expression detected by genome-wide analysis. BMC Genomics 14:106.

Sewall, T. C., Mims, C. W., and Timberlake, W. E. 1990. Conidium differentiation in *Aspergillus nidulans* wild-type and *wet-white* (*wetA*) mutant strains. Dev. Biol. 138:499-508.

Shore, P., and Sharrocks, A. D. 1995. The MADS-box family of transcription factors. Eur. J. Biochem. 229:1-13.

Thai, M. V., Guruswamy, S., Cao, K. T., Pessin, J. E., and Olson, A. L. 1998. Myocyte enhancer factor 2 (MEF2)-binding site is required for GLUT4

gene expression in transgenic mice. Regulation of MEF2 DNA binding activity in insulin-deficient diabetes. J. Biol. Chem. 273:14285-14292.

van West, P., Kamoun, S., Van 't Klooster, J. W., and Govers, F. 1999. Internuclear gene silencing in *Phytophthora infestans*. Mol. Cell 3:339-348.

Vu, A. L., Leesutthiphonchai, W., Ah-Fong, A. M. V., and Judelson, H. S. 2019. Defining transgene insertion sites and off-target effects of homology-based gene silencing informs the application of functional genomics tools in *Phytophthora infestans*. Mol. Plant- Microbe Interact. 32:915-927.

Wieser, J., Lee, B. N., Fondon, J. W. 3rd, and Adams, T. H. 1994. Genetic requirements for initiating asexual development in *Aspergillus nidulans*. Curr. Genet. 27:62-69.

Winter, K. U., Weiser, C., Kaufmann, K., Bohne, A., Kirchner, C., Kanno, A., Saedler, H., and Theißen, G. 2002. Evolution of class B floral homeotic proteins: obligate heterodimerization originated from homodimerization. Mol. Biol. Evol.19:587-596.

Xiang, Q. J., and Judelson, H. S. 2014. Myb transcription factors and light regulate sporulation in the oomycete *Phytophthora infestans*. PLoS One 9:92086.

Yu, J. H. 2006. Heterotrimeric G protein signaling and RGSs in *Aspergillus nidulans*. J. Microbiol. 44:145-154.

Yu, Y. T. 1996. Distinct domains of myocyte enhancer binding factor-2A determining nuclear localization and cell type-specific transcriptional activity. J. Biol. Chem. 271:24675-24683.

Zahn, L. M., Kong, H., Leebens-Mack, J. H., Kim, S., Soltis, P. S., Landherr, L. L., Soltis, D. E., dePamphilis, C. W., and Ma, H. 2005. The evolution of the SEPALLATA subfamily of MADS-box genes: a preangiosperm origin with multiple duplications throughout angiosperm history. Genetics 169:2209-2223.

Zhao, M., New, L., Kravchenko, V. V., Kato, Y., Gram, H., di Padova, F., Olson, E. N., Ulevitch, R. J., and Han, J. 1999. Regulation of the MEF2 family of transcription factors by p38. Mol. Cell. Biol. 19:21-30.